

Endocytic Trafficking in *Toxoplasma gondii*

by

Olivia Lauren McGovern

**A dissertation submitted in partial fulfillment
of the requirements for the degree of
Doctor of Philosophy
(Microbiology and Immunology)
in The University of Michigan
2018**

Doctoral Committee:

**Professor Vern. B. Carruthers, Chair
Professor Ronald W. Holz
Professor Mary X. D. O’Riordan
Professor Joel Swanson**

Olivia L. McGovern

livmcgov@umich.edu

ORCID iD: 0000-0001-7216-5021

© Olivia L. McGovern 2018

DEDICATION

This dissertation is dedicated to my dad, Lawrence Edward McGovern. I know he would be proud.

ACKNOWLEDGMENTS

I would like to thank my advisor, Dr. Vern Carruthers for his guidance and support throughout my graduate career, especially support for my pursuit of the Epidemic Intelligence Service (EIS). Whether it was honing skills for critical thinking, experimental design, troubleshooting or communication of my work in the lab, or giving me the freedom to pursue extracurricular activities to get experience in the public health realm, the training I received in Vern's lab have made me an independent scientist and prepared me for the next phase of my career. I would also like to thank my thesis committee, Drs. Mary O'Riordan, Joel Swanson and Ronald Holz for their guidance in developing my thesis project, constructive critique of my work, crafting a manuscript for publication and for supporting me in my career development.

I am also grateful to my labmates, who were always there to encourage me. Your helpful feedback in lab meeting and consultation on how to perform new experiments have been invaluable in the success of my projects. I would also like to thank the coauthors and collaborators. Without your hard work and dedication, the work in this thesis would not have been possible. Reagents contributed by collaborators were also invaluable. Your contributions are greatly appreciated and have been highlighted within each chapter.

I also want to acknowledge all of my mentors that lead up to graduate school. Thank you Mrs. Neyhard for applying to my first internship for me when I had no idea what an internship was. Thank you to Dr. Gerda Breitwieser and Dr. Kenneth Loparo for developing me as a young scientist during my summer internships, to Dr. Jonathan Southard and Dr. Bob Hinrichsen for your personal and professional support during my undergraduate studies that has continued until now, and to Dr. Judy Yanowitz who taught me so much about the kind of scientist and mentor I wanted to be and pushing me bring out my best as a technician in your lab. I would not have made it to graduate school if it were not for all of you.

Finally, I would also like to thank my friends and family who have supported me throughout graduate school. Whether it was words of encouragement, a much-needed hug, sharing an inside joke, or coming to visit me in Ann Arbor I appreciated it all. In particular, I need to thank my wife Maura Barrett, who has also believed in me and supported me. Thank you so much for listening to all of my practice talks and knowing when I needed a good laugh. I can't wait to start the next chapter of our life.

TABLE OF CONTENTS

DEDICATION	ii
ACKNOWLEDGMENTS	iii
LIST OF FIGURES	viii
GLOSSARY OF TERMS	x
ABSTRACT	xvi
Chapter 1 Introduction	1
1.1 Introduction to <i>Toxoplasma gondii</i> and toxoplasmosis	1
1.2 <i>T. gondii</i> ingests host protein from within a parasitophorous vacuole	2
1.3 Mechanisms of endocytosis at the plasma membrane in model organisms	4
1.4 Endocytic trafficking across the <i>T. gondii</i> PVM and plasma membrane	8
1.5 Endocytic trafficking to the lysosome in model organisms	10
1.6 Trafficking to the <i>T. gondii</i> VAC through a plant-like exocytic system?	12
1.7 Summary and chapter outline	14
1.8 References	15
Chapter 2 Intersection of endocytic and exocytic systems in <i>Toxoplasma gondii</i>	25
2.1 Abstract	25
2.2 Introduction	26
2.3 Results	27
2.3.1 Localization of the TGN/ELC marker GalNac-YFP	27
2.3.2 Ingested proteins traverse ELCs	29
2.3.3 Ingested proteins reach the VAC for CPL-dependent digestion within 30 min	33
2.3.4 Promicroneme proteins are detected in all cell cycle phases	35
2.3.5 Prorhoptry proteins are detected in S and M/C phases	37

2.3.6 Ingestion is active throughout the cell cycle.....	38
2.3.7 Ingested host protein trafficking intersects with microneme protein trafficking.....	40
2.4 Discussion	43
2.4.1 Trafficking of ingested proteins.....	43
2.4.2 Cell cycle dependence of microneme and rhoptry biogenesis.....	43
2.4.3 Cell cycle dependence of <i>T. gondii</i> ingestion.....	44
2.4.4 Intersection of endocytosis and exocytosis in <i>T. gondii</i>	45
2.4.5 A model for sorting in the <i>T. gondii</i> endolysosomal system.....	45
2.5 Materials and methods	47
2.6 Notes and notable contributions	52
2.7 References	53
Chapter 3 <i>T. gondii</i> endocytosis does not require DrpB	59
3.1 Abstract.....	59
3.2 Introduction.....	60
3.3 Results.....	62
3.3.1 DrpB localizes to the TGN and ELCs.....	62
3.3.2 Ingested protein colocalizes with DrpB.....	64
3.3.3 DrpB is not required for endocytosis of host cytosol.....	66
3.3.4 DrpB is not required for downstream trafficking to the VAC.....	68
3.4 Discussion	70
3.4.1 Does endocytic traffic in <i>T. gondii</i> resemble traffic in plants?.....	70
3.4.2 DrpB-independent does not necessarily mean dynamin-independent.....	71
3.4.3 Expression of ddGFP-DrpB K72A enhances <i>T. gondii</i> endocytosis.....	71
3.5 Materials and methods	72
3.6 Notes and notable contributions	76
3.7 References	77
Chapter 4 Discussion	81
4.1 Overview.....	81
4.2 Ongoing and future work for mechanisms of trafficking across the PVM.....	86

4.3 Ongoing and future work for mechanisms of trafficking across the parasite plasma membrane	88
4.4 Ongoing and future work for mechanisms of trafficking to the VAC	90
4.5 Sorting receptors for endocytic cargo	92
4.6 Tools for testing predictable and unpredictable targets	94
4.7 The importance of host protein ingestion	96
4.8 Conclusion	97
4.9 References	97

LIST OF FIGURES

Figure 1-1. The intracellular niche of <i>T. gondii</i>	4
Figure 1-2. Mechanisms of endocytosis in model systems.....	7
Figure 1-3. Hypothetical models for ingestion across the PVM.....	9
Figure 1-4. Model for path and mechanisms of endocytic trafficking in plants and yeast/mammals.....	11
Figure 1-5. Hypothetical model for trafficking to the VAC.....	13
Figure 2-1. Localization of GalNac-YFP in RH GalNac-YFP parasites.....	28
Figure 2-2. Ingested host cytosolic mCherry is associated with the ELCs, VAC, and possibly the TGN.....	30
Figure 2-3. Harvested mCherry ⁺ parasites are viable and can invade HFF cells.....	31
Figure 2-4. Ingested mCherry colocalizes with GalNac-YFP in a CPB positive compartment.....	32
Figure 2-5. Host cytosolic mCherry is ingested into a non-digestive compartment before delivery to the VAC within 30 min.....	33
Figure 2-6. Peak colocalization with the GalNac-YFP ⁺ CPB/L ⁺ compartment coincides with rapid degradation of ingested material.....	33
Figure 2-7. <i>T. gondii</i> ingests host cytosolic mCherry within 7 min post-invasion.....	34
Figure 2-8. Microneme proteins are expressed in G, S and M/C phase.....	36
Figure 2-9. Rhoptry proteins are expressed in S and M/C phase.....	37
Figure 2-10. <i>T. gondii</i> ingests host cytosolic mCherry throughout its cell cycle.....	39
Figure 2-11. Validation of CHO-K1 imCherry cell line for detection of ingestion.....	41
Figure 2-12. Endocytic trafficking is merged with microneme biogenesis in <i>T. gondii</i>	42
Figure 2-13. Working model for trafficking and sorting of endocytic and exocytic cargoes in <i>T. gondii</i>	46
Figure 3-1. Recap of relevant findings from Chapter 2.....	60

Figure 3-2. Expression of dominant negative, but not wildtype ddGFP-DrpB leads to MIC3 secretion into the PV lumen.....	63
Figure 3-3. DrpB localizes to the TGN and ELCs.....	64
Figure 3-4. Ingested protein colocalizes with DrpB.....	65
Figure 3-5. DrpB is not required for endocytosis of ingested protein.....	67
Figure 3-6. DrpB is not required for trafficking of ingested protein to the VAC.....	69
Figure 4-1. Working model for host protein ingestion and overview of Chapter 4 discussion of ongoing work and future directions.....	83
Figure 4-2. Host ESCRT may contribute to ingestion.....	86
Figure 4-3. Hypothetical models for mechanisms of endocytosis.....	90
Figure 4-4. VSR2 colocalizes with VP1, an ELC marker.....	94

GLOSSARY OF TERMS

AID	auxin-inducible degradation, system in which proteins of interest fused to the auxin-inducible degron peptide are inducibly degraded in response to the plant hormone auxin
Alix	ESCRT-associated protein, binds to YPXL motifs in retroviral Gag proteins, and can link ESCRT-I to ESCRT-III by binding to Tsg101 and CHMP4, respectively
Amphiphysin	N-BAR protein associated with clathrin-mediated endocytosis
ANTH Domain	AP180 N-Terminal Homology Domain, membrane-binding domain associated with clathrin adaptor proteins
AP1	Adaptor complex central to clathrin-coated vesicle formation, links transmembrane cargoes to clathrin coat, required for secretory trafficking to the micronemes and rhoptries from the TGN in <i>Toxoplasma gondii</i>
AP180/CALM	accessory/cargo-specific adaptor for clathrin-mediated endocytosis
AP2	Adaptor complex central to clathrin-mediated endocytosis in mammalian cells, links transmembrane cargoes to clathrin coat
Apicoplast	residual chloroplast-like organelle in <i>Toxoplasma gondii</i>
Arf1	GTPase regulator of exocytic trafficking from the TGN and the CLIC/GEEC endocytic pathway in mammalian cells
ARHGAP10/21	Cdc42 GTPase activating protein associated with CLIC/GEEC
Arp2/3	interacts with N-WASP to promote branched cortical actin polymerization
ARTs	arresting-related-trafficking proteins, thought to act as scaffolds for enveloped virus budding and microvesicle formation at the plasma membrane, binds Nedd4 family ubiquitinases, Alix and Tsg101
Auxilin/GAK	cofactor that binds to clathrin and recruits HSC70 to clathrin-coated vesicles for uncoating
BAR Domain	protein domain that are thought to sense and/or promote membrane curvature, e.g. F-BAR and N-BAR domains
Cen2-EGFP	centrosome protein TgCentrin2, fused to the enhanced green fluorescent protein, EGFP
CHO-K1	Chinese Hamster Ovary cell line

CHO-K1 imCh	Chinese Hamster Ovary cell line with doxycycline-inducible mCherry expression
CHPM4	ESCRTIII component that can be recruited to retroviral budding sites by binding with Alix
Clathrin	coat protein required for clathrin-coated vesicle formation
CLIC/GEEC	endocytic pathway for uptake into GPI-anchored protein enriched early endosomal compartments (GEEC) derived from fusion of uncoated clathrin-independent carriers (CLICs)
Cortactin	target of Pak1 kinase, associates with N-WASP and Arp2/3 to enhance branched cortical actin polymerization
CORVET	class C core vacuole/endosome tethering factor complex, complex for homotypic fusion of Rab5 endosomes in mammalian, yeast and plant cells, made up of Vps3, Vps8, Vps11, Vps16, Vps 18 and Vps33
CPB	cathepsin B, VAC-associated protease
CPL	Cathepsin L, degradative protease localized to the VAC
Cytostome	mouth like structure, site of endocytosis into <i>Plasmodium spp.</i>
dd or ddFKBP	destabilization domain, leads to proteasomal degradation of a protein of interest in the absence of a stabilizing ligand Shield-1
ddGFP-DrpB K72A	dominant-negative DrpB GTPase mutant fused to the green fluorescent protein GFP and the ddFKBP destabilization domain conferring Shield-1-dependent expression
ddGFP-DrpB WT	wildtype DrpB fused to the green fluorescent protein GFP and the ddFKBP destabilization domain conferring Shield-1-dependent expression
DMSO	dimethyl sulfoxide, vehicle control for LHVS
DRP2	plant dynamin-related protein implicated in endocytosis at the plasma membrane, cell plate formation during cytokinesis and post-Golgi trafficking from the TGN and endosomes
DRP3	plant dynamin-related protein that participates in mitochondrial maintenance
DrpA	dynamin-related protein required for maintenance of the apicoplast in <i>Toxoplasma gondii</i>
DrpB	dynamin-related protein required for secretory trafficking to the micronemes and rhoptries from the TGN in <i>Toxoplasma gondii</i>
DrpC	dynamin-related protein of unknown function in <i>Toxoplasma gondii</i>
Dynamin	GTPases that drives vesicle scission and regulated fission and fusion of intracellular organelles, e.g. vps1 in yeast and DrpB in <i>Toxoplasma gondii</i>

ELCs	endosome-like compartments, collectively refers to the Rab5 and Rab7 endosomes in <i>Toxoplasma gondii</i>
Endophilin	N-BAR protein associated with clathrin-mediated endocytosis and FEME
ENTH Domain	Epsin N-terminal Homology Domain, membrane-binding domain associated with clathrin adaptor proteins
EPS15/EPS15R	scaffold protein for clathrin-mediated endocytosis
Epsin	accessory/cargo-specific adaptor for clathrin-mediated endocytosis
ESCRT	Endosomal Sorting Complex Required for Transport, five complexes that are recruited sequentially: ESCRT-0, ESCRT-I, ESCRT-II, ESCRT-III and Vps4, required for budding of vesicles away from the host cell cytosol for intraluminal vesicle formation, enveloped virus budding, and maturation of the TGN into multivesicular endosomes in plants
EtOH	ethanol, vehicle control for Shield-1
F-CHO1/2	F-BAR protein important for nucleation of clathrin-mediated endocytosis
FEME	Fast endophilin-mediated endocytosis, clathrin-independent process
Frm3	formin protein in <i>Toxoplasma gondii</i> , function is unknown, but it capable of polymerizing linear actin filaments <i>in vitro</i>
G phase	growth phase of the cell cycle
GalNac-YFP	UDP-GalNac:polypeptide N-acetylgalactosaminyl-transferase fused to YFP, TGN and ELC marker in <i>Toxoplasma gondii</i>
GAPs	GTPase activating proteins, stimulate GTP hydrolysis activity of GTPase proteins
GEFs	guanine nucleotide exchange factors, stimulate exchange of GDP for GTP for GTPase proteins
GFP	green fluorescent protein
GFP-DrpB	dynamain related protein B fused to GFP, TGN and ELC marker in <i>Toxoplasma gondii</i>
GRA17/GRA23	Components of the hypothetical nutrient pore in the PVM
GRA2	structural component require for biogenesis of the IVN
GRAF1	BAR domain protein and Cdc42 GTPase activating protein associated with CLIC/GEEC
GRAs	proteins contained within and secreted from the parasite's secretory organelles called the dense granules
GRASP55	Cis-medial Golgi marker in <i>Toxoplasma gondii</i>

GTPase	guanine triphosphatase enzyme, active in GTP-bound state, inactive in GDP-bound state
H.O.S.T.s	Host Organelle Sequestering Tubulo-structures, mechanism used by <i>T. gondii</i> to scavenge host cholesterol/lysosomes
HIP1R	accessory adaptor for clathrin-mediated endocytosis, links clathrin coat to actin cytoskeleton
HOPS	homotypic fusion and vacuole protein sorting, complex for endosomal fusion with lysosomes in mammalian, yeast and plant cells Vps39, Vps41, Vps11, Vps16, Vps 18 and Vps33
HSC70	heat shock cognate protein and ATPase that drives uncoating of clathrin-coated vesicles
IMC1	component of the inner membrane complex of <i>Toxoplasma gondii</i> , a system of flattened membranous sacs beneath the parasite plasma membrane
Intersectin 1 and 2	scaffold proteins for clathrin-mediated endocytosis
IVN	intravacuolar network, system of membrane tubules emanating from PVM into the PV lumen
LHVS	morpholinurea-leucine-homophenylalanine-vinyl phenyl sulfone, covalent, irreversible inhibitor of cathepsin L
M/C phase	mitosis and cytokinesis phase of the cell cycle
mCherry	red fluorescent protein
Mgm1	yeast dynamin-related protein that participates in mitochondrial maintenance
MIC3	soluble microneme protein, secreted into the PV lumen in response to DrpB K72A expression
Microneme	regulated secretory organelle of <i>Toxoplasma gondii</i>
Micropore	mouth like structure, hypothetical site of endocytosis into <i>Toxoplasma gondii</i>
N-WASP	complex that interacts with Arp2/3 to promote branched cortical actin polymerization
NHE3	Vacuolar type Na ⁺ /H ⁺ exchanger in <i>Toxoplasma gondii</i>
Pak1	kinase, downstream target of Rac1 GTPase
PI(3,4)P ₂	phosphatidylinositol 3,4 bisphosphate, lipid associated with endocytosis at the plasma membrane
PI3P	phosphitidyl-3-phosphate, lipid typically associated with Rab5 endosomes, or the apicoplast in the case of <i>Toxoplasma gondii</i>
PIP ₂	phosphatidylinositol 4,5 bisphosphate or PI(4,5)P ₂ , lipid associated with plasma membrane and endocytosis

PIP ₃	phosphatidylinositol 3,4,5 triphosphate or PI(3,4,5)P ₃ , lipid associated with plasma membrane and endocytosis
proM2AP	immature form of the microneme protein M2AP with a propeptide
proMIC5	immature form of the microneme protein MIC5 with a propeptide
proRON4	immature form of the rhoptry protein RON4 with a propeptide
PV	parasitophorous vacuole, intracellular compartment where <i>T. gondii</i> replicates within the host cell
PVM	parasitophorous vacuole membrane
Rab5	GTPase regulator of trafficking to and homotypic fusion with the Rab5 endosome in mammalian, yeast and plant cells
Rab7	GTPase regulator of endosomal fusion with lysosomes in mammalian, yeast and plant cells
RBCs	red blood cells
Rho GTPases	family of small GTPases associated with regulation of cytoskeletal elements, e.g. RhoA, Rac1 and Cdc42
Rhoptry	regulated secretory organelle of <i>Toxoplasma gondii</i>
S phase	synthesis phase of the cell cycle
SAG1	major surface antigen of <i>Toxoplasma gondii</i>
SAND1/Mon1-Ccz1	Rab7 GEF, mediates Rab5 to Rab7 switch in mammalian, yeast and plant cells
Sh-1	Shield-1, stabilizing ligand that allows the post-translational stabilization of proteins fused to the ddFKPB or dd destabilization domain
Sortillin	sorting receptor that binds to lysosomal proteins in the lumen of the TGN and escorts them to endosomal compartments for delivery to the lysosome, see TgSORTLR for function in <i>Toxoplasma gondii</i>
TgEpsL	Epsin-like protein associated with AP1 at the TGN in <i>Toxoplasma gondii</i>
TGN	trans-Golgi network
TgPI-1	dense granule protein, constitutively secreted into the PV lumen
TgSORTLR	sortillin, receptor for sorting of micronemes and rhoptry proteins from the TGN to the ELCs in <i>Toxoplasma gondii</i>
TPLATE	plant-specific nucleation complex for clathrin-mediated endocytosis, eight subunit complex
Tsg101	ESCRT-I component, binds to PT/SAP motifs in retroviral Gag proteins

VAC	vacuolar compartment/plant-like vacuole, a lysosome-like organelle in <i>Toxoplasma gondii</i>
Vps1	yeast dynamin-related protein implicated in endocytosis at the plasma membrane, secretory trafficking from the TGN, trafficking from the TGN to the vacuole/lysosome, post-Golgi trafficking from the TGN and endosomes and fission and fusion of lysosomes
Vps4	ATPase and final member of the ESCRT complex, recruited by ESCRT-III complex and mediates recycling of ESCRT complexes back to the cytosol and scission of intraluminal vesicles or enveloped viruses
VSR	vacuolar sorting receptors found in plants (for example BP80), type 1 transmembrane protein with a luminal protease-associated (PA) domain for cargo binding and epidermal growth factor (EGF) domains which may bind calcium, and a short cytoplasmic domain for sorting, escorts cargo from the ER to TGN in plants,
VSR1	plant-like vacuolar sorting receptor of unknown function in <i>Toxoplasma gondii</i>
VSR2	plant-like vacuolar sorting receptor of unknown function in <i>Toxoplasma gondii</i>

ABSTRACT

Host cytosolic proteins are endocytosed by *Toxoplasma gondii* and proteolytically degraded in a Cathepsin L (CPL)-dependent manner in its lysosome-like compartment called the vacuolar compartment/plant-like vacuole (referred to as the VAC). The exact contribution of host protein ingestion to *T. gondii* virulence is unknown, but CPL-dependent protein degradation is important in both acute and chronic stages of infection. Therefore, the host protein ingestion pathway could provide a novel pool of drug targets, however we understand very little about this pathway works, including the route and mechanisms of endocytic trafficking. Plant-like features suggest *T. gondii* endocytic trafficking involves transit through the trans-Golgi network (TGN) and endosome-like compartments (ELCs) en route to the VAC, and conservation of classical endocytic players like clathrin, dynamin, Rab5 and Rab7 suggest endocytic trafficking will resemble model systems. However, trafficking to the parasite's secretory organelles called micronemes and rhoptries proceeds through the TGN and ELCs and requires clathrin, dynamin, and Rab5. Using fluorescence microscopy and colocalization analysis, we show that host cytosolic proteins were endocytosed within 7 min post-invasion, trafficked through ELCs en route to the VAC, and were degraded within 30 min. Ingested protein colocalized with UDP-GalNAc:polypeptide N-acetylgalactosaminyl-transferase fused to YFP (GalNAc-YFP) and the dynamin related protein B fused to GFP (GFP-DrpB), which are typically used as specific markers of the TGN, but these markers labeled both the TGN and ELCs in our hands. Therefore, we could not definitively interpret if ingested protein is trafficked through the TGN. Ingested host proteins also colocalized with immature microneme proteins, proM2AP and proMIC5 but not the immature rhoptry protein proRON4, indicating that endocytic trafficking of ingested protein intersects with exocytic trafficking of microneme proteins. Further, sorting mechanisms will be required to ensure ingested proteins are destroyed in the VAC and microneme proteins arrive intact to the microneme organelles. Finally, conditional expression of a dominant-negative

mutant of DrpB did not inhibit uptake or delivery of ingested host proteins to the VAC, indicating that DrpB is not required for *T. gondii* endocytosis. This work sheds light on the underlying mechanisms of *T. gondii* endocytosis, but much is left to be discovered. Future studies will investigate the role of other proteins classically involved in endocytosis and will aim to discover parasite specific proteins involved in this process.

Chapter I

Introduction

1.1 Introduction to *Toxoplasma gondii* and toxoplasmosis

Apicomplexa is a phylum of single-celled, eukaryotic, obligate intracellular parasites that contains two of the most successful pathogens on the planet, *Toxoplasma gondii* and *Plasmodium spp.* *Plasmodium spp.* caused 216 million cases of malaria and 445,000 deaths worldwide in 2016 alone.¹ *T. gondii*, while not as notorious in the public's eye, has an incredible host range. This parasite is thought to infect any nucleated cell in warm-blooded animals from the land, air and sea.²⁻⁴ Initially, *T. gondii* rapidly disseminates to establish a systemic acute infection before differentiating into slow growing tissue cysts that are thought to persist for the lifetime of the host.⁵ Vertical transmission can occur with acute infection during pregnancy and lead to miscarriage.^{6, 7} Reactivation of chronic tissue cysts in immunocompromised or congenitally infected individuals can result in seizures, encephalitis, cognitive deficits, blindness and death.^{6, 7} Currently, 6.7% of individuals in the United States and 2 billion people worldwide are chronically infected with *T. gondii* and susceptible to reactivated infection.^{8, 9} There is no cure for chronic toxoplasmosis, and acute toxoplasmosis requires prolonged treatment that is often poorly tolerated.¹⁰ Thus, it is imperative to better understand the fundamental aspects of infection in order to identify better treatment options and to minimize the burden of toxoplasmosis.

The focus of this dissertation is an endocytic pathway in which *T. gondii* ingests proteins from the cytosol of the cell it infects, and degrades them in a cathepsin L (CPL)-dependent manner.¹¹ In acute stage parasites lacking CPL, the ability to degrade proteins from the host cell is greatly inhibited, parasite growth is inhibited by 30% *in vitro*, and virulence is reduced fifty-fold *in vivo*.¹¹ In the chronic stage, CPL-deficient parasites accumulate autophagic vesicles, die *in vitro*, and have severely reduced cyst burden *in vivo*.¹² Ongoing studies are working to determine whether chronic stage parasites also

undergo endocytosis from the host cell. Although, the exact contribution of host protein ingestion to virulence is not known, because CPL is important for degradation of proteins acquired from the host cell and parasite-derived proteins, these virulence defects suggest breakdown of endocytic material could be important to the parasite. Yet we understand very little about *T. gondii* endocytosis including its underlying mechanisms and exact contribution to virulence. An analogous endocytic pathway for ingestion of host cytosol in *Plasmodium spp.* is essential for amino acid scavenging, and targeting this pathway has been a successful therapeutic strategy.¹³⁻¹⁵ However, this pathway is also poorly understood. Therefore, studying the *T. gondii* ingestion pathway in the acute stage, which is the focus of this thesis, could be valuable for several reasons. First, there is potential for future discovery of novel therapeutic targets against acute and chronic toxoplasmosis. Second, acute stage host protein ingestion in *T. gondii* could serve as a model for understanding the enigmatic biology of chronic stage *T. gondii* infection and for understanding host protein ingestion in *Plasmodium spp.* To begin understanding the ingestion pathway in *T. gondii*, we can look to characterized mechanisms of endocytosis in model systems such as yeast, mammalian and plant cells and to host protein ingestion by *Plasmodium spp.* In this introductory chapter, these points will be discussed along with what is known about endocytic and exocytic trafficking within *T. gondii*. From this, hypothetical models for endocytic trafficking in *T. gondii* will be built to serve as a framework for work performed for this dissertation.

1.2 *T. gondii* ingests host protein from within a parasitophorous vacuole

As an obligate intracellular parasite, *T. gondii* survival revolves around establishing a favorable niche for replication and survival within host cells. For *T. gondii*, this niche is the parasitophorous vacuole (PV), and its formation is coupled to parasite invasion of host cells (Figure 1-1). During *T. gondii* invasion, the host plasma membrane is pushed in toward the cytosol and pinched off once invasion is complete. This cloak of host-derived membrane provides a protective barrier that resists fusion with host lysosomes and prevents autophagic destruction of the parasite.¹⁶⁻¹⁹ However, the PV also represents a barrier to accessing nutrients in the host cell cytosol for which it is auxotrophic, including amino acids like tryptophan, arginine and tyrosine.^{20, 21} Constitutive secretion of parasite

proteins from secretory organelles called dense granules (GRAs) into the PV lumen helps overcome this barrier as shown in Figure 1-1. A hypothetical nutrient pore made up of GRA17 and GRA23 is inserted into the PV membrane (PVM) and allows diffusion of molecules with molecular weights less than 1.3 kilodaltons (e.g. sugars, amino acids and nucleotides)^{22, 23}, which could be taken up by transporters at the parasite plasma membrane²⁴⁻²⁸. GRA2, 4 and 6 promote formation of a system of membrane tubules invaginated from the PVM called the intravacuolar network (IVN), which is thought to act like intestinal villi, increasing surface area of the PVM for maximum nutrient exchange.²⁹⁻
³¹ Finally, GRA7 has been implicated in scavenging cholesterol from the host cell via structures called Host Organelle Sequestering Tubulo-structures (H.O.S.T.s). In H.O.S.T.s, host lysosomes are recruited to the PV on microtubules, engulfed in PV membrane invaginations and pinched off, presumably by GRA7, to form lysosome-containing vesicles in the PV lumen.³²

In *T. gondii* ingestion, host cytosol is taken up into the parasite and trafficked to the parasite's lysosome-like compartment called the vacuolar compartment/plant-like vacuole (hereafter referred to as the VAC) where they are degraded.¹¹ To track this process, fluorescent proteins like the green fluorescent protein, GFP, or the red fluorescent protein, mCherry, are expressed in the host cytosol as non-specific tracers that can be visualized by microscopy. GFP and mCherry (molecular weights of 27.0 and 28.8 kilodaltons) are too large to diffuse through the GRA17/GRA23 pore. Therefore, *T. gondii* does not have direct access to the host cytosolic proteins it consumes in the ingestion pathway, and ingestion of host protein will require active transport across both the PVM and the parasite plasma membrane in order to reach the VAC. Host protein ingestion is not affected by loss of GRA7, but the ability of *T. gondii* to ingest host proteins is reduced by 40% in parasites lacking GRA2.¹¹ This precludes a H.O.S.T.-like mechanism and suggests the IVN contributes to host protein ingestion. In addition to its suggested role in nutrient exchange, the IVN also acts as a structural component to organize replicated parasites into a characteristic rosette pattern within the PV.³³ Since the role of GRA2 was determine in mature replicated vacuoles, the IVN could contribute directly through ingestion of IVN tubules or IVN-derived vesicles (Figure 1-1) or indirectly via organization of parasites within the PV. Beyond this, the mechanisms for trafficking

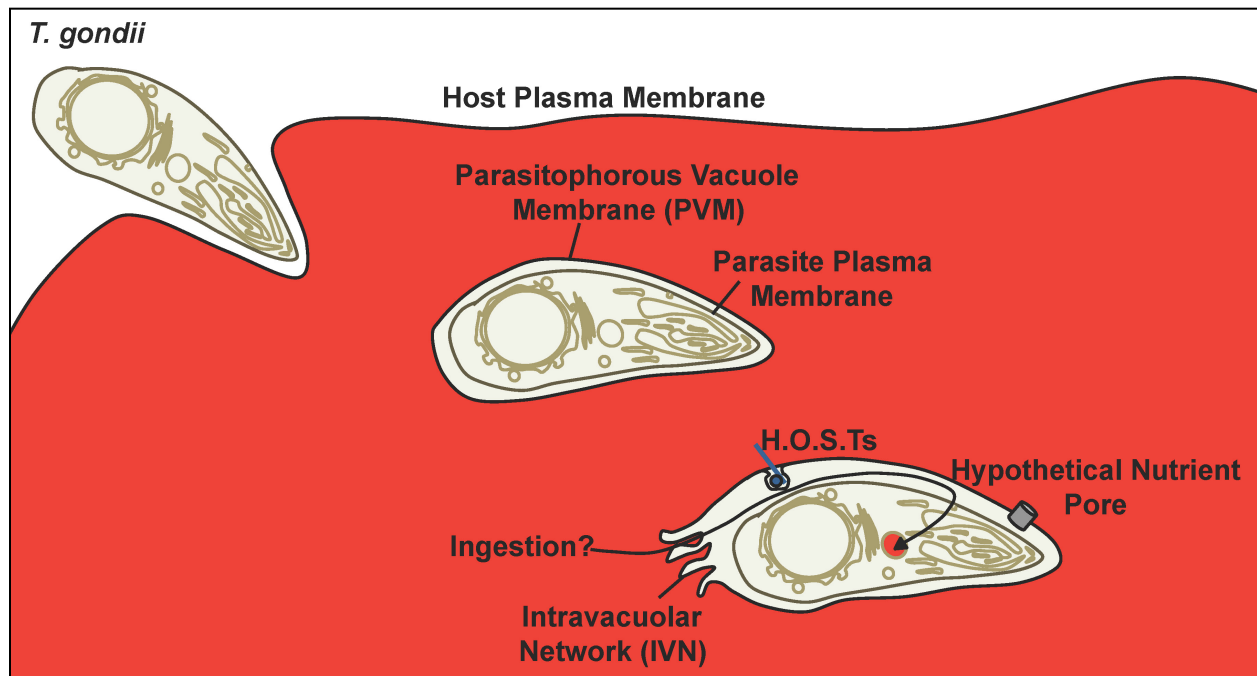


Figure 1-1. The intracellular niche of *T. gondii*. *Toxoplasma gondii* forms a parasitophorous vacuole (PV) as it invades host cells. Trafficking across the PV membrane may include a hypothetical nutrient pore (GRA17/GRA23: grey cylinder), a system of membrane tubules invaginated from the PV membrane called the intravacuolar network (driven by GRA2, 4 and 6), or an active trafficking pathway for acquiring cholesterol in LDL particles (blue circle) from the host cell with the help of microtubules (blue line) called H.O.S.T.s (associated with GRA7). Ingested protein substrates cannot diffuse across the hypothetical nutrient pore. Ingestion does require GRA2 but not GRA7, suggesting ingested protein trafficking across the PVM could occur via the IVN as indicated by the arrow from the host cell to the interior of the parasite.

across the PVM and parasite plasma membrane, and the path and mechanisms of endocytic trafficking to the VAC are not known. Most simply, *T. gondii* endocytosis can be broken down into two steps. First, material from the host cell cytosol is taken up across the PVM and parasite plasma membrane into endocytic vesicles in the parasite cytoplasm. Second, these endocytic cargoes are delivered to the VAC for degradation. To begin understanding how *T. gondii* endocytosis works, we can look to model systems such as yeast, mammals and plants.

1.3 Mechanisms of endocytosis at the plasma membrane in model organisms

In this section, characterized mechanisms for generating endocytic vesicles at the plasma membrane in model systems will be described. It should be noted that in these model systems, the cell has direct access to endocytic cargoes and the plasma membrane is the only membrane barrier to overcome. *T. gondii*, on the other hand, must endocytose material across both the PVM and the parasite plasma membrane. This is an

important consideration that will be discussed later in the context of the parasite. Endocytosis involves bending of the plasma membrane in toward the cytosol and scission of the plasma membrane to form endocytic vesicles. Mechanisms underlying this process will be divided into three categories, clathrin-dependent, clathrin-independent/dynamin-dependent, and clathrin and dynamin-independent, and are depicted in Figure 1-2.

There are two forms of endocytosis that require characteristic coats visible by electron microscopy, clathrin-mediated endocytosis and caveolar endocytosis. *T. gondii* does not express caveolin/cavin proteins required for caveolar endocytosis and thus this mechanism will not be further discussed.³⁴ In mammalian cells, clathrin-mediated endocytosis facilitates internalization of transmembrane receptors. First, a nucleation complex is formed. F-BAR domain proteins FCHO1/2 and the clathrin adaptor complex for endocytosis AP2 bind to phosphatidylinositol 4,5 bisphosphate (PI(4,5)P₂ or PIP₂) at the plasma membrane and recruit scaffolding proteins EPS15, EPS15R and intersectin 1 and 2, which cluster together to nucleate clathrin-mediated endocytosis.^{35, 36} AP2 serves as a major hub that binds to cytosolic domains of transmembrane cargoes and recruits accessory adaptors like AP180/CALM, epsins and HIP1R, which can also bind to specific transmembrane cargoes.^{35, 36} AP2 together with the accessory adaptors then recruit clathrin to form the clathrin coat.^{35, 36} Membrane bending is progressively promoted by BAR domains in FCHO1/2, insertion of amphipathic helices in membrane-binding ENTH (Epsin N-Terminal Homology Domain) and ANTH (AP180 N-Terminal Homology Domain) domains of epsin and CALM, respectively, and polymerization of a curved clathrin lattice that encases the forming vesicle which may drive and/or stabilize membrane curvature.^{35, 36} The actin nucleation and branching-promoting proteins N-WASP and Arp2/3 are then recruited and drive polymerization of actin coupled to the clathrin coat through interactions with epsin and HIP1R. This is thought to push against the plasma membrane, elongating the neck of the forming vesicle and further promoting membrane bending through tensile pressure.^{35, 37, 38} Vesicle scission is mediated by recruitment of the N-BAR proteins endophilin and amphiphysin which are thought to restrict the vesicle neck and also recruit the GTPase dynamin.^{35, 39} Dynamin forms a coil around the neck of budding vesicle and hydrolyzes GTP to drive membrane scission.⁴⁰ Finally, the vesicle is uncoated and

clathrin coat components are recycled back to the cytosol by the heat shock cognate protein HSC70 and its cofactor auxillin/GAK.^{35, 36}

Clathrin-mediated endocytosis in yeast largely resembles mechanisms in mammalian cells.⁴¹ However, the exact role of dynamin in yeast endocytosis is controversial. Dynamin is thought to act as a “pinchase” that forms a coil around vesicle necks and hydrolyzes GTP to squeeze and sever the membrane to form endocytic vesicles.⁴² A recent study showed that the dynamin-related protein vps1 is recruited to sites of clathrin-mediated endocytosis at the plasma membrane, a dominant-negative vps1 mutant severely inhibits endocytosis, and is able to tubulate liposomes *in vitro* indicating vps1 can likely directly contribute to membrane bending.⁴³ However, 22% of clathrin-mediated endocytic sites lack vps1, and other studies suggest that the role of dynamin in membrane scission is indirect through its role in actin organization.⁴³⁻⁴⁵ Membrane scission in this case is thought to be driven by concerted action of actin and BAR-domain proteins like amphiphysin.^{41, 43, 44, 46} Nevertheless, vps1 is required for efficient scission of endocytic vesicles in yeast. Additionally, AP2 seems to play a less central role in yeast. Whereas knockout of AP2 in mice is lethal and knockdown in mammalian cells leads to greater than 90% block in clathrin-mediated endocytosis, AP2 knockouts in yeast are viable and its only demonstrated role in clathrin-mediated endocytosis is for uptake of the yeast toxin K28.^{36, 47-49}

Plants also undergo clathrin-mediated endocytosis, but AP2 is also not essential and FCHO1/2 homologs have not been identified.⁵⁰ Instead, an ancestral nucleation complex called TPLATE seems to be more central to plant endocytosis. The TPLATE complex has protein-protein interaction domains found in the scaffold proteins EPS15 and intersectin1 and 2, interacts with AP2, two ANTH domain-containing adaptor proteins, clathrin, and dynamin.⁵⁰

Clathrin-independent endocytosis is generally less understood and has been characterized mostly in mammalian cells. These pathways are diverse but are united by their requirement of actin polymerization and regulation by GTPase proteins RhoA, Rac1, and Cdc42. These GTPases cycle between active GTP-bound and inactive GDP-bound states that are regulated by GTPase activating proteins (GAPs), which stimulate GTP

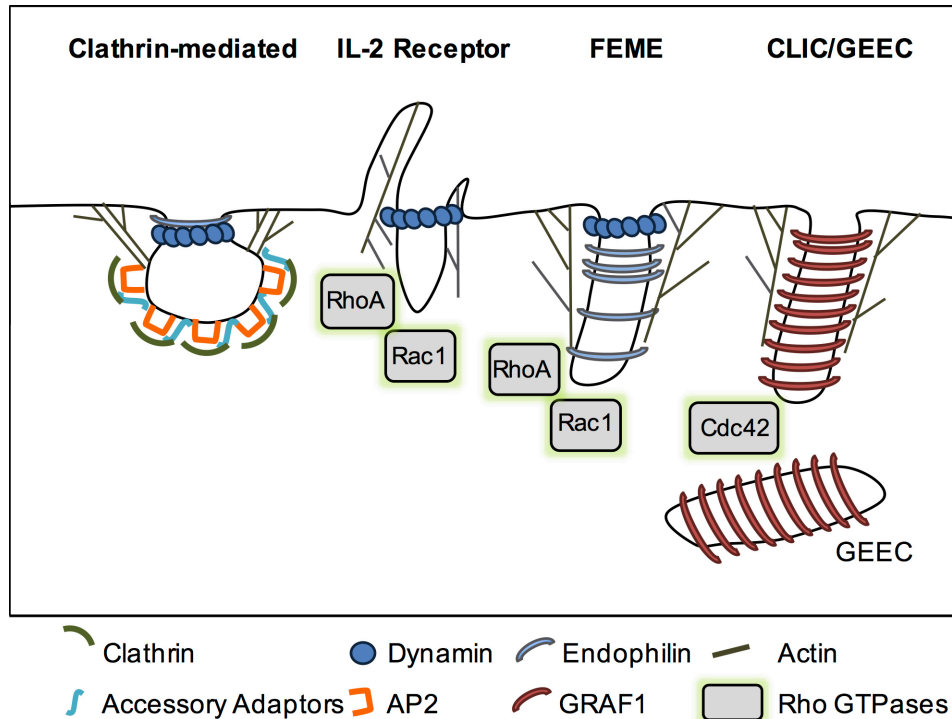


Figure 1-2. Mechanisms of endocytosis in model systems. Note that these models are simplified from the text to depict key differentiating features of each pathway. See text for full description of endocytic mechanisms. Fast endophilin-mediated endocytosis (FEME), clathrin-independent carriers/ GPI-anchored protein enriched early endosomal compartments (CLIC/GEEC).

hydrolysis, and guanine nucleotide exchange factors (GEFs), which exchange GDP for GTP.⁵¹ The pathways described below are not exhaustive in terms of clathrin-independent mechanisms of endocytosis, but are representative examples to illustrate the key role of actin in clathrin-independent endocytosis.

Clathrin-independent endocytosis may require dynamin. For example, the IL-2 (interleukin 2) receptor endocytosis pathway is dynamin-dependent and requires activation of RhoA and local production of phosphatidylinositol 3,4,5 triphosphate (PI(3,4,5)P₃ or PIP₃) to the recruit and activate Rac1.^{46, 52, 53} WIRS motifs in the IL-2 receptor recruit the WAVE complex, and activated Rac1 recruits the N-WASP complex, which leads to recruitment of Arp2/3 to stimulate actin filament nucleation and branching. Rac1 also activates its target kinase Pak1 to phosphorylate cortactin, which also associates with N-WASP to enhance actin polymerization.^{46, 52} Fast endophilin-mediated endocytosis (FEME) mediates endocytosis of transmembrane proteins like activated G-protein coupled receptors. In FEME the protein lamellipodin binds to phosphatidylinositol 3,4 bisphosphate (PI(3,4)P₂) in the plasma membrane, and recruits the N-BAR protein

endophilin. Endophilin is thought to induce membrane curvature itself and recruits N-WASP, Arp2/3, and dynamin to drive actin polymerization and endocytic vesicle formation.⁵² This process is regulated by Rac1, RhoA and Pak1, which also likely mediate N-WASP and Arp 2/3 recruitment.⁵⁴

Other clathrin-independent mechanisms are dynamin-independent, like CLIC/GEEC, which can mediate uptake of GPI-anchored proteins, transmembrane proteins and bulk uptake of fluid-phase markers into GPI-anchored protein enriched early endosomal compartments (GEEC) derived from fusion of uncoated clathrin-independent carriers (CLICs).^{55, 56} In CLIC/GEEC, cycling of Cdc42 activity is required for productive endocytosis. Both Cdc42 activation and inactivation are required for productive actin polymerization, and the small GTPase Arf1 recruits the Cdc42 GAP protein ARHGAP10/21 to mediate Cdc42 inactivation.^{46, 52} Activated Cdc42 also recruits the GAP GRAF1, which regulates Cdc42 and also has a BAR domain that is thought to contribute to membrane curvature and work together with forces generated by actin polymerization to drive membrane fission.^{46, 52, 57}

1.4 Endocytic trafficking across the *T. gondii* PVM and plasma membrane

How endocytosis across both the PVM and parasite plasma membrane is accomplished has not been determined in *T. gondii*, but the related *Plasmodium spp.* parasites provide some insight into how this may occur. *Plasmodium spp.* parasites also replicate in a PV in red blood cells (RBCs) and consume RBC cytosol from within this niche. Electron microscopy studies show RBC cytosol is taken up across the PVM and parasite plasma membrane simultaneously. The PVM extends inward toward a mouth-like structure at the parasite plasma membrane called the cytostome, and both membranes are pinched off into the parasite cytoplasm resulting in RBC cytosol encased in two layers of membrane derived from parasite plasma membrane and PVM.^{58, 59} *T. gondii* has an analogous mouth-like structure called the micropore that is proposed to be a site of endocytosis. Electron microscopy studies show vesicles in the parasite cytoplasm near the micropore that appear to contain material from the PV lumen, and consistent with a *Plasmodium*-like model of endocytosis, vesicle-like structures sometimes occupy the micropore.⁶⁰ A few things should be noted about these

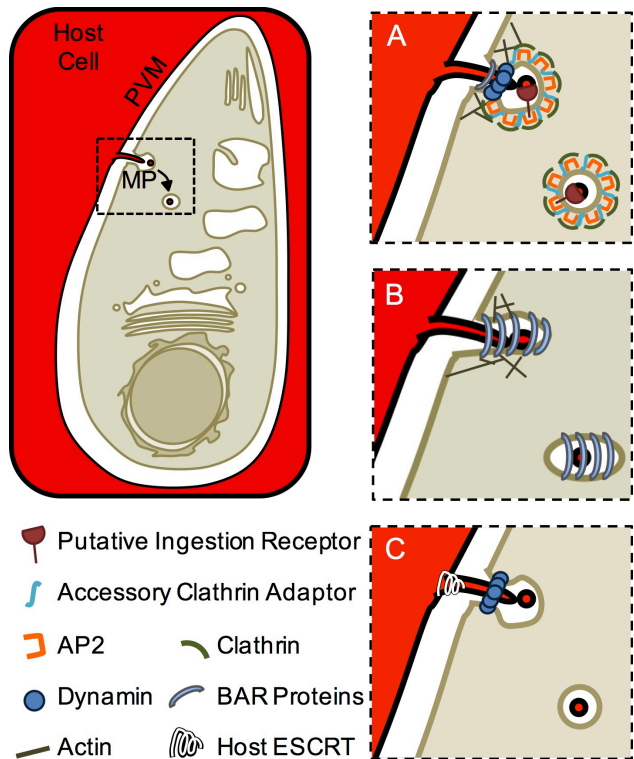


Figure 1-3. Hypothetical models for ingestion across the PVM and parasite plasma membrane.

Ingested proteins are proposed to be taken up across PVM and parasite plasma membrane is proposed to occur at the micropore into double membrane vesicles as in *Plasmodium spp.* Mechanisms could resemble model systems and depend on coats, dynamin, and actin. Examples of **A** clathrin-mediated or **B** clathrin-independent processes, represented by CLIC-GEEC are depicted. **C**. Scission of endocytic vesicles may also require host proteins for pinching of the PVM as depicted by possible recruitment of host ESCRT machinery.

observations. First, it is impossible to say if these are free vesicles or if the membranes are continuous with the PVM, as described for *Plasmodium spp.*, without serial sectioning. Second, electron microscopy studies provide a single snapshot in time, so whether these vesicle-like structures are there by coincidence or being trafficked in or out of the parasite cannot be concluded. Finally, micropores are present in acute and chronic stages of infection, but micropores occupied by vesicles have only been observed in the chronic cyst stage. Nevertheless, based on *Plasmodium spp.*

RBC ingestion and requirement of GRA2, our hypothetical model of acute stage host protein ingestion is that host proteins are ingested by endocytosis of IVN tubules or IVN-derived vesicles at the micropore (Figure 1-3). If IVN tubules or IVN-derived vesicles are ingested, then integral or

peripheral membrane proteins exposed on the luminal face of the PVM could mediate interactions with receptors on the parasite surface. Therefore, uptake across the parasite plasma membrane could be receptor-mediated (Figure 1-3A).

Electron microscopy also shows that the micropore sometimes appears bare and other times appears to have a proteinaceous coat.⁶⁰ This suggests that both coat-dependent and coat-independent mechanisms of endocytosis may occur (Figure 1-3A and B), and since *T. gondii* does not express caveolin or cavin, the coat is most likely clathrin.³⁴ Conservation of classical endocytic players like clathrin, dynamin-related proteins, epsin-like proteins, and actin suggest that *T. gondii* endocytosis may resemble model systems. However, clathrin, actin, the dynamin-related proteins DrpA and DrpB,

and the epsin-like protein TgEpsL have not been localized to the plasma membrane and have characterized roles in parasite motility (actin), maintenance of a chloroplast-like organelle called the apicoplast (DrpA), or exocytic trafficking to the parasite's unique secretory organelles called micronemes and rhoptries (clathrin, DrpB and TgEpsL, discussed further in Section 1.6).⁶¹⁻⁶⁶ Small, transient populations at the plasma membrane could be overlooked like the yeast dynamin-related protein Vps1. Vps1 predominantly localizes to internal organelles like the trans-Golgi network (TGN), and localization to endocytic sites at the plasma membrane only became apparent with the use of specialized microscopic methods for isolated imaging of the plasma membrane like total internal reflection fluorescence microscopy.⁴³ Further, the roles for these proteins mentioned above in endocytosis have not been tested, and other potential mediators of endocytosis such as AP2 or BAR-domain containing proteins have not been studied.

Finally, trafficking endocytosed material across both the PVM and parasite plasma membrane may require added machinery (Figure 1-3C). For example, dynamin and actin are required for RBC endocytosis in *Plasmodium spp.*, but it is not known if they are sufficient for pinching off both the parasite plasma membrane and the PVM.⁶⁷ Additional parasite proteins in the PV lumen could orchestrate pinching off of the PVM, or host proteins may be hijacked to perform this function. The host Endosomal Sorting Complex Required for Transport (ESCRT) complex is a rational candidate for this job. ESCRT normally drives budding of vesicles away from the host cell cytoplasm and into the lumen of endosomes in the host cell, and is hijacked by retroviruses like HIV for budding from the plasma membrane.^{68, 69} Host ESCRT could be recruited to the PVM to perform a similar function and bud vesicles into the PV lumen.

1.5 Endocytic trafficking to the lysosome in model organisms

Once host cytosol has been internalized into endocytic vesicles in *T. gondii*, it will next be transported to the lysosome-like VAC. In yeast and mammals, endocytosed cargoes, whether they are derived from clathrin-mediated or clathrin-independent endocytosis, are trafficked sequentially through the Rab5 endosome, Rab7 endosome and then the lysosome.^{46, 70} These trafficking events are coordinated by the Rab GTPases Rab5 and Rab7, which mediate endosome maturation and fusion with the lysosome.

Rab5 activity is maintained by its GEF, RABGEF1/Rabex5, and recruits the class C core vacuole/endosome tethering factor (CORVET) complex, which drives homotypic fusion with other Rab5 endosomes.⁷⁰⁻⁷³ Rab5 also recruits the phosphatidylinositol-3-kinase (PI3K) to generate phosphatidylinositol-3-phosphate (PI3P), which mediates recruitment of ESCRT.^{70, 74} Endocytosed solutes and ligands released from their receptors already occupy the lumen of the endosome to be sent to the lysosome, but ESCRT is required to target transmembrane proteins for lysosomal degradation through budding of intraluminal vesicles away from the cytosol and into the lumen of Rab5 and Rab7 endosomes. PI3P along with RABGEF1/Rabex5 also recruits the Rab7 GEF, SAND1/Mon1-Ccz1, mediating endosome maturation via a Rab5/Rab7 switch. SAND1/Mon1-Ccz1 dissociates RABGEF1/Rabex5, leading to loss of Rab5 and recruitment of Rab7.^{75, 76} Finally, CORVET (composed of VPS3, 8, 11, 16, 18, and 33) is converted to form the homotypic fusion and vacuole protein sorting (HOPS) complex, which mediates fusion with the lysosome.^{75, 76} CORVET and HOPS share four core proteins (VPS11, 16, 18 and 33) that are retained in the switch, while VPS3 and 8 are switched out for VPS39 and 41.⁷⁷

The mechanisms that govern endocytic trafficking in plants are less well-understood, but there are clear differences from yeast and mammals. First, plants deliver endocytosed cargoes initially to the TGN before trafficking through the Rab5 endosome, Rab7 endosome and finally to the lysosome.^{50, 78, 79} The Rab5 endosomes are

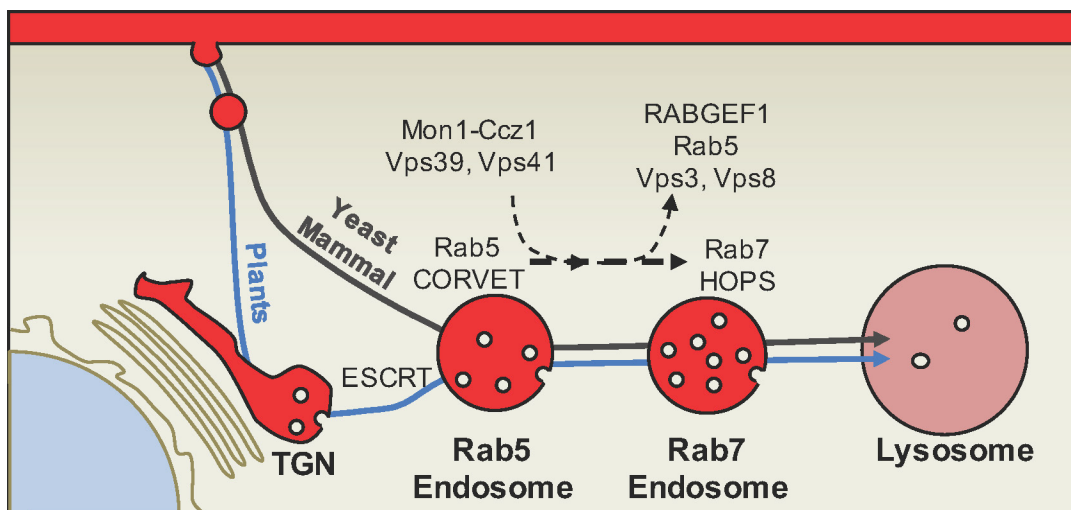


Figure 1-4. Model for path and mechanisms of endocytic trafficking in plants (blue line) and yeast/mammals (dark grey line).

multivesicular compartments derived by ESCRT-dependent maturation of the TGN (Figure 1-4).⁸⁰ Plants also have a homologous SAND1/Mon1-Ccz1 complex that acts as a Rab7 GEF and mediates conversion from Rab5 to Rab7 on its endosomes.^{81, 82} Homologs of HOPS and CORVET are also present in plants.⁸³ However, the function of CORVET has not been studied, and the existence of a HOPS complex is inferred from studies of VPS16 and VPS41. VPS16 regulates biogenesis and fusion with the lysosome and interacts with two more putative HOPS complex members VPS11 and VPS33 at late endosomal and lysosomal membranes.⁸⁴⁻⁸⁶ Vps41 also localizes to the late endosomal and lysosome membranes, interacts with Rab7, and is important for lysosomal fusion.⁸⁷

1.6 Trafficking to the *T. gondii* VAC through a plant-like exocytic system?

Toxoplasma has a conserved basic endomembrane structure including a TGN, endosome-like compartments (ELCs) marked by Rab5 and Rab7, and a lysosome-like VAC. *T. gondii* also belongs to the phylum Apicomplexa, which has evolutionary origins that are thought to predate the split between plants and animals and share features of both.⁸⁸ In relation to plants in particular, *T. gondii* possesses a plant-specific vacuolar pyrophosphatase proton pump and an aquaporin in the VAC and a plant-specific Rab5 isoform.^{89, 90} *T. gondii* expresses three Rab5 isoforms, Rab5A, Rab5B and Rab5C. Rab5A and Rab5C resembles conventional Rab5 and are C-terminally geranylated while Rab5B is N-terminally myristoylated like the plant-specific Rab5 isoform Ara6.^{90, 91} This suggests endocytic trafficking in *T. gondii* most likely resembles plants, and endocytosed material would be delivered initially to the TGN, then to Rab5 and Rab7-marked ELCs, and finally to the VAC (Figure 1-5A). Alternatively, endocytic trafficking could resemble yeast and mammals, despite other plant-like features, and deliver endocytosed material initially to the ELCs before reaching the VAC (Figure 1-5B). Conservation of Rab5, Rab7, and the HOPS complex suggest mechanisms of endocytic trafficking likely resemble those of model organisms.

However, the *T. gondii* endocytic system was thought to be adapted specifically for exocytic trafficking for secretion. Apicomplexa are named for the unique organelles found at their apical end called micronemes and rhoptries (Figure 1-5). Micronemes and rhoptries are regulated secretory organelles that are normally secreted only during

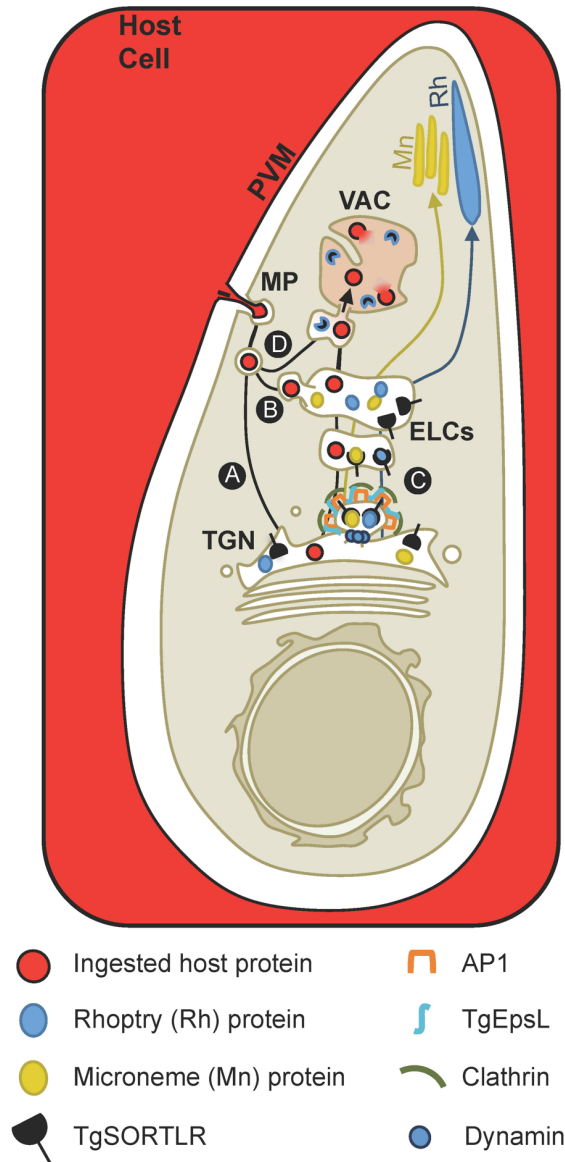


Figure 1-5. Hypothetical model for trafficking to the VAC. Endocytic trafficking (black lines) may proceed through **A** a plant-like or **B** a yeast/mammal-like endocytic system, which has the potential to intersect with **C** exocytic trafficking (yellow to micronemes and blue like to rhoptries) to the micronemes and rhoptries. TgSORTLR, clathrin, dynamin (DrpB), AP1 and TgEPsL mediate sorting of microneme and rhoptry proteins at the TGN, but sorting from the ELCs is undefined. Alternatively, endocytic trafficking may go directly to the VAC **D** as proposed in one emerging model for *Plasmodium spp.* ingestion of RBC cytoplasm.

invasion and egress, and they mediate parasite motility, host cell attachment, invasion, defense against host immune attack, and pore-formation and host cell lysis during host cell egress.^{63, 92-101} Trafficking to the micronemes and rhoptries proceeds through the TGN and ELCs (Figure 1-5C), and requires clathrin, DrpB, Rab5A, Rab5C, the Rab5A GEF Vps9, and the HOPS complex. Interference with the function of any of these proteins is lethal and leads to aberrant secretion of microneme and rhoptry proteins into the PV lumen presumably through rerouting to the dense granule constitutive secretion pathway.^{61, 66, 90, 102-105} However, whether the *T. gondii* endolysosomal system is also used for endocytic trafficking to the VAC, and whether any of these proteins contribute to endocytic trafficking in *T. gondii* is not known.

The potential for mixing of endocytic and exocytic cargoes poses an interesting problem given that endocytosed host protein is delivered to the VAC for degradation, and microneme and rhoptry proteins must be delivered to their respective organelles in order to coordinate parasite invasion, egress and defense against host immune attack.^{63, 92-}

¹⁰¹ Emerging models of endocytosis in

Plasmodium spp. offer two possible ways for these cargoes to avoid interaction altogether. *Plasmodium spp.* also make microneme and rhoptry organelles, and the path

of endocytic trafficking to its lysosome is not known. However, ingestion of RBC cytosol and biogenesis of microneme organelles occur at different times during the cell cycle.¹⁰⁶⁻¹¹⁰ So even if these cargoes traverse the same endolysosomal compartments, they never do so at the same time. In this case, mechanisms for trafficking to the micronemes versus the lysosome may be switched on or off at exclusive times during the cell cycle. Alternatively, one model of RBC endocytosis predicts that endocytic vesicles generated from the cytostome fuse directly with the lysosome, avoiding the endosomal compartments altogether (Figure 1-5D).¹¹¹

If endocytic and exocytic trafficking do intersect in the TGN or ELCs, sorting will be required. Microneme and rhoptry protein sorting is partially understood (Figure 1-5C). The sorting receptor sortillin (TgSORTLR) binds to soluble microneme and rhoptry proteins in the TGN, and the clathrin adaptor protein complex AP1 is thought to recognize the cytoplasmic portion of TgSORTLR or transmembrane microneme and rhoptry proteins.^{66, 112} AP1 also interacts with the epsin-like protein TgEpsL, and together they are thought to recruit clathrin for sorting from TGN to the ELCs via clathrin-coated vesicles that are pinched off by DrpB.^{64, 66} How the microneme and rhoptry proteins are sorted from ELCs is unknown. Host-protein-containing vesicles may be sorted in a similar manner using sorting receptors that recognize parasite proteins embedded in the PVM-derived vesicle membrane. Alternatively, the endocytosed vesicles could behave like soluble cargo that lack receptors or sorting signals, which are by default delivered to the lysosome for degradation via a bulk flow pathway, which even occurs for endocytosed red fluorescent protein, RFP, delivered to the TGN in plants.^{70, 113, 114} Therefore, determining the path that ingested proteins take to reach the VAC and when the parasite is actively ingesting host proteins compared to biogenesis of microneme and rhoptry organelles will have important implications for regulation of the endolysosomal system in *T. gondii*.

1.7 Summary and chapter outline

Our current hypothetical model predicts that ingested host proteins are taken across the PVM and parasite plasma membrane at the micropore into double membrane vesicles in the host cell cytoplasm, like in *Plasmodium spp.* Based on plant-like features,

we favor a model where these vesicles are then trafficked through a plant-like endocytic system, proceeding sequentially through the TGN, ELCs and VAC. However, how and when ingested proteins are delivered to the VAC for degradation remains undefined. This dissertation addresses these aspects of *T. gondii* endocytosis and is split into two parts. Chapter 2 includes an observational study that explores two phenomena: the path of endocytic trafficking to the VAC and the spatiotemporal relationship between endocytic trafficking to the VAC and exocytic trafficking to micronemes and rhoptries. Chapter 3 is a functional study exploring the role of DrpB in *T. gondii* endocytosis. Finally, Chapter 4 will include a summary of findings from Chapters 2 and 3 as well as a discussion of ongoing efforts and projected future directions for this body of work.

1.8 References

1. WHO . World malaria report 2017. *World Health Organization, Geneva*. 2017.
2. Gibson AK, Raverty S, Lambourn DM, Huggins J, Magargal SL, Grigg ME. Polyparasitism is associated with increased disease severity in *Toxoplasma gondii*-infected marine sentinel species. *PLoS Negl Trop Dis*. 2011;5(5):e11142. doi: 10.1371/journal.pntd.0001142 [doi].
3. Guo M, Mishra A, Buchanan RL, et al. A Systematic Meta-Analysis of *Toxoplasma gondii* Prevalence in Food Animals in the United States. *Foodborne Pathog Dis*. 2016;13(3):109-118. doi: 10.1089/fpd.2015.2070 [doi].
4. Dubey JP. A review of toxoplasmosis in wild birds. *Vet Parasitol*. 2002;106(2):121-53.
5. Montoya JG, Liesenfeld O. Toxoplasmosis. *Lancet*. 2004;363(9425):1965-1976. doi: 10.1016/S0140-6736(04)16412-X.
6. Montoya J, Giraldo L, Efron B, et al. Infectious complications among 620 consecutive heart transplant patients at Stanford University Medical Center. *Clin Infect Dis*. 2001;33:629-640.
7. Hoffmann S, Batz MB, Morris JG, Jr. Annual cost of illness and quality-adjusted life year losses in the United States due to 14 foodborne pathogens. *J Food Prot*. 2012;75(7):1292-1302. doi: 10.4315/0362-028X.JFP-11-417 [doi].
8. Pappas G, Roussos N, Falagas ME. Toxoplasmosis snapshots: global status of *Toxoplasma gondii* seroprevalence and implications for pregnancy and congenital

- toxoplasmosis. *Int J Parasitol.* 2009;39(12):1385-1394. doi: 10.1016/j.ijpara.2009.04.003 [doi].
9. Jones JL, Kruszon-Moran D, Rivera HN, Price C, Wilkins PP. *Toxoplasma gondii* seroprevalence in the United States 2009-2010 and comparison with the past two decades. *Am J Trop Med Hyg.* 2014;90(6):1135-1139. doi: 10.4269/ajtmh.14-0013 [doi].
 10. Alday PH, Doggett JS. Drugs in development for toxoplasmosis: advances, challenges, and current status. *Drug Des Devel Ther.* 2017;11:273-293. doi: 10.2147/DDDT.S60973 [doi].
 11. Dou Z, McGovern O, Di Cristina M, Carruthers V. *Toxoplasma gondii* ingests and digests host cytosolic proteins. *mBio.* 2014;5(4):e01188-14.
 12. Di Cristina M, Dou Z, Lunghi M, et al. *Toxoplasma* depends on lysosomal consumption of autophagosomes for persistent infection. *Nat Microbiol.* 2017;2:17096. doi: 10.1038/nmicrobiol.2017.96 [doi].
 13. Meshnick SR. Artemisinin: mechanisms of action, resistance and toxicity. *Int J Parasitol.* 2002;32(13):1655-1660. doi: S0020751902001947 [pii].
 14. Slater AF. Chloroquine: mechanism of drug action and resistance in *Plasmodium falciparum*. *Pharmacol Ther.* 1993;57(2-3):203-235. doi: 0163-7258(93)90056-J [pii].
 15. Liu J, Istvan ES, Gluzman IY, Gross J, Goldberg DE. *Plasmodium falciparum* ensures its amino acid supply with multiple acquisition pathways and redundant proteolytic enzyme systems. *Proc Natl Acad Sci U S A.* 2006;103(23):8840-8845. doi: 0601876103 [pii].
 16. Mordue D, Hakansson S, Niesman IR, Sibley LD. *Toxoplasma gondii* resides in a vacuole that resists fusion with host cell endocytic and exocytic vesicular trafficking pathways. *Exp Parasitol.* 1999;92:87-99.
 17. Mordue DG, Sibley LD. Intracellular fate of vacuoles containing *Toxoplasma gondii* is determined at the time of formation and depends on the mechanism of entry. *J Immunol.* 1997;159(9):4452-4459.
 18. Mordue DG, Desai N, Dustin M, Sibley LD. Invasion by *Toxoplasma gondii* establishes a moving junction that selectively excludes host cell plasma membrane proteins on the basis of their membrane anchoring. *J Exp Med.* 1999;190(12):1783-1792.
 19. Ling YM, Shaw MH, Ayala C, et al. Vacuolar and plasma membrane stripping and autophagic elimination of *Toxoplasma gondii* in primed effector macrophages. *J Exp Med.* 2006;203(9):2063-2071. doi: jem.20061318 [pii].

20. Blader IJ, Koshy AA. Toxoplasma gondii development of its replicative niche: in its host cell and beyond. *Eukaryot Cell*. 2014;13(8):965-976. doi: 10.1128/EC.00081-14 [doi].
21. Marino ND, Boothroyd JC. Toxoplasma growth in vitro is dependent on exogenous tyrosine and is independent of AAH2 even in tyrosine-limiting conditions. *Exp Parasitol*. 2017;176:52-58. doi: S0014-4894(16)30401-5 [pii].
22. Gold DA, Kaplan AD, Lis A, et al. The Toxoplasma Dense Granule Proteins GRA17 and GRA23 Mediate the Movement of Small Molecules between the Host and the Parasitophorous Vacuole. *Cell Host Microbe*. 2015;17(5):642-652. doi: 10.1016/j.chom.2015.04.003 [doi].
23. Schwab JC, Beckers CJM, Joiner KA. The parasitophorous vacuole membrane surrounding intracellular *Toxoplasma gondii* functions as a molecular sieve. *Proc Natl Acad Sci USA*. 1994;91:509-513.
24. Blume M, Rodriguez-Contreras D, Landfear S, et al. Host-derived glucose and its transporter in the obligate intracellular pathogen *Toxoplasma gondii* are dispensable by glutaminolysis. *Proc Natl Acad Sci U S A*. 2009;106(31):12998-13003. doi: 10.1073/pnas.0903831106.
25. Rajendran E, Hapuarachchi SV, Miller CM, et al. Cationic amino acid transporters play key roles in the survival and transmission of apicomplexan parasites. *Nat Commun*. 2017;8:14455. doi: 10.1038/ncomms14455 [doi].
26. De Koning HP, Al-Salabi MI, Cohen AM, Coombs GH, Wastling JM. Identification and characterisation of high affinity nucleoside and nucleobase transporters in *Toxoplasma gondii*. *Int J Parasitol*. 2003;33(8):821-831. doi: S0020751903000912 [pii].
27. Chiang CW, Carter N, J. SW, Jr, et al. The adenosine transporter of *Toxoplasma gondii* identification by insertional mutagenesis, cloning, and recombinant expression. *J Biol Chem*. 1999;274(49):35255-35261.
28. Schwab JC, Afifi Afifi M, Pizzorno G, Handshumacher RE, Joiner KA. *Toxoplasma gondii* tachyzoites possess an unusual plasma membrane adenosine transporter. *Mol Biochem Parasitol*. 1995;70:59-69.
29. Mercier C, Dubremetz JF, Rauscher B, Lecordier L, Sibley LD, Cesbron-Delauw MF. Biogenesis of nanotubular network in *Toxoplasma* parasitophorous vacuole induced by parasite proteins. *Mol Biol Cell*. 2002;13(7):2397-409.
30. Sibley LD, Niesman IR, Parmley SF, Cesbron-Delauw MF. Regulated secretion of multi-lamellar vesicles leads to formation of a tubulo-vesicular network in host-cell vacuoles occupied by *Toxoplasma gondii*. *J Cell Sci*. 1995;108 (Pt 4)(Pt 4):1669-1677.

31. Labruyere E, Lingnau M, Mercier C, Sibley LD. Differential membrane targeting of the secretory proteins GRA4 and GRA6 within the parasitophorous vacuole formed by *Toxoplasma gondii*. *Mol Biochem Parasitol*. 1999;102(2):311-324.
32. Coppens I, Dunn JD, Romano JD, et al. *Toxoplasma gondii* sequesters lysosomes from mammalian hosts in the vacuolar space. *Cell*. 2006;125(2):261-74.
33. Travier L, Mondragon R, Dubremetz JF, et al. Functional domains of the *Toxoplasma* GRA2 protein in the formation of the membranous nanotubular network of the parasitophorous vacuole. *Int J Parasitol*. 2008;38(7):757-773. doi: 10.1016/j.ijpara.2007.10.010.
34. Lige B, Romano JD, Sampels V, Sonda S, Joiner KA, Coppens I. Introduction of caveolae structural proteins into the protozoan *Toxoplasma* results in the formation of heterologous caveolae but not caveolar endocytosis. *PLoS One*. 2012;7(12):e51773. doi: 10.1371/journal.pone.0051773 [doi].
35. Kaksonen M, Roux A. Mechanisms of clathrin-mediated endocytosis. *Nat Rev Mol Cell Biol*. 2018. doi: 10.1038/nrm.2017.132 [doi].
36. McMahon HT, Boucrot E. Molecular mechanism and physiological function. *Nat Rev Mol Cell Biol*. 2011;12(8):517-533. doi: 10.1038/nrm3151 [doi].
37. Mooren OL, Galletta BJ, Cooper JA. Roles for actin assembly in endocytosis. *Annu Rev Biochem*. 2012;81:661-686. doi: 10.1146/annurev-biochem-060910-094416 [doi].
38. Goode BL, Eskin JA, Wendland B. Actin and endocytosis in budding yeast. *Genetics*. 2015;199(2):315-358. doi: 10.1534/genetics.112.145540 [doi].
39. Dawson JC, Legg JA, Machesky LM. Bar domain proteins: a role in tubulation, scission and actin assembly in clathrin-mediated endocytosis. *Trends Cell Biol*. 2006;16(10):493-498. doi: S0962-8924(06)00221-2 [pii].
40. Hinshaw JE. Dynamin and its role in membrane fission. *Annu Rev Cell Dev Biol*. 2000;16:483-519. doi: 10.1146/annurev.cellbio.16.1.483 [doi].
41. Weinberg J, Drubin DG. Clathrin-mediated endocytosis in budding yeast. *Trends Cell Biol*. 2012;22(1):1-13. doi: 10.1016/j.tcb.2011.09.001 [doi].
42. Ferguson SM, De Camilli P. Dynamin, a membrane-remodelling GTPase. *Nat Rev Mol Cell Biol*. 2012;13(2):75-88. doi: 10.1038/nrm3266 [doi].
43. Smaczynska-de R,II, Allwood EG, Aghamohammadzadeh S, Hetteema EH, Goldberg MW, Ayscough KR. A role for the dynamin-like protein Vps1 during endocytosis in yeast. *J Cell Sci*. 2010;123(Pt 20):3496-3506. doi: 10.1242/jcs.070508 [doi].

44. Yu X, Cai M. The yeast dynamin-related GTPase Vps1p functions in the organization of the actin cytoskeleton via interaction with Sla1p. *J Cell Sci.* 2004;117(Pt 17):3839-3853. doi: 10.1242/jcs.01239 [doi].
45. Palmer SE, Smaczynska-de R,II, Marklew CJ, et al. A dynamin-actin interaction is required for vesicle scission during endocytosis in yeast. *Curr Biol.* 2015;25(7):868-878. doi: 10.1016/j.cub.2015.01.061 [doi].
46. Mayor S, Parton RG, Donaldson JG. Clathrin-independent pathways of endocytosis. *Cold Spring Harb Perspect Biol.* 2014;6(6):10.1101/cshperspect.a016758. doi: 10.1101/cshperspect.a016758 [doi].
47. Huang KM, D'Hondt K, Riezman H, Lemmon SK. Clathrin functions in the absence of heterotetrameric adaptors and AP180-related proteins in yeast. *EMBO J.* 1999;18(14):3897-3908. doi: 10.1093/emboj/18.14.3897 [doi].
48. Carroll SY, Stirling PC, Stimpson HE, Giesselmann E, Schmitt MJ, Drubin DG. A yeast killer toxin screen provides insights into a/b toxin entry, trafficking, and killing mechanisms. *Dev Cell.* 2009;17(4):552-560. doi: 10.1016/j.devcel.2009.08.006 [doi].
49. Motley A, Bright NA, Seaman MN, Robinson MS. Clathrin-mediated endocytosis in AP-2-depleted cells. *J Cell Biol.* 2003;162(5):909-918. doi: 10.1083/jcb.200305145 [doi].
50. Paez Valencia J, Goodman K, Otegui MS. Endocytosis and Endosomal Trafficking in Plants. *Annu Rev Plant Biol.* 2016;67:309-335. doi: 10.1146/annurev-arplant-043015-112242 [doi].
51. Bos JL, Rehmann H, Wittinghofer A. GEFs and GAPs: critical elements in the control of small G proteins. *Cell.* 2007;129(5):865-877. doi: S0092-8674(07)00655-1 [pii].
52. Ferreira APA, Boucrot E. Mechanisms of Carrier Formation during Clathrin-Independent Endocytosis. *Trends Cell Biol.* 2018;28(3):188-200. doi: S0962-8924(17)30208-8 [pii].
53. Spiering D, Hodgson L. Dynamics of the Rho-family small GTPases in actin regulation and motility. *Cell Adh Migr.* 2011;5(2):170-180. doi: 14403 [pii].
54. Boucrot E, Ferreira AP, Almeida-Souza L, et al. Endophilin marks and controls a clathrin-independent endocytic pathway. *Nature.* 2015;517(7535):460-465. doi: 10.1038/nature14067 [doi].
55. Kirkham M, Fujita A, Chadda R, et al. Ultrastructural identification of uncoated caveolin-independent early endocytic vehicles. *J Cell Biol.* 2005;168(3):465-476. doi: jcb.200407078 [pii].

56. Howes MT, Kirkham M, Riches J, et al. Clathrin-independent carriers form a high capacity endocytic sorting system at the leading edge of migrating cells. *J Cell Biol.* 2010;190(4):675-691. doi: 10.1083/jcb.201002119 [doi].
57. Lundmark R, Doherty GJ, Howes MT, et al. The GTPase-activating protein GRAF1 regulates the CLIC/GEEC endocytic pathway. *Curr Biol.* 2008;18(22):1802-1808. doi: 10.1016/j.cub.2008.10.044 [doi].
58. Aikawa M, Hepler PK, Huff CG, Sprinz H. The feeding mechanism of avian malarial parasites. *J Cell Biol.* 1966;Feb;28(2):355-373.
59. Slomianny C. Three-dimensional reconstruction of the feeding process of the malaria parasite. *Blood Cells.* 1990;16(2-3):369-378.
60. Nichols BA, Chiappino ML, Pavesio CE. Endocytosis at the micropore of *Toxoplasma gondii*. *Parasitol Res.* 1994;80(2):91-98.
61. Pieperhoff MS, Schmitt M, Ferguson DJ, Meissner M. The role of clathrin in post-Golgi trafficking in *Toxoplasma gondii*. *PLoS One.* 2013;8(10):e77620. doi: 10.1371/journal.pone.0077620 [doi].
62. Wetzel DM, Hakansson S, Hu K, Roos D, Sibley LD. Actin filament polymerization regulates gliding motility by apicomplexan parasites. *Mol Biol Cell.* 2003;14(2):396-406.
63. Bargieri D, Lagal V, Andenmatten N, Tardieux I, Meissner M, Ménard R. Host Cell Invasion by Apicomplexan Parasites: The Junction Conundrum. *PLoS Pathog.* 2014 Sep 18;10(9):e1004273. doi: 10.1371/journal.ppat.1004273. eCollection 2014 Sep.
64. Breinich MS, Ferguson DJ, Foth BJ, et al. A dynamin is required for the biogenesis of secretory organelles in *Toxoplasma gondii*. *Curr Biol.* 2009;19(4):277-286. doi: 10.1016/j.cub.2009.01.039.
65. van Dooren GG, Reiff SB, Tomova C, Meissner M, Humbel BM, Striepen B. A novel dynamin-related protein has been recruited for apicoplast fission in *Toxoplasma gondii*. *Curr Biol.* 2009;19(4):267-276. doi: 10.1016/j.cub.2008.12.048.
66. Venugopal K, Werkmeister E, Barois N, et al. Dual role of the *Toxoplasma gondii* clathrin adaptor AP1 in the sorting of rhoptry and microneme proteins and in parasite division. *PLoS Pathog.* 2017 Apr 21;13(4):e1006331.
67. Milani KJ, Schneider TG, Taraschi TF. Defining the Morphology and Mechanism of the Hemoglobin Transport Pathway in *Plasmodium falciparum* Infected Erythrocytes. *Eukaryot Cell.* 2015. doi: EC.00267-14 [pii].
68. Wollert T, Yang D, Ren X, Lee HH, Im YJ, Hurley JH. The ESCRT machinery at a glance. *J Cell Sci.* 2009;122(Pt 13):2163-2166. doi: 10.1242/jcs.029884 [doi].

69. Fujii K, Hurley JH, Freed EO. Beyond Tsg101: the role of Alix in 'ESCRTing' HIV-1. *Nat Rev Microbiol.* 2007;5(12):912-916. doi: nrmicro1790 [pii].
70. Scott CC, Vacca F, Gruenberg J. Endosome maturation, transport and functions. *Semin Cell Dev Biol.* 2014;31:2-10. doi: 10.1016/j.semcdb.2014.03.034 [doi].
71. Balderhaar HJ, Lachmann J, Yavavli E, Brocker C, Lurick A, Ungermann C. The CORVET complex promotes tethering and fusion of Rab5/Vps21-positive membranes. *Proc Natl Acad Sci U S A.* 2013;110(10):3823-3828. doi: 10.1073/pnas.1221785110 [doi].
72. van der Kant R, Jonker CT, Wijdeven RH, et al. Characterization of the Mammalian CORVET and HOPS Complexes and Their Modular Restructuring for Endosome Specificity. *J Biol Chem.* 2015;290(51):30280-30290. doi: 10.1074/jbc.M115.688440 [doi].
73. Perini ED, Schaefer R, Stoter M, Kalaidzidis Y, Zerial M. Mammalian CORVET is required for fusion and conversion of distinct early endosome subpopulations. *Traffic.* 2014;15(12):1366-1389. doi: 10.1111/tra.12232 [doi].
74. Schmidt O, Teis D. The ESCRT machinery. *Curr Biol.* 2012;22(4):R116-20. doi: 10.1016/j.cub.2012.01.028 [doi].
75. Mizuno-Yamasaki E, Rivera-Molina F, Novick P. GTPase networks in membrane traffic. *Annu Rev Biochem.* 2012;81:637-659. doi: 10.1146/annurev-biochem-052810-093700 [doi].
76. Numrich J, Ungermann C. Endocytic Rabs in membrane trafficking and signaling. *Biol Chem.* 2014;395(3):327-333. doi: 10.1515/hsz-2013-0258 [doi].
77. Solinger JA, Spang A. Tethering complexes in the endocytic pathway: CORVET and HOPS. *FEBS J.* 2013;280(12):2743-2757. doi: 10.1111/febs.12151 [doi].
78. Dettmer J, Hong-Hermesdorf A, Stierhof Y, Schumacher K. Vacuolar H⁺-ATPase activity is required for endocytic and secretory trafficking in Arabidopsis. *Plant Cell.* 2006;18:715-730.
79. Yu M, Liu H, Dong Z, et al. The dynamics and endocytosis of Flot1 protein in response to flg22 in Arabidopsis. *J Plant Physiol.* 2017;215:73-84. doi: S0176-1617(17)30130-X [pii].
80. Scheuring D, Viotti C, Kruger F, et al. Multivesicular bodies mature from the trans-Golgi network/early endosome in Arabidopsis. *Plant Cell.* 2011;23(9):3463-3481. doi: 10.1105/tpc.111.086918 [doi].
81. Ebine K, Inoue T, Ito J, et al. Plant vacuolar trafficking occurs through distinctly regulated pathways. *Curr Biol.* 2014;24(12):1375-1382. doi: S0960-9822(14)00529-6 [pii].

82. Singh MK, Kruger F, Beckmann H, et al. Protein delivery to vacuole requires SAND protein-dependent Rab GTPase conversion for MVB-vacuole fusion. *Curr Biol*. 2014;24(12):1383-1389. doi: S0960-9822(14)00530-2 [pii].
83. Klinger CM, Klute MJ, Dacks JB. Comparative genomic analysis of multi-subunit tethering complexes demonstrates an ancient pan-eukaryotic complement and sculpting in Apicomplexa. *PLoS One*. 2013;8(9):e76278. doi: 10.1371/journal.pone.0076278 [doi].
84. Rojo E, Zouhar J, Kovaleva V, Hong S, Raikhel NV. The AtC-VPS protein complex is localized to the tonoplast and the prevacuolar compartment in Arabidopsis. *Mol Biol Cell*. 2003;14(2):361-369. doi: 10.1091/mbc.E02-08-0509 [doi].
85. Ahmed SU, Rojo E, Kovaleva V, et al. The plant vacuolar sorting receptor AtELP is involved in transport of NH₂-terminal propeptide-containing vacuolar proteins in Arabidopsis thaliana. *J Cell Biol*. 2000;149(7):1335-1344.
86. Ebine K, Okatani Y, Uemura T, et al. A SNARE complex unique to seed plants is required for protein storage vacuole biogenesis and seed development of Arabidopsis thaliana. *Plant Cell*. 2008;20(11):3006-3021. doi: 10.1105/tpc.107.057711 [doi].
87. Hao L, Liu J, Zhong S, Gu H, Qu LJ. AtVPS41-mediated endocytic pathway is essential for pollen tube-stigma interaction in Arabidopsis. *Proc Natl Acad Sci U S A*. 2016;113(22):6307-6312. doi: 10.1073/pnas.1602757113 [doi].
88. Baldauf SL. The deep roots of eukaryotes. *Science*. 2003;300(5626):1703-1706. doi: 10.1126/science.1085544 [doi].
89. Miranda K, Pace DA, Cintron R, et al. Characterization of a novel organelle in *Toxoplasma gondii* with similar composition and function to the plant vacuole. *Mol Microbiol*. 2010;76(6):1358-1375. doi: 10.1111/j.1365-2958.2010.07165.x [doi].
90. Kremer K, Kamin D, Rittweger E, et al. An Overexpression Screen of *Toxoplasma gondii* Rab-GTPases Reveals Distinct Transport Routes to the Micronemes. *PLoS Pathog*. 2013;9(3):e1003213. doi: 10.1371/journal.ppat.1003213; 10.1371/journal.ppat.1003213.
91. Ebine K, Miyakawa N, Fujimoto M, Uemura T, Nakano A, Ueda T. Endosomal trafficking pathway regulated by ARA6, a RAB5 GTPase unique to plants. *Small GTPases*. 2012;3(1):23-27.
92. Dowse T, Soldati D. Host cell invasion by the apicomplexans: the significance of microneme protein proteolysis. *Curr Opin Microbiol*. 2004;7(4):388-396. doi: 10.1016/j.mib.2004.06.013.

93. Hunter CA, Sibley LD. Modulation of innate immunity by *Toxoplasma gondii* virulence effectors. *Nat Rev Microbiol.* 2012;10(11):766-778. doi: 10.1038/nrmicro2858; 10.1038/nrmicro2858.
94. Carey KL, Jongco AM, Kim K, Ward GE. *The Toxoplasma gondii* rhoptry protein ROP4 is secreted into the parasitophorous vacuole and becomes phosphorylated in infected cells. *Eukaryot Cell.* 2004;3(5):1320-30.
95. Besteiro S, Michelin A, Poncet J, Dubremetz J, Lebrun M. Export of a *Toxoplasma gondii* Rhoptry Neck Protein Complex at the Host Cell Membrane to Form the Moving Junction during Invasion. *PLoS Pathog.* 2009;Feb;5(2):e1000309.
96. Etheridge RD, Alaganan A, Tang K, Lou HJ, Turk BE, Sibley LD. The *Toxoplasma* pseudokinase ROP5 forms complexes with ROP18 and ROP17 kinases that synergize to control acute virulence in mice. *Cell Host Microbe.* 2014 May 14;15(5):537-550.
97. Huynh MH, Carruthers VB. A *Toxoplasma gondii* Ortholog of Plasmodium GAMA Contributes to Parasite Attachment and Cell Invasion. *mSphere.* 2016;1(1):10.1128/mSphere.00012-16. eCollection 2016 Jan-Feb. doi: 10.1128/mSphere.00012-16 [doi].
98. Huynh MH, Boulanger MJ, Carruthers VB. A conserved apicomplexan microneme protein contributes to *Toxoplasma gondii* invasion and virulence. *Infect Immun.* 2014;82(10):4358-4368. doi: 10.1128/IAI.01877-14 [doi].
99. Sidik SM, Huet D, Ganesan SM, et al. A Genome-wide CRISPR Screen in *Toxoplasma* Identifies Essential Apicomplexan Genes. *Cell.* 2016;166(6):1423-1435.e12. doi: 10.1016/j.cell.2016.08.019 [doi].
100. Kafsack BF, Pena JD, Coppens I, Ravindran S, Boothroyd JC, Carruthers VB. Rapid membrane disruption by a perforin-like protein facilitates parasite exit from host cells. *Science.* 2009;323(5913):530-533. doi: 10.1126/science.1165740.
101. Guerin A, Corrales RM, Parker ML, et al. Efficient invasion by *Toxoplasma* depends on the subversion of host protein networks. *Nat Microbiol.* 2017;2(10):1358-1366. doi: 10.1038/s41564-017-0018-1 [doi].
102. Harper JM, Huynh MH, Coppens I, Parussini F, Moreno S, Carruthers VB. A cleavable propeptide influences *Toxoplasma* infection by facilitating the trafficking and secretion of the TgMIC2-M2AP invasion complex. *Mol Biol Cell.* 2006;17(10):4551-4563. doi: E06-01-0064 [pii]; 10.1091/mbc.E06-01-0064 [doi].
103. Parussini F, Coppens I, Shah PP, Diamond SL, Carruthers VB. Cathepsin L occupies a vacuolar compartment and is a protein maturase within the endo/exocytic system of *Toxoplasma gondii*. *Mol Microbiol.* 2010;76(6):1340-1357. doi: 10.1111/j.1365-2958.2010.07181.x.

104. Sakura T, Sindikubwabo F, Oesterlin LK, et al. A Critical Role for *Toxoplasma gondii* Vacuolar Protein Sorting VPS9 in Secretory Organelle Biogenesis and Host Infection. *Sci Rep*. 2016 Dec 14;6:38842-doi: 10.1038/srep38842.
105. Morlon-Guyot J, Pastore S, Berry L, Lebrun M, Daher W. *Toxoplasma gondii* Vps11, a subunit of HOPS and CORVET tethering complexes, is essential for the biogenesis of secretory organelles. *Cell Microbiol*. 2015;17(8):1157-1178. doi: 10.1111/cmi.12426 [doi].
106. Krugliak M, Zhang J, Ginsburg H. Intraerythrocytic *Plasmodium falciparum* utilizes only a fraction of the amino acids derived from the digestion of host cell cytosol for the biosynthesis of its proteins. *Mol Biochem Parasitol*. 2002;Feb;119(2):249-256.
107. Hanssen E, Knoechel C, Dearnley M, et al. Soft X-ray microscopy analysis of cell volume and hemoglobin content in erythrocytes infected with asexual and sexual stages of *Plasmodium falciparum*. *J Struct Biol*. 2012;177(2):224-232. doi: 10.1016/j.jsb.2011.09.003 [doi].
108. Bakar NA, Klonis N, Hanssen E, Chan C, Tilley L. Digestive-vacuole genesis and endocytic processes in the early intraerythrocytic stages of *Plasmodium falciparum*. *J Cell Sci*. 2010;123:441-450; doi: 10.1242/jcs.061499.
109. Francis SE, Gluzman IY, Oksman A, et al. Molecular characterization and inhibition of a *Plasmodium falciparum* aspartic hemoglobinase. *EMBO J*. 1994 Jan 15;13(2):306-317.
110. Margos G, Bannister LH, Dluzewski AR, Hopkins J, Williams IT, Mitchell GH. Correlation of structural development and differential expression of invasion-related molecules in schizonts of *Plasmodium falciparum*. *Parasitology*. 2004 Sep;129(Pt 3):273-287.
111. Lazarus MD, Schneider TG, Taraschi TF. A new model for hemoglobin ingestion and transport by the human malaria parasite *Plasmodium falciparum*. *J Cell Sci*. 2008;121(11):1937-1949. doi: 10.1242/jcs.023150 [doi].
112. Sloves PJ, Delhaye S, Mousseaux T, et al. *Toxoplasma* sortilin-like receptor regulates protein transport and is essential for apical secretory organelle biogenesis and host infection. *Cell Host Microbe*. 2012;11(5):515-527. doi: 10.1016/j.chom.2012.03.006; 10.1016/j.chom.2012.03.006.
113. Brillada C, Rojas-Pierce M. Vacuolar trafficking and biogenesis: a maturation in the field. *Curr Opin Plant Biol*. 2017 Aug 31;40:77-81. doi: 10.1016/j.pbi.2017.08.005. [Epub ahead of print].
114. Kunzl F, Fruholz S, Fassler F, Li B, Pimpl P. Receptor-mediated sorting of soluble vacuolar proteins ends at the trans-Golgi network/early endosome. *Nat Plants*. 2016;2:16017. doi: 10.1038/nplants.2016.17 [doi].

Chapter 2

Intersection of endocytic and exocytic systems in *Toxoplasma gondii*

2.1 Abstract

Host cytosolic proteins are endocytosed by the intracellular parasite *Toxoplasma gondii* and degraded in its lysosome-like compartment, the vacuolar compartment/plant-like vacuole, hereafter referred to as the VAC. Conserved endocytic components and plant-like features suggest endocytic trafficking in *T. gondii* involves transit through endosome-like compartments (ELCs) marked by Rab5 and Rab7 as in other eukaryotes and potentially through the trans-Golgi network (TGN) as in plants. However, exocytic trafficking to regulated secretory organelles, micronemes and rhoptries, also proceeds through ELCs and requires classical endocytic components like clathrin, dynamin and Rab5. Therefore, endocytic and exocytic trafficking may intersect in *T. gondii*, but the dynamics and route of endocytic trafficking remain undefined. Using fluorescence microscopy and colocalization analysis, we found the following. Host cytosolic proteins are endocytosed within 7 min post-invasion, trafficked through ELCs and potentially the TGN en route to the VAC, and are degraded within 30 min. Endocytosis of host-derived proteins and microneme/rhoptry biogenesis occur simultaneously and microneme synthesis occurs throughout the cell cycle, whereas rhoptry protein synthesis occurs in S and M/C phases. Finally, ingested host proteins colocalize with immature promicroneme proteins, proM2AP and proMIC5, in transit to the micronemes, but not with the immature prorhoptry protein proRON4. Collectively, these findings are consistent with endocytic trafficking of ingested protein intersecting with exocytic trafficking of microneme proteins and suggests sorting mechanisms are required for proper targeting of endocytic exocytic cargoes.

2.2 Introduction

Endocytosis is pathway by which material is taken up across the plasma membrane and trafficked to the lysosome for digestion. An analogous pathway was recently discovered in the obligate intracellular eukaryotic parasite, *Toxoplasma gondii*, termed the ingestion pathway. In *T. gondii* ingestion, proteins acquired from the host cell cytosol are trafficked across the parasitophorous vacuole (PV) and parasite plasma membrane to a lysosome-like compartment within the parasite termed the vacuolar compartment/plant-like vacuole (VAC/PLV; the term VAC will be used hereafter) for degradation.¹ However, how ingested cargoes are delivered to the VAC is not known.

Endocytic trafficking to the lysosome is highly conserved among eukaryotes with a slight variation observed in plants. In mammalian and yeast cells, endocytic cargoes are delivered sequentially to the Rab5 compartment, the Rab7 compartment and finally to the lysosome.² Plant cells, on the other hand, initially deliver endocytosed cargoes to the trans-Golgi network (TGN), followed by sequential movement through the Rab5 compartment, the Rab7 compartment and finally the lysosome for degradation.³ *Toxoplasma* has a conserved endomembrane structure including a TGN, endosome-like compartments (ELCs) marked by Rab5 and Rab7, and the lysosome-like VAC, and also expresses the essential machinery for endocytic trafficking to lysosomes including clathrin, dynamin, Rab5 and Rab7.⁴ The presence of a plant-like lysosome and a plant-specific proton pump within the *T. gondii* endolysosomal system suggests that endocytic trafficking in *T. gondii* may resemble trafficking in plants, as proposed by *Pieperhoff et al.*^{5, 6} However, exocytic trafficking of proteins destined for the parasite's regulated secretory organelles, the micronemes and rhoptries, proceeds through the TGN and ELCs, and requires clathrin, dynamin and Rab5 for transit.^{5, 7-13} In contrast to the ingestion pathway, which leads to the destruction of its cargo, many microneme and rhoptry proteins have propeptides that are cleaved off during transit to the microneme and rhoptry organelles, but must otherwise remain intact to orchestrate parasite invasion, egress and defense against host immune attack.¹⁴⁻²⁴ Without these exocytic proteins and organelles, the parasite cannot establish a successful infection.

How *T. gondii* regulates and ensures proper targeting of endocytic and exocytic cargo is unclear, but other eukaryotic systems reveal several possible mechanisms.

Endocytic and exocytic trafficking may be spatially regulated like certain GPI-anchored proteins that traffic directly to the plasma membrane from the TGN, avoiding endosomes in mammalian cells.²⁵ Alternatively, these processes may be temporally regulated. In *Plasmodium spp.*, endocytosis of red blood cell cytoplasm is most active in G1 and early S phase, whereas microneme organelle biogenesis occurs later in the late S and mitosis and cytokinesis (M/C) phases of its cell cycle.²⁶⁻³⁰ Another scenario is that endocytic and exocytic trafficking intersect and require sorting mechanisms to ensure proper targeting. This is illustrated by the TGN in plants, which serves as a sorting station for endocytic and exocytic cargoes, or by transferrin receptors in mammalian cells, which traffic through endosomes before reaching the plasma membrane.^{25, 31}

In this study, we determine the temporal and spatial relationships between endocytic and exocytic trafficking within *T. gondii*. We find that host cytosolic proteins are ingested during or immediately following invasion and are trafficked through the ELCs and potentially the TGN en route to the VAC for degradation in 30 min. Host protein ingestion and microneme/rhoptry biogenesis occur simultaneously. Ingestion and microneme biogenesis occur throughout the cell cycle, whereas rhoptry biogenesis is restricted to the S and M/C phases. Finally, ingested proteins colocalize with newly synthesized microneme but not rhoptry proteins. Taken together, our work suggests that endocytic trafficking of ingested protein intersects with exocytic trafficking of microneme proteins.

2.3 Results

2.3.1 Localization of the TGN/ELC marker GalNac-YFP

Plant-like features of *T. gondii* led to the prediction that ingested proteins follow a plant-like endocytic route through the TGN and ELCs en route to the VAC. To test if the endocytic trafficking is plant-like in *T. gondii*, we generated a parasite line stably expressing UDP-GalNac:polypeptide N-acetylgalactosaminyl-transferase fused to YFP (GalNac-YFP), typically used as a specific TGN marker.³² Consistent with TGN localization, GalNac-YFP appeared in a centrally located structure that overlapped substantially with, or was just apical to, the Golgi marker GRASP55-mRFP (Figure 2-1). Interestingly, GalNac-YFP overlapped best with NHE3, a vacuolar type Na⁺/H⁺

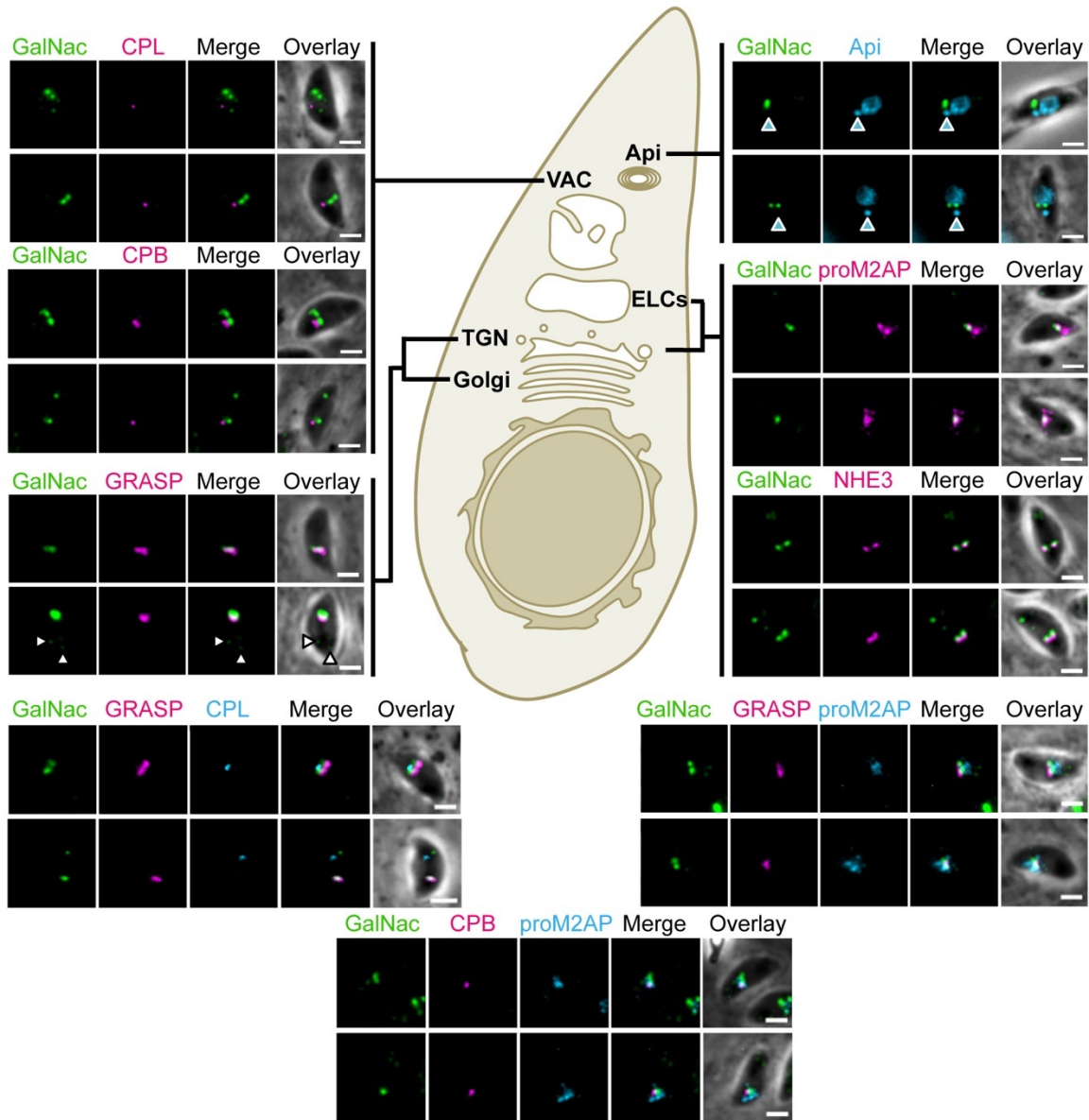


FIGURE 2-1 Localization of GalNac-YFP in RH GalNac-YFP parasites. Representative images for localization of GalNac-YFP in RH GalNac-YFP parasites. GalNac-YFP parasites or GalNac-YFP parasites transiently transfected to express GRASP55-RFP were stained with DAPI to label the apicoplast or CPB, CPL, NHE3 and/or proM2AP using antibody staining. The best localization was seen with NHE3 and GRASP55-RFP, which showed perfect overlap or slightly offset localization. As previously observed, proM2AP also showed significant overlap, but with more anterior signal than NHE3. CPL, CPB and the apicoplast showed rare overlap with GalNac-YFP. Blue arrowhead indicates the apicoplast, and white arrows indicate “Golgi-free” GalNac-YFP signal. Images are representative of two biological replicates. Scale bars: 2 μ m.

exchanger, in the central region of the parasite despite previous observations that NHE3 partially colocalized with the VAC.³³ Therefore, we interpret NHE3 to be an ELC marker that partially overlaps with the TGN, similar to the established ELC marker proM2AP, the immature proform of the microneme protein M2AP.^{7, 34} GalNac-YFP also partially overlapped with proM2AP, but rarely colocalized with the VAC-localized proteases

cathepsin B (CPB) and cathepsin L (CPL) or the parasite's residual chloroplast-like organelle called the apicoplast (Figure 2-1, blue arrowheads for apicoplast). We also observed that some parasites had GalNac-YFP-labeled structures that were not associated with GRASP55-mRFP (Figure 2-1, white arrowheads). These structures are reminiscent of "Golgi-free" TGN bodies in plants³⁵ This observation together with substantial overlap with the ELC markers proM2AP and NHE3, suggests GalNac-YFP occupies the TGN, ELCs, and perhaps additional sites.

2.3.2 Ingested proteins traverse ELCs

The ability of *T. gondii* to ingest proteins from the host cytosol can be monitored using fluorescent protein reporters, such as the red fluorescent protein mCherry, expressed in host cytosol (Figure 2-2A). Chinese hamster ovary (CHO-K1) cells transiently transfected with a plasmid encoding cytosolic mCherry are infected with *T. gondii* and incubated to allow consumption of host cytosol. Parasites are then purified from host cells and analyzed by fluorescence microscopy. In our previous study, accumulation of ingested host protein was enhanced by the absence of the VAC-localized protease CPL or by treatment with a CPL inhibitor, morpholinurea-leucine-homophenylalanine-vinyl phenyl sulfone (LHVS).¹ When LHVS-dependent accumulation of ingested host protein ingestion is detected, the ingestion pathway is considered to be active, and localization of the ingested protein can be assessed by determining the percentage of ingested mCherry puncta overlapping with endolysosomal system markers (%Colocalized).

To determine which endolysosomal compartments ingested protein traffics through on the way to the VAC, GalNac-YFP or WT (RH) parasites retrieved from mCherry-expressing CHO-K1 cells were treated and processed as shown in Figure 2-2A and stained with antibodies against proM2AP, NHE3, or CPB. As a negative control, the apicoplast, a compartment that is in the same region as, but distinct from, the endolysosomal system, was stained with DAPI as a test for random colocalization. Ingestion was found to be active in both strains (Figure 2-2B and C), and localization analysis revealed that ingested protein significantly colocalized with GalNac-YFP,

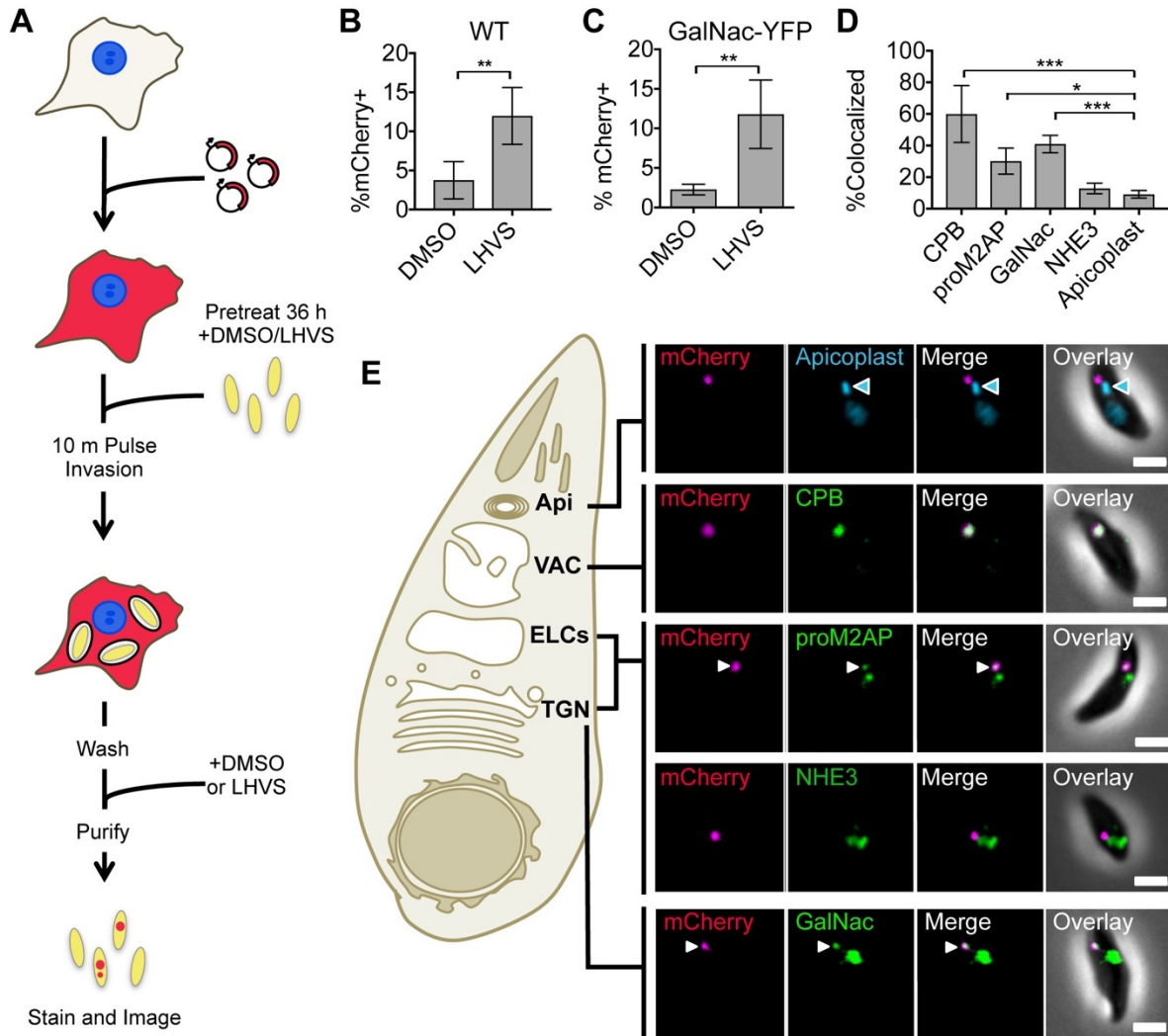


Figure 2-2. Ingested host cytosolic mCherry is associated with the ELCs, VAC, and possibly the TGN. A, Experimental design for detection and localization of host cytosolic protein ingestion. CHO-K1 cells were transiently transfected with a plasmid encoding cytosolic mCherry fluorescent protein 18-24 h before synchronous invasion for 10 min with *T. gondii* parasites (pretreated with 1 μ M LHVS or the vehicle control DMSO for 36 h). Parasites were allowed to ingest host cytosol for 3 h in the presence of 1 μ M LHVS or DMSO before being purified, stained and analyzed by fluorescence microscopy. B-C, Quantitation of ingestion of host cytosolic mCherry in WT or GalNac-YFP parasites treated with 1 μ M LHVS or DMSO. Shown is percentage of mCherry positive parasites, at least 200 parasites analyzed per condition, ratio paired t-test for B and C. D, Quantitation of colocalization of ingested mCherry with the indicated markers of the endolysosomal system. At least 30 ingested mCherry puncta per marker, one-way ANOVA with Dunnet's test for multiple comparisons to colocalization with the apicoplast. E, Representative images for localization of ingested mCherry in LHVS-treated parasites from B and C relative to the apicoplast using DAPI staining, CPB, NHE3 or proM2AP using antibody staining, or GalNac-YFP. Scale bars: 2 μ m. Blue arrowhead indicates the apicoplast, and white arrows indicate areas of colocalization when the endolysosomal marker of interest has several puncta. All bars represent mean from 3 or more biological replicates with standard deviation error bars. * $p < 0.05$, ** $p < 0.01$, *** $p < 0.001$, otherwise not significant.

proM2AP and CPB, but not NHE3 when compared to the apicoplast (Figure 2-2D and E). Further, mCherry⁺ parasites are capable of invading new host cells, indicating that these

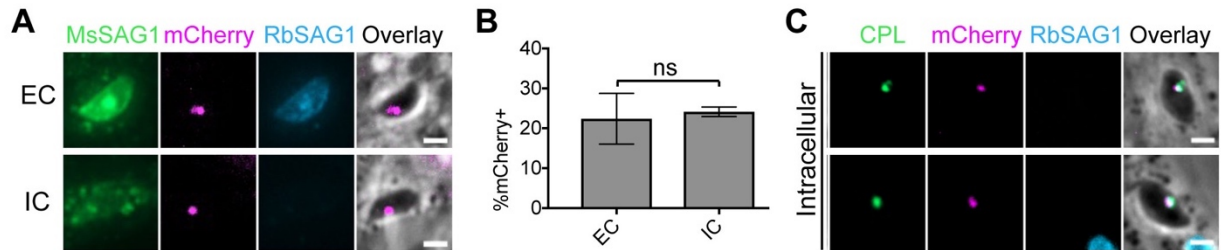


FIGURE 2-3 Harvested mCherry⁺ parasites are viable and can invade HFF cells. A, Representative images for mCherry associated with extracellular (EC) and intracellular (IC) parasites. Ingestion assay performed with RH parasites as described in Figure 2-2A using CHO mCherry cells (described in Figure 2-11A) to maximize mCherry⁺ parasites (see Figure 2-11C). Following harvest, parasites were resuspended in DMEM/10% cosmic calf serum/20 mM HEPES/2 mM L-glutamine/50 μ g/ml penicillin/streptomycin treated with 1 μ M LHVS to inhibit ingested mCherry turnover during the invasion period, and a green-blue invasion assay was performed. Rabbit anti-SAG1 (blue) indicates EC parasites and mouse anti-SAG1 (green) will label all parasites. Images are representative of two biological replicates. B, Quantitation of ingestion in EC versus IC parasites depicted in A. Shown is percentage of mCherry-positive parasites, at least 100 parasites analyzed for each of two biological replicates, unpaired two-sample t-test. C, Representative images for mCherry in IC parasites colocalizing with CPL. Parasites treated as in A, but stained with mouse anti-CPL instead of mouse anti-SAG1. CPL colocalized with 77.6% (13/17) ingested mCherry puncta, suggesting the mCherry is contained within the parasites. One biological replicate. Bars represent means, and error bars represent standard deviation. ns = not significant. Scale bars: 2 μ m.

parasites are viable, and uptake and colocalization is not due to loss of integrity during the purification process (Figure 2-3).

Why ingested protein colocalized significantly with GalNac-YFP, but not NHE3 despite their near perfect overlap in the central region of the parasite was puzzling. Further investigation revealed that most of the ingested mCherry that colocalized with GalNac-YFP also simultaneously colocalized with CPB (Figure 2-4A and B). This was not due to redistribution of GalNac-YFP in response to LHVS treatment since overlap of GalNac-YFP with CPB and CPL did not change with treatment (Figure 2-4C). GalNac-YFP also still showed substantial overlap with NHE3 in the central region of the parasite, and both GalNac-YFP and NHE3 showed only rare overlap with CPB when treated with LHVS (Figure 2-4D). Further analysis of the GalNac-YFP⁺CPB⁺ compartment showed that it was labeled with CPL, proM2AP and NHE3 (Figure 2-4E), implying it could be a subdomain of the ELCs or the VAC rather than the TGN. However, we cannot rule out the possibility that GalNac⁺CPB⁺ puncta represent a TGN subcompartment reserved for sorting of both ingested and biosynthetic cargoes to the ELCs and VAC. Although we can clearly distinguish localization of ingested protein from the apicoplast and NHE3 compartment, the dynamic localization of TGN markers within the apical region of the parasite makes their colocalization with ingested protein difficult to definitively interpret. Therefore, we cannot conclusively determine whether ingested proteins are trafficked

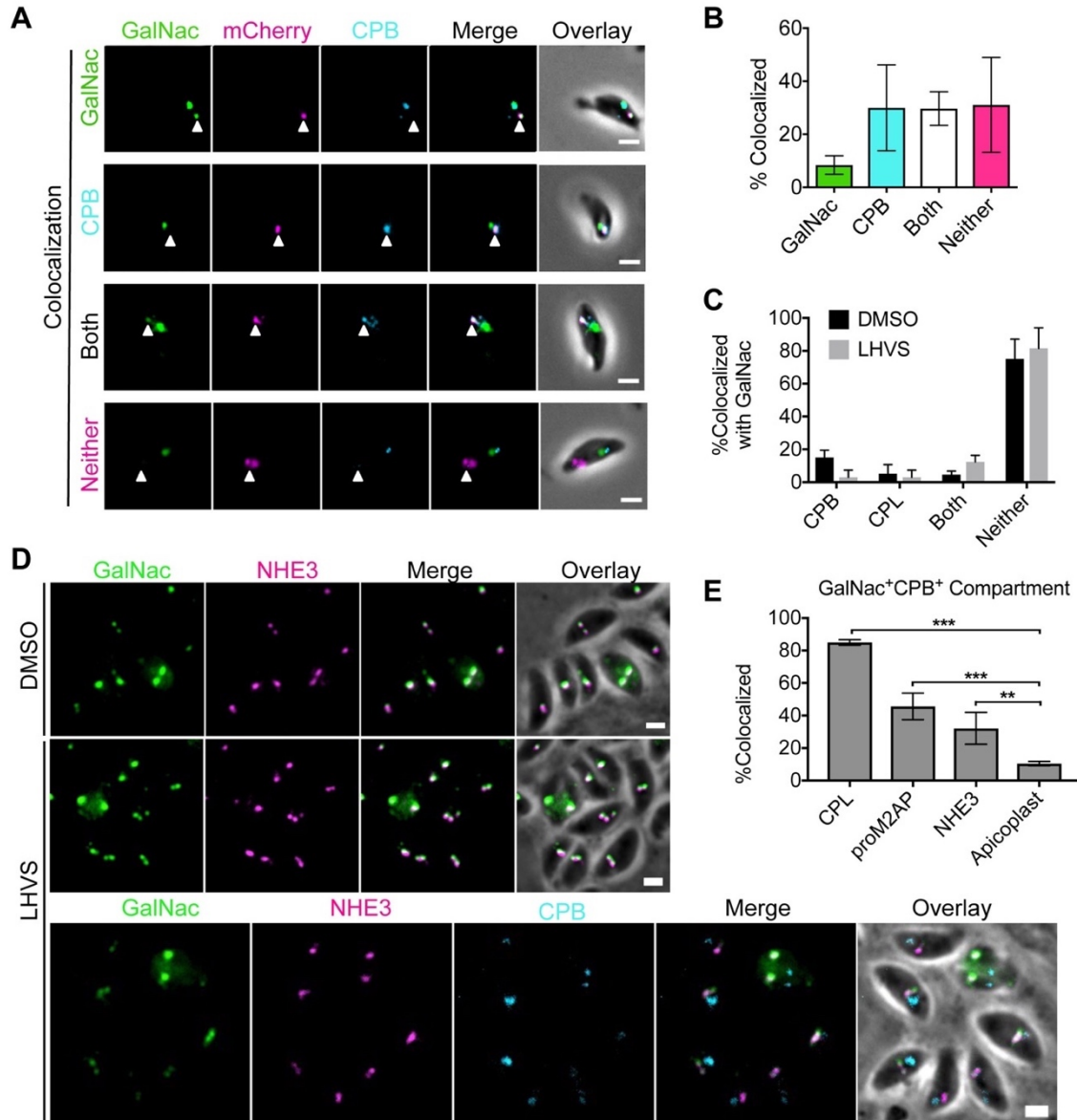


FIGURE 2-4 Ingested mCherry colocalizes with GalNac-YFP in a CPB positive compartment. A, Representative images for localization of ingested mCherry relative to GalNac-YFP and CPB in LHVS-treated GalNac-YFP parasites stained for CPB from Figure 2-2. From top to bottom are examples of ingested mCherry colocalized with GalNac-YFP only, CPB only, both GalNac-YFP and CPB, and neither GalNac-YFP or CPB. White arrows indicate localization of ingested mCherry accumulation. B, Quantitation of colocalization of ingested mCherry with GalNac-YFP and/or CPB in LHVS-treated GalNac-YFP parasites stained for CPB from Figure 2-2. Data are derived from 4 biological replicates with at least 30 ingested mCherry puncta analyzed per marker per replicate. C, Quantitation of colocalization of GalNac-YFP with CPB and CPL in DMSO and LHVS-treated parasites. HFF cells were synchronously invaded for 10 min with GalNac-YFP parasites (pretreated with 1 μ M LHVS or the vehicle control DMSO for 36 h), incubated in the presence of 1 μ M LHVS or DMSO, and fixed at 3 h post-invasion. Parasites were then stained with antibodies against CPB and CPL and analyzed by fluorescence microscopy. Data are derived from 2 biological replicates with at least 33 GalNac-YFP puncta analyzed per replicate. D, Representative images of GalNac-YFP distribution with DMSO or LHVS treatment. GalNac-YFP parasites were treated as in C and stained for NHE3 and CPB. Scale bars, 1 μ M. E, Quantitation of colocalization of the GalNac-YFP+CPB+ compartment with other endolysosomal system markers. GalNac-YFP parasites were treated as in C and stained for CPB and CPL, proM2AP, NHE3, or DAPI to label the apicoplast. Data are derived from 3 biological replicates with at least 20 GalNac-YFP+CPB+ puncta analyzed per marker per replicate, one way ANOVA with Dunnet's test for multiple comparisons to colocalization with the apicoplast, ** p,<0.01, ***p<0.001. All bars represent means, and error bars represent standard deviation. Scale bars: 2 μ m.

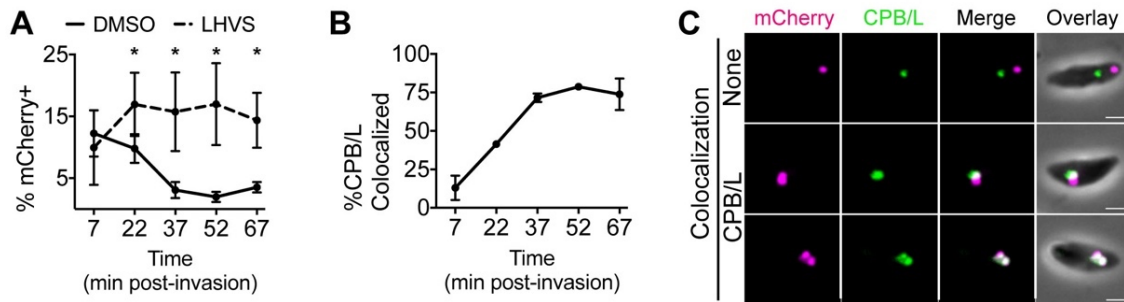


Figure 2-5. Host cytosolic mCherry is ingested into a non-digestive compartment before delivery to the VAC within 30 min. A, Time course of ingestion in DMSO or LHVS-treated GalNac-YFP parasites through 1 h post-invasion. Experiment performed as in Figure 2-2A, but with a 7 min invasion period and harvested at the indicated times. Shown is percentage of mCherry-positive parasites from analysis of at least 200 parasites analyzed per condition and time point. Ratio paired t-test comparing DMSO vs. LHVS treatment at each time point, * $p < 0.05$, otherwise not significant. B, Quantitation of colocalization of ingested mCherry with CPB/L in LHVS-treated parasites from A stained with mouse antibodies against both CPB and CPL. At least 30 ingested mCherry puncta were analyzed per marker and time point. C, Representative images for localization of ingested mCherry relative CPB/L. Scale bars, 2 μm : For all graphs, points represent the mean of 3 biological replicates, bars represent standard deviation.

through the TGN. Nevertheless, the data is consistent with ingested proteins trafficking through ELCs on the way to the VAC.

2.3.3 Ingested proteins reach the VAC for CPL-dependent digestion within 30 min

To better understand the dynamics of ingested protein trafficking to the VAC, GalNac-YFP parasites were prepared as shown in Figure 2-2A, purified at 15 min intervals through the first hour of infection, and LHVS-treated parasites were stained with antibodies against CPB and CPL to label the VAC. Parasite-associated mCherry was detected at the earliest time point (7 min post-invasion) and throughout the first hour of infection (Figure 2-5A). Intriguingly, accumulation of mCherry at 7 min post-invasion was independent of LHVS treatment (Figure 2-5A). Detection of ingested mCherry became increasingly dependent on LHVS treatment at 22 min post-invasion and beyond with ingestion in DMSO-treated parasites reaching the typically observed basal levels by 37 min post-invasion (Figure 2-5A). Colocalization of ingested mCherry with CPB/L increased as detection of ingested protein in DMSO-treated parasites

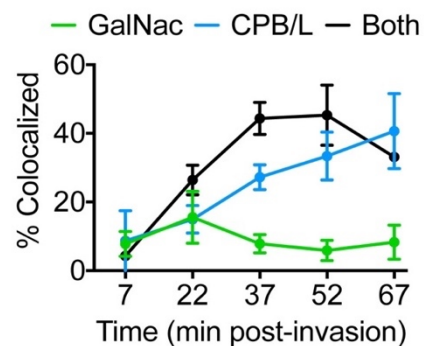


FIGURE 2-6 Peak colocalization with the GalNac-YFP+CPB/L+ compartment coincides with rapid degradation of ingested material. Quantitation of colocalization of ingested mCherry with GalNac YFP or CPB/L in LHVS-treated parasites from Figure 2-5. At least 30 ingested mCherry puncta analyzed per marker and time point. Points represent the mean of 3 biological replicates, bars represent standard deviation.

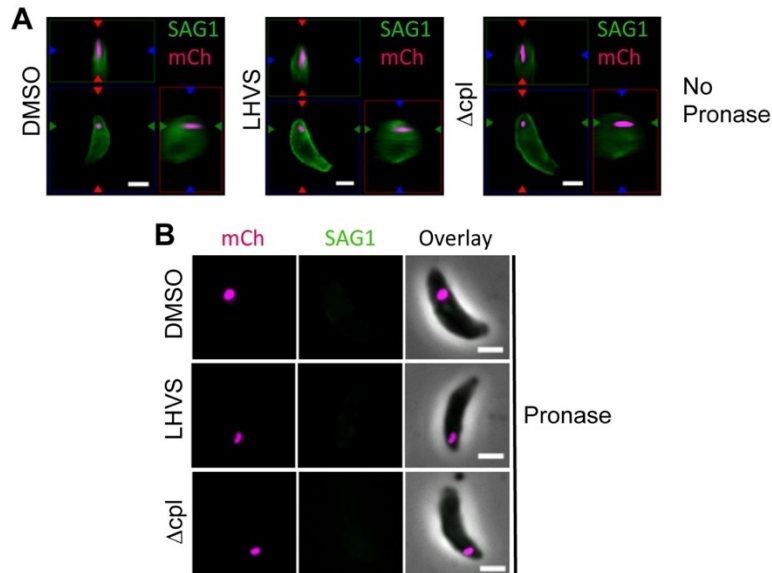


FIGURE 2-7 *T. gondii* ingests host cytosolic mCherry within 7 min post-invasion. A, mCherry accumulation is contained within the SAG1 surface outline of the parasites at 7 min post-invasion. Experiment performed as in Figure 2-5 with a 7 min invasion period, parasites were purified immediately following invasion (7 min post-invasion), and stained for the parasite surface marker SAG1. Unlike the samples in all other experiments in this study, no protease protection assay was performed (No Pronase), leaving SAG1 on the surface of the parasite. Shown are cut views from Z-stacks displaying a single plane that cuts through the center of the accumulated mCherry signal. B, mCherry accumulation, but not SAG1 is resistant to protease protection assay (Pronase). Experiment performed as in Figure 2-5 with a 7 min invasion period, parasites were purified immediately following invasion (7 min post-invasion), subjected to protease protection assay, and stained for the parasite surface marker SAG1. In parasites where SAG1 was digested off the parasite surface, mCherry accumulation remains. Images are derived from one biological replicate performed in GalNac-YFP parasites treated with DMSO or 1 μ M LHVS for 36 h or *RH* Δcpl parasites as indicated. Scale bars: 2 μ m.

decreased, and colocalization with CPB/L peaked at 37 min post-invasion (Figure 2-5B and C). Further, localization within the GalNac-YFP⁺CPB/L⁺ compartment also peaked at 37 min post-invasion (Figure 2-6), indicating that this compartment is digestive in nature, further supporting its identity as a subdomain of the ELCs or the VAC. Although external protease treatment of purified parasites is routinely performed to remove host protein sticking to the parasite surface, we wanted to ensure the mCherry accumulation was truly inside the parasite, especially at 7 minutes post-invasion. Deconvolution of Z-stack images confirmed that the mCherry accumulation was fully contained within the parasite (Figure 2-7A), and ingested mCherry was resistant to external protease treatment while the parasite surface protein SAG1 was not (Figure 2-7B). Taken together, these findings suggest that ingested host proteins are internalized either during or immediately after invasion, initially delivered into a non-proteolytic compartment and then trafficked to the VAC where they are degraded within 30 min.

2.3.4 Promicroneme proteins are detected in all cell cycle phases

Antibody staining against propeptides of microneme and rhoptry proteins label newly synthesized, immature promicroneme and prorhoptry proteins in transit to their respective organelles and possibly also cleaved propeptide, but not mature proteins in the microneme and rhoptry organelles. For example, staining for the propeptide of the microneme protein M2AP (proM2AP) or rhoptry protein ROP4 (proROP4) shows overlap with the TGN and ELCs but not the micronemes or rhoptries.^{7, 13, 34, 36} Therefore, the colocalization of ingested protein with proM2AP noted above suggests that endocytic trafficking to the VAC may intersect with exocytic trafficking to microneme and rhoptry organelles. An important limitation of this experiment, however, is that parasites were treated with LHVS for 36 h prior to infection to emulate detection of ingested host protein in the CPL knockout. Under these conditions, ingested host protein persists with a half-life of 2 to 3 h.¹ Persistent accumulation presumably occurs within the VAC, but trafficking might also be backed up in upstream compartments like the ELCs. Therefore, we cannot differentiate protein ingested several hours prior to fixation from actively trafficking, newly ingested protein. So while we conclude that proM2AP and ingested protein are trafficked through the ELCs, this experiment does not conclusively demonstrate that they occupy the ELCs at the same time under normal conditions. Nevertheless, how these cargoes can be trafficked through the same compartment, yet meet very different fates is unclear.

To test if endocytic and exocytic trafficking in *T. gondii* are temporally separated processes, we next sought to determine when during the cell cycle microneme or rhoptry biogenesis and ingestion occur. *T. gondii* divides by building daughter parasites within the mother cell in a process called endodyogeny and has a cell cycle characterized by three phases: G, S, M/C.³⁷ Progression through the *T. gondii* cell cycle can be monitored using two markers: TgCentrin2 (Cen2) which associates with the centrosome and additional apical structures, and IMC1 which associates with the inner membrane complex, a system of flattened membranous sacs beneath the parasite plasma membrane that outlines the periphery of the mother cell and newly forming daughter parasites.³⁸ In the G phase, parasites display a single mother IMC1 structure and a single centrosome. In S phase, the centrosome is duplicated and in M/C phase, two additional U-shaped IMC1 structures outlining the newly forming daughter cells will appear within

the IMC1 outline of the mother parasite. To test when microneme or rhoptry biogenesis occurs during the cell cycle, Cen2-EGFP parasites were stained with antibodies against IMC1 to determine cell cycle phase and against propeptides of microneme and rhoptry proteins, which in previous experiments have been associated with timing of microneme and rhoptry biogenesis.¹⁸

We first examined microneme protein synthesis using antibodies against proM2AP and proMIC5. proM2AP staining has been observed in all phases of the cell cycle, but to what extent remained unclear.^{7, 34} Parasites were analyzed at 4 to 6 h post-invasion when

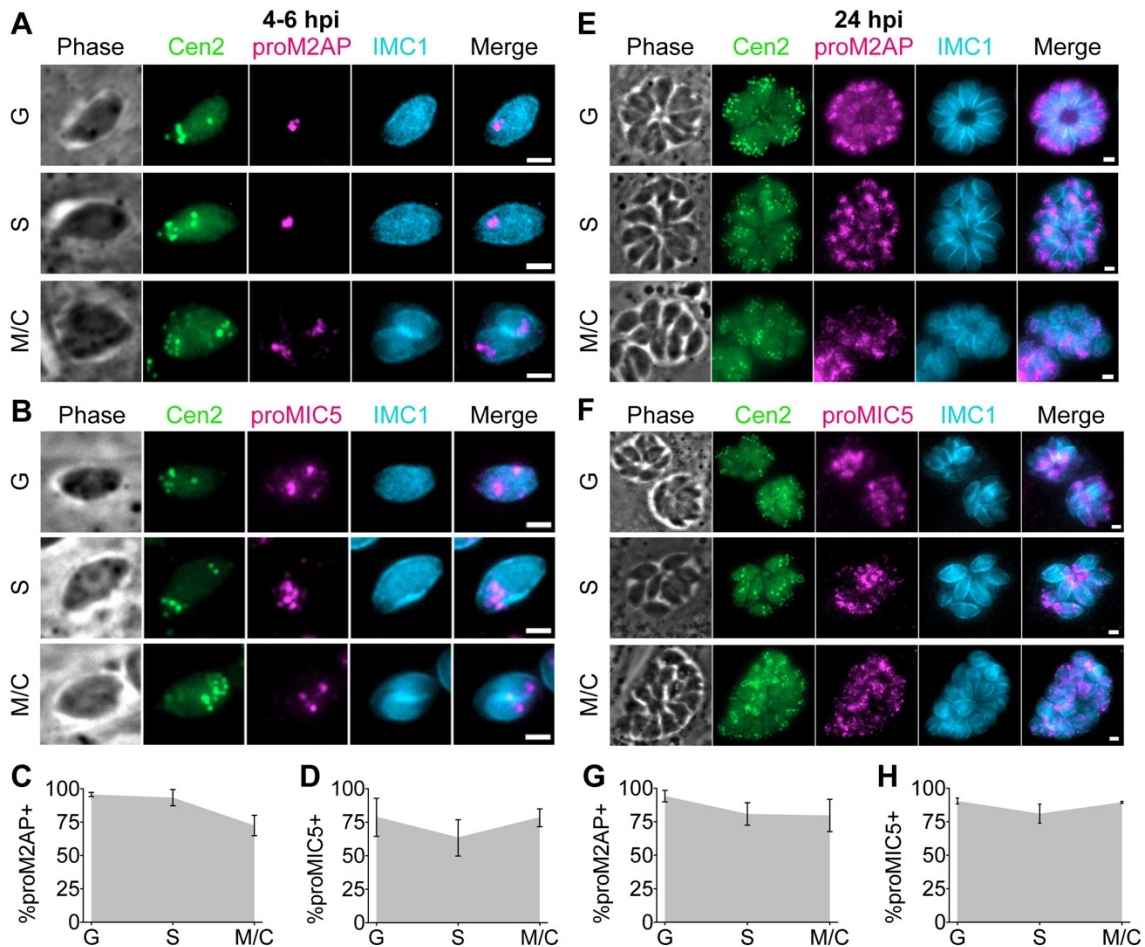


Figure 2-8. Microneme proteins are expressed in G, S and M/C phase. A and B, Representative images for detection of proM2AP or proMIC5 by immunofluorescent staining in G, S and M/C phase Cen2-EGFP vacuoles stained for IMC1 at 4 to 6 h post-invasion. C and D, Quantitation of percentage of Cen2-EGFP vacuoles positive for proM2AP or proMIC5 staining in G, S and M/C phase at 4 to 6 h post-invasion. E and F, Representative images for detection of proM2AP or proMIC5 by immunofluorescent staining in G, S and M/C phase Cen2-EGFP vacuoles stained for IMC1 at 24 h post-invasion. G and H, Quantitation of percentage of Cen2-EGFP vacuoles positive for proM2AP or proMIC5 staining in G, S and M/C phase at 24 h post-invasion. Error bars in all graphs represent standard deviation, and the point where the grey fill intersects the error bars represents the mean. Values derived from 3 biological replicates each with at least 100 total vacuoles and at least 30 vacuoles per cell cycle phase analyzed. Scale bars: 2 μ m.

parasites in all three phases of the cell cycle were present. proM2AP and proMIC5 were detected in G, S and M/C phases, and in the majority of parasite-containing vacuoles (Figure 2-8A through D). To ensure that this was not a product of pulse invasion into host cells or only characteristic of the first cell division, asynchronous, overnight cultures of parasites allowed to naturally invade host cells were also analyzed. Again, proM2AP and proMIC5 were detected in G, S and M/C phases and in the majority of parasite-containing vacuoles (Figure 2-8E through H), suggesting that microneme protein synthesis occurs throughout the cell cycle.

2.3.5 Prorhoptry proteins are detected in S and M/C phases

We next examined detection of rhoptry protein synthesis using antibody staining against proROP4 or proRON4, which is known to label M/C phase parasites.^{17, 39} The

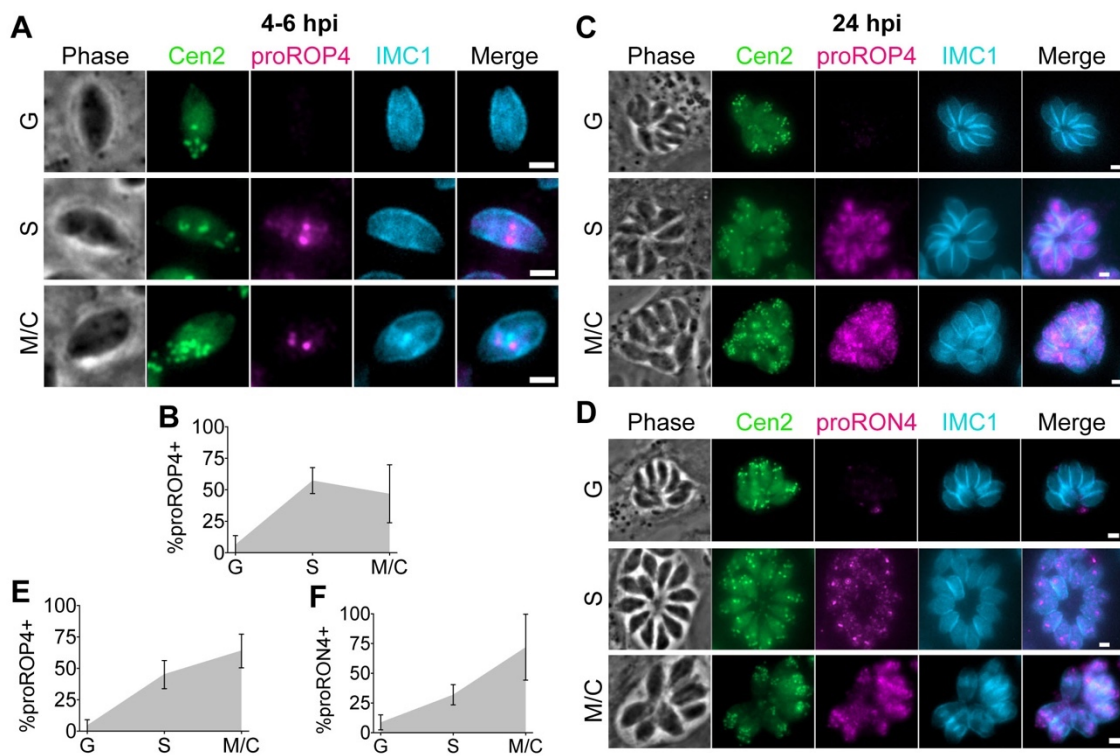


Figure 2-9. Rhoptry proteins are expressed in S and M/C phase. A, Representative images for detection of proROP4 by immunofluorescent staining in G, S and M/C phase Cen2-EGFP vacuoles at 4 to 6 h post-invasion. B, Quantitation of percentage of Cen2-EGFP vacuoles positive for proROP4 staining in G, S and M/C phase at 4 to 6 h post-invasion. C and D, Representative images for detection of proROP4 or proRON4 by immunofluorescent staining in G, S and M/C phase Cen2-EGFP vacuoles at 24 h post-invasion. E and F, Quantitation of percentage of Cen2-EGFP vacuoles positive for proROP4 or proRON4 staining in G, S and M/C phase at 24 h post-invasion. Error bars in all graphs represent standard deviation, and the point where the grey fill intersects the error bars represents the mean. Values are derived from 3 biological replicates each with at least 100 total vacuoles and at least 30 vacuoles per cell cycle phase analyzed. Scale bars: 2 μ m.

antibody mAb T5 4H1, used to detect proRON4, also detects the moving junction. As previously observed, staining of the moving junction remained on the PVM at 4 to 6 h post-invasion and could not be distinguished from staining within the parasites.^{18, 39}

Therefore, RON4 synthesis was only analyzed in asynchronous overnight cultures. proROP4 and proRON4 were detected in both S and M/C phases but were absent from nearly all parasite vacuoles in G phase at 4 to 6 or 24 h post-invasion (Figure 2-9). This suggests that rhoptry protein synthesis is restricted to later in the cell cycle and occurs in both S and M/C phases.

2.3.6 Ingestion is active throughout the cell cycle

We next sought to determine when during the cell cycle *T. gondii* ingests host proteins. To more precisely measure when parasites are ingesting protein from the host cell, LHVS treatment was reduced from 36 h to 30 min, adding LHVS immediately prior to parasite purification (Figure 2-10A). This is the time it takes to complete one ingestion event from uptake to turn over (Figure 2-5) and should reflect only recently ingested protein. Further, this treatment is shorter than the briefest phase of the cell cycle, M/C phase, which is estimated to last from 1 to 3 h.^{37, 40-42} To do this, the LHVS concentration had to be increased from 1 μ M to 50 μ M, but detection of ingested protein under this condition was indistinguishable from parasites treated with LHVS for 36 h (Figure 2-10B).

To test when during the cell cycle the ingestion pathway is active, Cen2-EGFP parasites were treated as in Figure 2-10A, purified at 4 to 6 h post-invasion when all cell cycle phases were observed (Figure 2-10C), and stained with antibodies against IMC1. Because promicroneme and prorhoptry proteins were detected with similar cell cycle dynamics during the first and subsequent cell division cycles (Figures 2-8 and 2-9), cell cycle dependence of ingestion was not analyzed at 24 h post-invasion for comparison. In samples where ingestion was active (Figure 2-10D), ingestion of mCherry was observed in parasites of all three cell cycle phases (Figure 2-10E). To determine if ingestion is down-regulated in any phase of the cell cycle, the percentage of mCherry positive parasites was also determined in G, S or M/C phase parasites. No significant differences

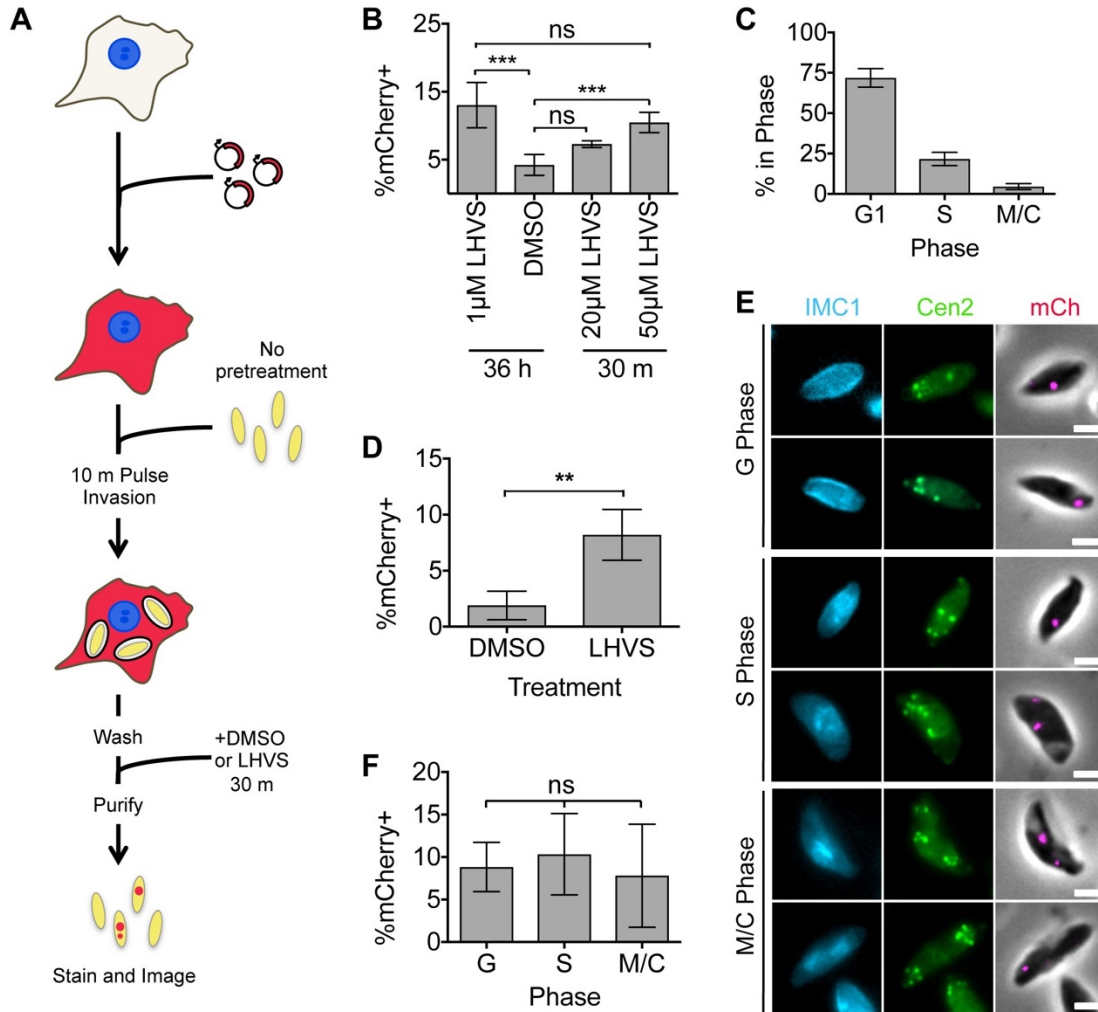


Figure 2-10. *T. gondii* ingests host cytosolic mCherry throughout its cell cycle. A, Experimental design for detection and localization of recently ingested host cytosolic protein ingestion. CHO-K1 cells were transiently transfected with a plasmid encoding cytosolic mCherry fluorescent protein 18-24 h before synchronous invasion for 10 min with untreated *T. gondii* parasites. 50 µM LHVS or DMSO added during the last 30 min of infection before being purified, stained and analyzed by fluorescence microscopy. B, Quantitation of ingestion in Cen2-EGFP parasites treated with DMSO or LHVS for 36 h or 30 m and purified at 3 h post-invasion. Shown is the percentage of mCherry-positive parasites; at least 200 parasites were analyzed per condition, One-way ANOVA with Tukey's multiple comparisons. C, Cell cycle phasing of LHVS-treated Cen2-EGFP parasites harvested at 4 to 6 h post-invasion to be quantitated for ingestion in D as determined by the pattern of Cen2-EGFP and antibody staining for IMC1. D, Quantitation of ingestion in DMSO or LHVS-treated Cen2-EGFP parasites at 4 to 6 h post-invasion. Shown is percentage of mCherry positive parasites, at least 200 parasites analyzed per condition, ratio paired t-test. E, Representative images for detection of ingested host cytosolic mCherry in parasites in G, S or M/C phase. F, Cell cycle phase-specific analysis of ingestion pathway activity. Percentage of mCherry positive parasites in each cell cycle phase from parasites in D was determined with at least 230 parasites in G phase, at least 55 parasites in S phase and at least 24 parasites in M/C phase analyzed, one-way ANOVA. All bars represent the mean of 4 biological replicates, error bars represent standard deviation, ** $p < 0.01$, ns = not significant, scale bars are 2 µm.

were observed, suggesting that ingestion was equally active during all phases of the cell cycle (Figure 2-10F).

2.3.7 Ingested host protein trafficking intersects with microneme protein trafficking

Although our results indicate that ingestion, microneme protein synthesis, and rhoptry protein synthesis are active during the same cell cycle phases and traffic through the ELCs, it is still possible that ingested proteins and microneme or rhoptry proteins could avoid interaction. For example, sequential rounds of ingestion and microneme or rhoptry synthesis could occur independent of the cell cycle. To determine if ingestion is down-regulated during microneme or rhoptry synthesis and if their trafficking paths intersect, as suggested by our findings in Figure 2-2, we compared the trafficking of newly ingested protein with that of newly synthesized microneme and rhoptry proteins en route to their respective apical secretory organelles.

To do this, a new cell line developed during the course of this study was used. These cells, termed CHO-K1 inducible mCherry cells (CHO-K1 imCh), produce cytosolic mCherry in response to induction with doxycycline (Figure 2-11A). mCherry is expressed in $76.0 \pm 0.42\%$ of doxycycline-treated CHO-K1 imCh cells compared to $18.6 \pm 4.3\%$ of transiently transfected CHO-K1 cells (Figure 2-11B). Consistent with the broader expression, we observed mCherry in $42.6 \pm 8.7\%$ of parasites treated with LHVS for 36 h. Also, ingested mCherry was detected in $16.5 \pm 4.1\%$ of parasites treated with LHVS for 30 min, although in this case the LHVS concentration had to be increased to $200 \mu\text{M}$ to consistently detect LHVS-dependent mCherry accumulation (Figure 2-11C and D). It should be noted that despite broader expression the mCherry fluorescence intensity of CHO-K1 imCh cells was about 2.8 times lower than transiently transfected CHO-K1 cells (Figure 2-11B). Thus, results from CHO-K1 imCh cells might still underrepresent the proportion of parasites that are actively ingesting host-derived protein.

To determine if ingestion is down-regulated during microneme or rhoptry biogenesis, parasites were allowed to ingest mCherry from doxycycline-treated CHO-K1 imCh cells and treated with LHVS for 30 min to exclusively detect newly ingested host protein. The parasites were then purified and stained for proM2AP, proMIC5 and proRON4 to detect newly synthesized microneme and rhoptry proteins. We attempted to detect proROP4, but the antibody did not work well in extracellular parasites. In samples where ingestion was active (Figure 2-12A), the activity of the ingestion pathway during microneme and rhoptry biogenesis was analyzed by determining the percentage of

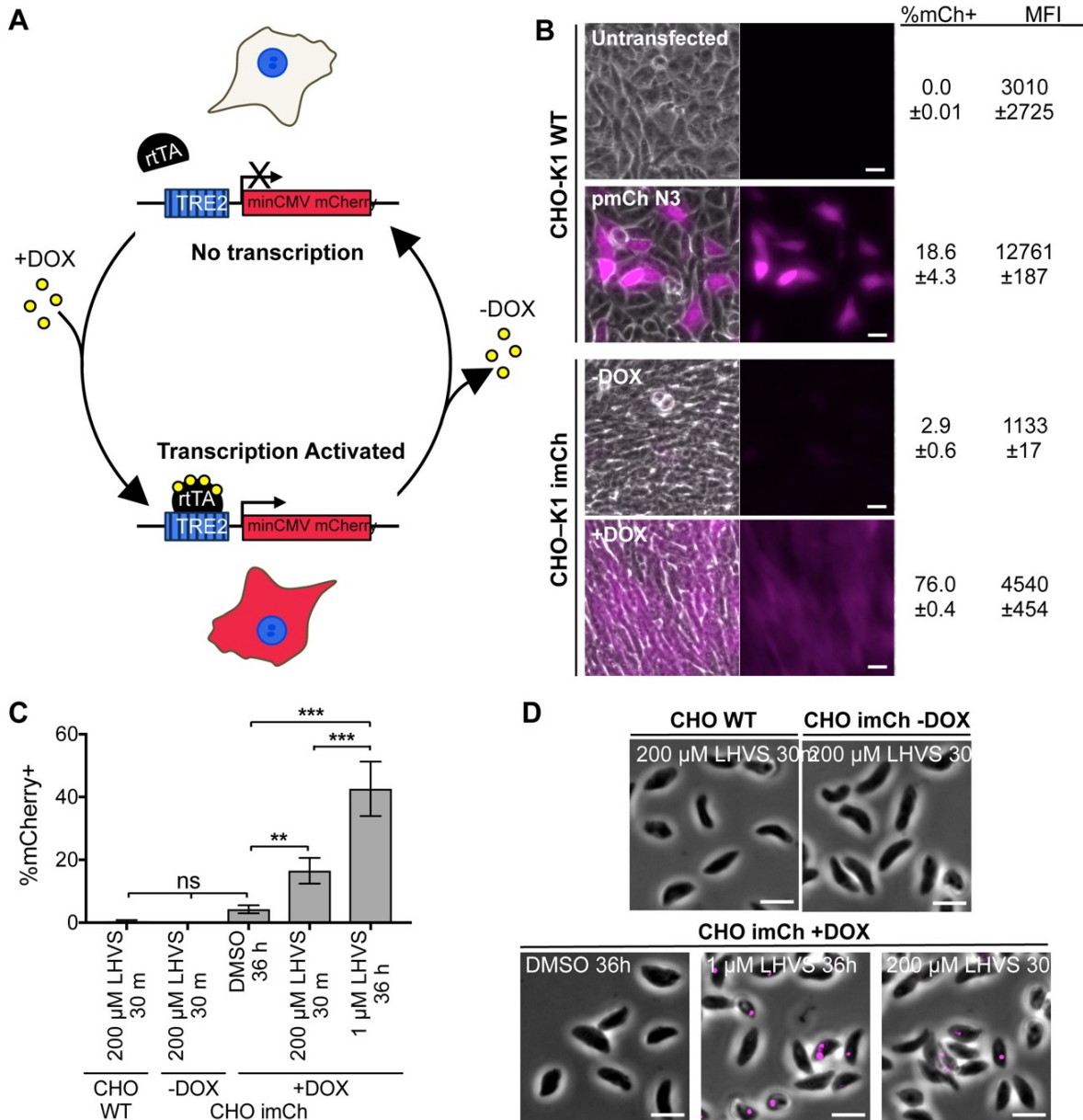


FIGURE 2-11 Validation of CHO-K1 imCherry cell line for detection of ingestion. A, Conceptual model for mCherry expression in CHO-K1 inducible mCherry (CHO-K1 imCh) cell. CHO-K1 cells that stably express mCherry under the control of the minimal CMV promoter and the tetracycline-responsive element (TRE) as well as the reverse tetracycline-controlled transactivator (rtTA) were generated. In the absence of tetracycline or its derivative doxycycline, rtTA cannot bind the TRE, and cytosolic mCherry transcription is repressed. In the presence of doxycycline, doxycycline will bind to rtTA and allow it to bind to the TRE and induce transcription of cytosolic mCherry. B, From top to bottom, representative images of mCherry detection in the parental CHO-K1 WT cell line, CHO-K1 WT cells transiently transfected with the pmCherry N3 plasmid, CHO-K1 imCh cells without DOX for 96 h and CHO-K1 imCh cells treated with 2 μ g/mL DOX for 96 h. To the right are values for the percentage of cells that are mCherry positive (%mCh⁺) and mean fluorescence intensity of the mCherry (MFI) as determined by flow cytometry. Data derived from 2 biological replicates with 20,000 cells analyzed per condition per replicate. Scale bar, 20 μ m. C, Quantitation of ingestion of host cytosolic mCherry from CHO-K1 WT, CHO-K1 WT cells transiently transfected to express cytosolic mCherry, CHO-K1 imCh cells without DOX for 96 h and CHO K1-imCh cells with 2 μ g/mL DOX for 96 h. Cells were synchronously invaded for 10 min with WT parasites treated with DMSO or LHSV as indicated, purified at 3 h post-invasion, fixed and analyzed by fluorescence microscopy. Shown is percentage of mCherry positive parasites with at least 200 parasites analyzed per condition, one-way ANOVA with Tukey's test for multiple comparisons, ** p<0.01, ***p<0.001, ns = not significant. D, Representative images of detection of ingested mCherry from parasites in C. Scale bars: 5 μ m.

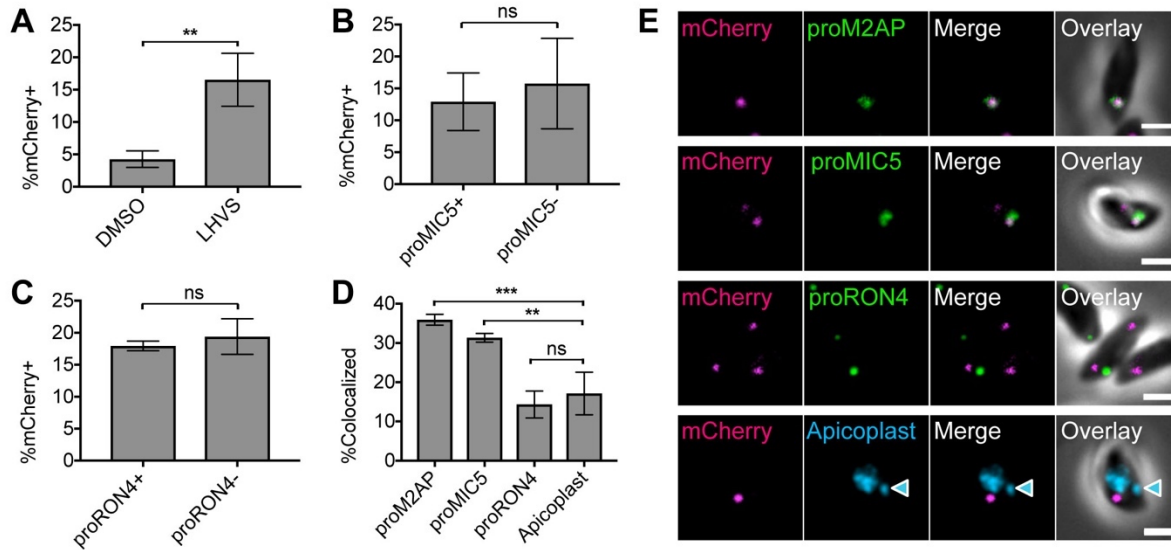


Figure 2-12. Endocytic trafficking is merged with microneme biogenesis in *T. gondii*. **A**, Quantitation of ingestion in DMSO or LHVS-treated WT parasites at 3 h post-invasion. Experiment carried out as in [Figure 2-11C](#) with infection of CHO-K1 imCh cells and 200 μ M LHVS treatment for 30 m to detect recently ingested mCherry only. Shown is percentage of mCherry positive parasites, at least 200 parasites analyzed per condition, unpaired t-test. **B**, Quantitation of ingestion pathway activity during microneme biogenesis by comparing proMIC5 positive and negative populations. Shown is percentage of mCherry positive parasites, at least 200 parasites analyzed for each proMIC5 positive and negative population, ratio paired t-test. **C**, Quantitation of ingestion pathway activity during rhoptry biogenesis by comparing proRON4 positive and negative populations. Shown is percentage of mCherry positive parasites, at least 200 parasites for each proRON4 positive and negative population, ratio paired t-test. **D**, Quantitation of colocalization of ingested mCherry with proM2AP, proMIC5, proRON4 or the apicoplast in LHVS-treated parasites from A stained with antibodies each marker. At least 30 ingested mCherry puncta analyzed per marker. **E**, Representative images of localization of ingested mCherry relative to proM2AP, proMIC5, proRON4 or the apicoplast (indicated by the blue arrow head). All bars represent the mean from 3 biological replicates, error bars represent standard deviation, ** $p < 0.01$, *** $p < 0.001$, ns = not significant, scale bars are 2 μ m.

mCherry⁺ parasites in populations expressing proMIC5 or proRON4 compared to populations of parasites that are negative for each of these markers. This analysis was not performed for proM2AP since 85.9 \pm 8.2% of parasites were expressing proM2AP. Ingestion pathway activity was not significantly different in proMIC5⁺ versus proMIC5⁻ or proRON4⁺ versus proRON4⁻ subpopulations, suggesting that ingestion is not down-regulated during microneme or rhoptry biogenesis (Figure 2-12B and C). Interestingly, even though ingestion is active during microneme and rhoptry biogenesis, ingested protein colocalized with proM2AP and proMIC5, but not proRON4 when compared to the apicoplast negative control (Figure 2-12D and E). Therefore, endocytic trafficking of ingested host proteins intersects with exocytic trafficking to micronemes, but not to rhoptries, suggesting that rhoptry trafficking may diverge earlier in the endolysosomal system such as the TGN or occupy functionally distinct ELCs.

2.4 Discussion

2.4.1 Trafficking of ingested proteins

Our data are consistent with ingested proteins trafficking through the ELCs on the way to the VAC, however we could not conclusively determine if ingested protein is trafficked through the TGN due to extensive localization of GalNac–YFP with ELC markers. Additionally, ingested protein colocalized with GalNac-YFP in a compartment that predominantly labeled with CPB and CPL and seems to be digestive in nature. This suggests an ELC or VAC-like identity for the GalNac-YFP⁺CPB/L⁺ compartment. Indeed, digestion of ingested proteins in prelysosomal compartments has been described in *Plasmodium* parasites. Haemozoin, a visible byproduct of hemoglobin digestion has been observed in transport vesicles en route to the lysosome-like organelle of *Plasmodium* called the digestive vacuole, suggesting that hemoglobin digestion begins and may even be complete before reaching the digestive vacuole.^{29, 43} Where digestion begins in *T. gondii* is unclear, but rapid digestion beginning soon after ingestion could explain why very few parasites have detectable levels of ingested protein in the absence of LHVS. Future use of super resolution microscopy and more precise endomembrane markers, especially of the TGN, will better define the localization of ingested protein. Finally, identifying a method for monitoring *T. gondii* ingestion using live-cell imaging will also be invaluable to determine the order that ingested proteins travel through the endolysosomal compartments, the rate of endocytosis, and whether every parasite undergoes endocytosis.

2.4.2 Cell cycle dependence of microneme and rhoptry biogenesis

Population-based transcriptomic studies and live cell imaging of fluorescently-tagged microneme and rhoptry proteins suggest that microneme and rhoptry organelles are made de novo during daughter cell formation once per cell cycle in M/C phase.^{41, 44} However, transcript levels do not necessarily correspond to protein levels, and fluorescent tagging of microneme and rhoptry proteins will label both immature protein in transit and mature protein within the microneme and rhoptry organelles. Our data suggests that microneme proproteins are present in all phases of the cell cycle, whereas expression of rhoptry proproteins is limited to S and M/C phase. It should be noted that antibodies used

for this study may detect cleaved propeptides, which could persist after mature microneme and rhoptry proteins are further trafficked with an unknown half-life. However, the pattern of protein expression that we observe mirrors expression patterns in transcriptomic data. Microneme transcript levels are decreased in G phase, but remain high throughout the cell cycle, whereas rhoptry protein transcripts show a much sharper drop in the G phase.⁴⁴ Previous work found that expression of promicroneme and prorhoptry proteins is mutually exclusive such that parasites express one or the other, but not both.¹⁸ Together the findings imply that microneme biogenesis occurs in multiple waves during the cell cycle with a pause during a portion of S or M/C phase for rhoptry production. In future studies, live cell imaging of fluorescent protein timers, which change color over time indicating time since synthesis, would be informative in more accurately determining when microneme and rhoptry biogenesis occurs.^{45, 46}

2.4.3 Cell cycle dependence of *T. gondii* ingestion

Endocytosis persists, but is down-regulated during the M/C phase of the cell cycle in mammalian cells.⁴⁷⁻⁴⁹ Similar observations have been made in *Plasmodium* parasites, which undergo schizogony. This process involves a G1/trophozoite stage followed by multiple rounds of nuclear division in S phase and segmentation into many parasites in M/C phase. Endocytosis in *Plasmodium* parasites begins in G1 and is thought to remain active until the fourth nuclear division of the S phase.²⁷⁻³⁰ However, examples of *Plasmodium* segmenters that appear to ingest red blood cell cytoplasm during the final stages of daughter cell formation have been observed.⁵⁰ We find that ingested host cytosolic proteins can be detected in *T. gondii* parasites of all cell cycle phases. Ingestion does not appear to be significantly down-regulated in any phase of the cell cycle. However, it should be noted that we were not able to enrich for M/C phase parasites. Attempts to synchronize cell cycle progression by pulse invasion as observed by Gaji *et al.*⁴² were unsuccessful, because mechanically liberated parasites used to infect mCherry expressing CHO cells were not homogeneously in G0 (data not shown). This limited our power to detect a decrease in ingestion in the M/C phase.

2.4.4 Intersection of endocytosis and exocytosis in *T. gondii*

Ingested protein colocalizes with proM2AP and proMIC5, but not proRON4. This suggests that endocytic trafficking to the VAC intersects with exocytic trafficking to the micronemes, which contrasts with the distinct phases of endocytosis and microneme biogenesis in *Plasmodium* parasites. Microneme biogenesis begins late in the fourth nuclear division, when endocytosis is shut down.^{27, 30} On the other hand, synthesis of *Plasmodium* rhoptry proteins has been observed as early as the G1/trophozoite stage.^{26, 51, 52} Accordingly, endocytosis and rhoptry synthesis likely occur at the same time, opening the possibility that endocytic and exocytic trafficking also intersect in *Plasmodium*. Further, the intersection of ingested protein and microneme protein trafficking in *T. gondii* implies the existence of sorting mechanisms that ensure ingested proteins are delivered to the VAC for destruction and microneme proteins remain intact and are delivered to the microneme organelles. We speculate the existence of yet unidentified receptors for sorting of cargoes to their target organelles, discussed further below.

2.4.5 A model for sorting in the *T. gondii* endolysosomal system

Taken together, we propose the following working model for intracellular trafficking in *T. gondii* (Figure 2-13). Because *T. gondii* replicates inside a PV, ingested proteins must traverse both the PV membrane (PVM) and the parasite plasma membrane. Studies of hemoglobin ingestion by *Plasmodium*, which also reside in a PV, showed that red blood cell cytoplasm is simultaneously taken up across the PVM and parasite plasma membrane through a mouth-like structure called the cytostome, producing double-membrane transport vesicles.^{43, 50} Vesicles have been seen in the cytostome-like structure of *T. gondii* called the micropore⁵³, which is thought to be a site of endocytosis in the parasite, although there is no direct evidence for this. Our initial studies demonstrated that the intravacuolar network (IVN), a system of PVM-associated, membranous tubules extending into the PV lumen, is important for acquiring host proteins.¹ Using *Plasmodium* as a model, we propose that host cell cytoplasm is taken up into double-membrane transport vesicles potentially via the micropore in *T. gondii*. These transport vesicles are proposed to be the non-digestive compartment occupied at

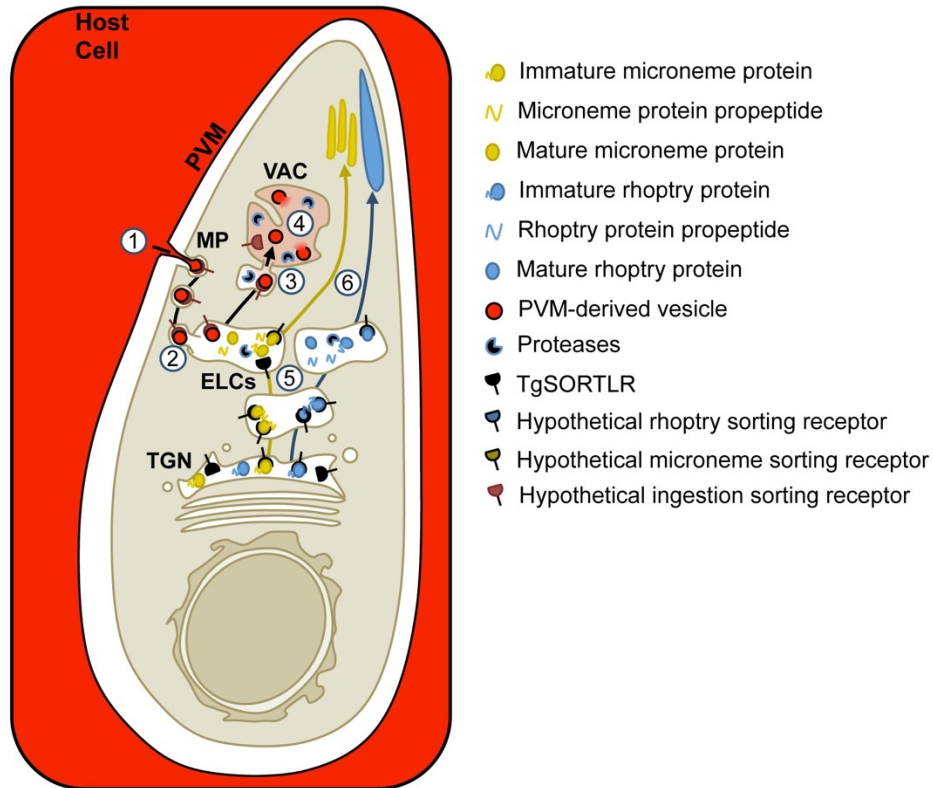


Figure 2-13. Working model for trafficking and sorting of endocytic and exocytic cargoes in *T. gondii*. 1. Host cell cytosol (red) is taken up across the PVM and parasite plasma membrane into double membrane transport vesicles at the micropore (MP). 2. These transport vesicles then fuse with the ELCs and deliver the host cytosol-containing, PVM-derived vesicles to the ELC lumen, where we propose ingested protein trafficking intersects with trafficking of microneme proteins. 3. Fusion of the ELCs with the VAC would then deliver the PVM-derived vesicles to the lumen of the VAC. How the PVM-derived vesicles are sorted away from the microneme proteins is unclear. Trafficking to the VAC may represent a bulk flow pathway independent of receptor-mediated uptake and sorting, or it could require unidentified receptors that recognize parasite proteins associated with the PVM-derived vesicles. This model depicts the possibility of receptor-mediated uptake of PVM-derived vesicles at the parasite plasma membrane and escorting them all the way to the VAC. 4. In the VAC, the PVM-derived vesicles are presumably ruptured by parasite lipases, releasing host cytosolic proteins and exposing them to degradation by parasite proteases. 5. Immature microneme and rhoptry proteins are escorted to the ELCs by TgSORTLR where their propeptides are cleaved off by proteases. However, trafficking at some point diverges so that trafficking of microneme proteins intersect with ingested protein, but rhoptry proteins do not and may occupy a distinct subset of ELCs. 6. Microneme and rhoptry proteins are sorted from the ELCs to their respective organelles by unknown mechanisms that likely involve unidentified receptors.

7 min post-invasion and could be derived from endocytosis of IVN tubules or vesicles derived from the PVM. Active ingestion at 7 min post-invasion (Figure 2-5A) before the IVN is formed favors the existence of PVM vesicles. The IVN may contribute to ingestion indirectly through its role in organizing parasites within the PV.^{54, 55} We could not conclusively determine if ingested protein colocalized with the TGN, but our data is consistent with trafficking through the ELCs. Our model represents a conservative interpretation of the data, predicting yeast or mammal-like endocytic trafficking. In this case, transport vesicles will fuse with the ELCs, releasing PVM-derived vesicles into the

ELC lumen. The PVM-derived vesicles are then delivered to the VAC where they are digested. Intersection of ingested protein trafficking with exocytic trafficking to the micronemes is predicted to occur in the ELCs. How micronemes, rhoptries and ingested protein vesicles are further sorted from the ELCs to their respective target organelles is unclear and likely requires additional, unidentified sorting receptors including potential transmembrane receptors on the parasite surface that could escort PVM-derived vesicles to the VAC. Future studies will seek to better understand the molecular mechanisms of ingested protein trafficking to the VAC and sorting away from microneme proteins. Discovery of plant-like features will be particularly interesting and will provide potential targets for development of novel therapeutics that are divergent from the mammalian cells that *T. gondii* infects.

2.5 Materials and methods

Host Cell and Parasite Culture

All cells and parasites were maintained in a humidified incubator at 37°C with 5% CO₂. CHO-K1 cells (ATCC® CCL-61™) were maintained in Ham's F12 supplemented with 10% FBS, 20 mM HEPES, and 2 mM L-glutamine. HFF cells (ATCC® CRL-1634™) were maintained in Dulbecco's modified Eagle's medium (DMEM) supplemented with 10% Cosmic Calf serum, 20 mM HEPES, 2 mM L-glutamine, and 50µg/ml penicillin/streptomycin. *Toxoplasma gondii* parasites were maintained by serial passaging in HFF cells. Centrin2-EGFP parasites were kindly provided by Dr. Ke Hu of Indiana University and were maintained in the presence of 1 µM pyrimethamine.³⁸

Generation of Parasite Lines

To generate the GalNac-YFP strain, 50µg of the pTUB GalNac YFP CAT plasmid⁵⁶ was transfected into 1.7x10⁷ RH parasites by electroporation in a 4 mm gap cuvette using a Bio-Rad Gene Pulser II set to exponential decay program with 1500 V, 25 µF capacitance and no resistance. Transfected parasites were cultured in HFF cells in the presence of chloramphenicol. Once chloramphenicol-resistance was established, clones were obtained by limiting dilution of the population and confirmed by immunofluorescence.

Transient Transfection of *Toxoplasma*

50µg of the pDHFR GRASP55-mRFP plasmid⁵⁶ was transfected into 1×10^8 GalNac-YFP parasites by electroporation in a 4 mm gap cuvette in the presence of 1% DMSO using a Bio-Rad Gene Pulser II set to exponential decay with 2400 V, 25 µF capacitance and 24 Ω resistance. Transfected parasites were cultured in HFF cells for 24 to 48 h before experimentation.

Chemicals and Reagents

Morpholine urea-leucyl-homophenyl-vinylsulfone phenyl (LHVS) was kindly provided in powdered form by Dr. Matthew Bogyo at Stanford University. LHVS was dissolved in DMSO, and applied with a final DMSO concentration of 0.1-1%.

Plasmids

pCMV mCherry N3 plasmid was kindly provided by Dr. Jonathan Howard Instituto Gulbenkian de Ciecia.⁵⁷ pTUB-GalNac-YFP CAT⁵⁶ and pDHFR GRASP55-mRFP³² plasmids were kindly provided by Dr. David Roos at University of Pennsylvania. pTRE2hyg plasmid (Clontech Cat# 631014) was generously provided by Dr. Christiane Wobus at the University of Michigan.

Transfection of CHO-K1 Cells

CHO-K1 cells were plated in 35 mm dishes and transfected when they reached 70-80% confluency. Each dish was transfected with 2 µg of pCMV mCherry N3 plasmid using the X-TREMEGENE 9 Transfection Reagent (Roche, Cat# 6365787001) using a 3:1 ratio of plasmid to transfection reagent in Opti-MEM (Gibco, Cat#31985062) and a total final volume of 200 µl. Cells were then incubated overnight at 37°C and infected at 18-24 h post-transfection.

Synchronized Invasion

Synchronous invasion was accomplished using the ENDO Buffer Method of invasion⁵⁸ with the following modifications. Briefly, parasite cultures were purified by scraping, syringing, and passing through a 3µm filter and then pelleted by spinning at 1000xg for

10 min. The pellet was then resuspended to $1-3 \times 10^7$ parasites per 1 mL in ENDO Buffer (44.7 mM K_2SO_4 , 10mM $MgSO_4$, 106mM sucrose, 5 mM glucose, 20 mM Tris- H_2SO_4 , 3.5 mg/ml BSA, pH 8.2) for infection of 35 mm dishes, $0.3-1 \times 10^7$ parasites per 1 mL ENDO Buffer for infection of 8-well chamber slides. Host cells were rinsed once with ENDO Buffer, and then 1 mL of ENDO Buffer-parasite suspension was added to each 35 mm dish or 100 μ l of ENDO Buffer-parasite suspension was added to each chamber of an 8-well chamber slide. Parasites were allowed to settle at 37°C for 10 min before the ENDO Buffer was removed and replaced with twice the volume of Invasion Media (Ham's F12/3% Cosmic Calf Serum/20 μ M HEPES). Parasites were allowed to invade at 37°C for 7 or 10 min as indicated. Cells were washed three times with warm media to remove uninvaded parasites and placed back at 37°C until ready for purification or fixation.

Protease Protection Assay

Protease protection assay was performed as in reference 3. Briefly, purified parasites were pelleted for 10 min at 1000xg at 4°C, supernatant was removed, and resuspended in 250 μ l of freshly prepared 1 mg/mL Pronase (Roche, Cat# 10165921001)/0.01% Saponin/PBS and incubated at 12°C for 1 h. Reaction was stopped with the addition of 5 mL ice cold PBS.

Intracellular Fluorescent Protein Acquisition Assay for assessment of ingestion and colocalization with ELCs

Transfected CHO-K1 cells were synchronously invaded by the ENDO Buffer method with *T. gondii* parasites, treated with LHVS or equal volume of DMSO, and purified at the indicated times post-invasion as previously described.¹ All steps are performed on ice or at 4°C unless otherwise noted. Infected cells were washed twice with ice-cold PBS to remove any extracellular parasites, and intracellular parasites were liberated and purified by scraping and syringing with a 5/8" 25g needle before passing through a 3 μ m filter. Parasites were then subjected to the protease protection assay. Parasites were then pelleted by spinning at 1000xg for 10 min and washed three times in ice cold PBS before depositing on Cell-Tak (Corning, Cat# 354240) coated chamber slides. Parasites were fixed with 4% formaldehyde at room temperature, permeabilized with 0.1% Triton X-100,

and stained with antibodies as indicated. Parasites were imaged at 63x with an AxioCAM MRm camera-equipped Zeiss Axiovert Observer Z1 inverted fluorescence microscope. Ingestion of host mCherry was scored manually as mCherry positive or mCherry negative. Colocalization of ingested mCherry with endolysosomal markers was scored manually with each ingested mCherry spot being scored using a binary measure of colocalized or not, giving a readout of percent ingested mCherry puncta colocalized with a given endolysosomal system marker within each experiment. Ingested mCherry puncta were scored as colocalized if they showed any overlap, and there was no differentiation between complete or partial colocalization. As a negative control indicating random colocalization, colocalization of ingested host protein with the apicoplast was determined, since the apicoplast is in the same general region as the proposed endosomal compartments but is expected to be separate from endocytic trafficking. An independent, blinded observer validated the colocalization findings by reanalyzing 15 percent of the colocalization data. Their findings confirmed the reported results.

Immunofluorescent Antibody Labeling

Purified parasites or chamberslides were fixed with 4% formaldehyde for 20 min, and washed 3 times with PBS for 5 min each. Slides were then permeabilized with 0.1% TritonX-100 for 10 min, rinsed three times in PBS, blocked with 10%FBS/0.01% Triton X-100/PBS, and incubated in primary antibody diluted in wash buffer (1% FBS/1% NGS/0.01% Triton X-100/PBS) for 1 h at room temperature. The following primary antibodies and dilutions were used in this study. Affinity purified rabbit anti-CPL (1:100)⁵⁹, mouse anti-CPB (1:100)⁶⁰, affinity purified rabbit anti-proM2AP (1:400)⁷, rabbit anti-P30 (SAG1) (1:1000)⁶¹ kindly provided by Dr. John Boothroyd at Stanford University, affinity purified mouse anti-SAG1 (US Biological) (1:1000), affinity purified rabbit proMIC5 (1:100)¹⁰, mouse α RON4 mAb T5 4H1 (1:100) kindly provided by Jean-Francois Dubremetz³⁹, rabbit α proROP4 UVT70 (1:3000) and mouse anti-IMC1 (1:1000) kindly provided by Dr. Gary Ward of University of Vermont^{17, 62}, and rabbit anti-IMC1 (1:1000) kindly provided by Dr. Con Beckers of University of North Carolina, Chapel Hill.⁶² Slides were washed three times and then incubated in Alex Fluor goat anti-mouse, anti-rabbit, anti-rat secondary antibody (Invitrogen Molecular Probes) diluted (1:1000) in wash buffer

for 1 h at room temperature. Slides were washed three times and mounted in Mowiol before imaging at 63x with an AxioCAM MRm camera-equipped Zeiss Axiovert Observer Z1 inverted fluorescence microscope.

Generating CHO-K1 inducible mCherry Cells

A plasmid expressing mCherry under a tetracycline-inducible minimal CMV promoter was generated by inserting mCherry into the pTRE2hyg plasmid (Clontech Cat# 631014) using Gibson Assembly. mCherry was amplified from the pmCherry N3 plasmid using the forward primer 5'-ctagtcagctgacgcgtgatggtgagca agggcgag-3' and reverse primer 5'-tcgatcggccgcgctagttactgtacagctcgtc-3'. The pTRE2 plasmid was cut within the multiple cloning site using NheI, and mCherry was inserted by homologous recombination using Gibson Assembly Master Mix (NEB, Cat# E2611S) to generate the plasmid pTRE2-mCherry. Insertion was confirmed by sequencing. pTRE2-mCherry and pTet-On (Clontech, Cat# 631018), expressing the reverse tet-responsive transcriptional activator, were cotransfected into CHO-K1 cells and selected with 200 µg/mL hygromycin B (Invitrogen, Cat# 10687010) and 400 µg/mL geneticin (Invitrogen, Cat# 10131035). After recovery from drug selection, the cells were maintained in culture with 200µg/mL hygromycin B and 400 µg/mL geneticin, sorted for the brightest mCherry signal following treatment with doxycycline (Clontech, Cat# 63111) by live fluorescence-associated cell sorting and cloned out. Clones were chosen based on screening for lack of signal in the absence of doxycycline and intensity of mCherry following treatment with addition of 1 µg/mL doxycycline for 48 h. Fluorescence intensity as compared to transiently transfected CHO-K1 WT cells was evaluated using flow cytometry using a BD LSRFortessa Cell Analyzer with FACSDiva software.

Green-blue invasion assay for viability of mCherry+ parasites

Ability of mCherry+ parasites to invade host cells was determined using a modified red-green invasion assay.⁶³ The intracellular fluorescent protein acquisition assay was performed with RH parasites treated with 1µM LHVS for 36 h harvested from iCHO imCh cells at 3 hpi with the following modifications. Protease protection assay was not performed, and instead, parasites were resuspended in 100 µl DMEM/10% Cosmic Calf

serum/20 mM HEPES/2 mM L-glutamine/50µg/ml penicillin/streptomycin/1µM LHVS and allowed to invade HFF cells in an 8-chamber slide for 30 min at 37°C. Treatment with 1 µM LHVS during the invasion period was performed to prevent mCherry degradation. The chamber slide was then gently washed to remove uninvaded and unattached parasites, fixed with 4% formaldehyde for 20 min, and washed 3 times with PBS for 5 min each. Extracellular parasites were stained by blocking with 10%FBS/PBS followed by incubation with rabbit anti-SAG-1 diluted in wash buffer without detergent (1% FBS/1% NGS/PBS) for 1 h at room temperature. Both intracellular and extracellular parasites were then stained with mouse anti-SAG-1 or mouse anti-CPL according to the immunofluorescent antibody labeling protocol above beginning with Triton X-100 permeabilization.

2.6 Notes and notable contributions

Data in this chapter was published in *Traffic*:

McGovern OL, Rivera-Cuevas Y, Kannan G, Narwold A, Jr, Carruthers VB. Intersection of Endocytic and Exocytic Systems in *Toxoplasma gondii*. *Traffic*. 2018. doi: 10.1111/tra.12556 [doi].

Author contributions are as follows. Olivia McGovern and Vern Carruthers designed experiments. Data in Figures 2-2 and 2-5 was generated and analyzed by Olivia McGovern, and Yolanda Rivera-Cuevas carried out a blinded analysis of 15% of the colocalization data to validate Olivia's findings and method for analyzing colocalization. Experiments for Figures 2-9 and 2-10 were carried out and analyzed by Yolanda Rivera-Cuevas and Andrew Narwold, Jr. The CHO-K1 imCherry cell line used to generate data in Figures 2-3, 2-11 and 2-12 in this study was created by Geetha Kannan. CHO-K1 imCherry cells were prepared for flow cytometry by Olivia McGovern, and Geetha Kannan and a collaborator (mentioned below) contributed equally to collecting and analyzing flow cytometry data in Figure 2-11. Data for all other figures was collected and analyzed by Olivia McGovern.

Other contributions are as follows. The ingestion assay used in this study was

originally designed by Zhicheng Dou and was modified by Olivia McGovern to include synchronized invasion and reduced LHVS treatment times. A special thank you to Ronald Holz for his suggestion to reduce LHVS treatment to more accurately measure when host protein ingestion is occurring, which made experiments in Figure 2-10 and 2-12 possible. Sophina Taitano and Geetha Kannan contributed equally to collecting and analyzing flow cytometry data in Figure 2-12. We gratefully acknowledge funding to support this work including NIH T32 Molecular Mechanisms of Microbial Pathogenesis (5T32AI007528 to Olivia McGovern), NIH Ruth L. Kirschstein F31- Diversity (1F31AI118274-01 to Olivia McGovern), and ASM Robert D. Watkins Graduate Research Fellowship (to Olivia McGovern) and an NIH operating grant (R01AI120607 to Vern Carruthers). We thank our colleagues for the generous contribution of reagents essential for this study including Ke Hu, David Roos, Matthew Bogoyo, Jonathan Howard, Christiane Wobus, Peter Bradley, Jean-Francois Dubremetz, Gustavo Arrizabalaga, Gary Ward, and Con Beckers.

2.7 References

1. Dou Z, McGovern O, Di Cristina M, Carruthers V. *Toxoplasma gondii* ingests and digests host cytosolic proteins. *mBio*. 2014;5(4):e01188-14.
2. Stenmark H. Rab GTPases as coordinators of vesicle traffic. *Nat Rev Mol Cell Biol*. 2009;10(8):513-525. doi: 10.1038/nrm2728 [doi].
3. Dettmer J, Hong-Hermesdorf A, Stierhof Y, Schumacher K. Vacuolar H⁺-ATPase activity is required for endocytic and secretory trafficking in Arabidopsis. *Plant Cell*. 2006;18:715-730.
4. Tomavo S, Slomianny C, Meissner M, Carruthers VB. Protein trafficking through the endosomal system prepares intracellular parasites for a home invasion. *PLoS Pathog*. 2013;9(10):e1003629. doi: 10.1371/journal.ppat.1003629 [doi].
5. Pieperhoff MS, Schmitt M, Ferguson DJ, Meissner M. The role of clathrin in post-Golgi trafficking in *Toxoplasma gondii*. *PLoS One*. 2013;8(10):e77620. doi: 10.1371/journal.pone.0077620 [doi].
6. Miranda K, Pace DA, Cintron R, et al. Characterization of a novel organelle in *Toxoplasma gondii* with similar composition and function to the plant vacuole. *Mol Microbiol*. 2010;76(6):1358-1375. doi: 10.1111/j.1365-2958.2010.07165.x [doi].
7. Harper JM, Huynh MH, Coppens I, Parussini F, Moreno S, Carruthers VB. A cleavable propeptide influences *Toxoplasma* infection by facilitating the trafficking and secretion of the TgMIC2-M2AP invasion complex. *Mol Biol Cell*.

- 2006;17(10):4551-4563. doi: E06-01-0064 [pii]; 10.1091/mbc.E06-01-0064 [doi].
8. Kremer K, Kamin D, Rittweger E, et al. An Overexpression Screen of *Toxoplasma gondii* Rab-GTPases Reveals Distinct Transport Routes to the Micronemes. *PLoS Pathog.* 2013;9(3):e1003213. doi: 10.1371/journal.ppat.1003213; 10.1371/journal.ppat.1003213.
 9. Breinich MS, Ferguson DJ, Foth BJ, et al. A dynamin is required for the biogenesis of secretory organelles in *Toxoplasma gondii*. *Curr Biol.* 2009;19(4):277-286. doi: 10.1016/j.cub.2009.01.039.
 10. Brydges SD, Harper JM, Parussini F, Coppens I, Carruthers VB. A transient forward-targeting element for microneme-regulated secretion in *Toxoplasma gondii*. *Biol Cell.* 2008;100(4):253-264. doi: 10.1042/BC20070076.
 11. Sangare LO, Alayi TD, Westermann B, et al. Unconventional endosome-like compartment and retromer complex in *Toxoplasma gondii* govern parasite integrity and host infection. *Nat Commun.* 2016;7:11191. doi: 10.1038/ncomms11191 [doi].
 12. Sloves PJ, Delhaye S, Mouveaux T, et al. *Toxoplasma* sortilin-like receptor regulates protein transport and is essential for apical secretory organelle biogenesis and host infection. *Cell Host Microbe.* 2012;11(5):515-527. doi: 10.1016/j.chom.2012.03.006; 10.1016/j.chom.2012.03.006.
 13. Venugopal K, Werkmeister E, Barois N, et al. Dual role of the *Toxoplasma gondii* clathrin adaptor AP1 in the sorting of rhoptry and microneme proteins and in parasite division. *PLoS Pathog.* 2017 Apr 21;13(4):e1006331.
 14. Bargieri D, Lagal V, Andenmatten N, Tardieux I, Meissner M, Ménard R. Host Cell Invasion by Apicomplexan Parasites: The Junction Conundrum. *PLoS Pathog.* 2014 Sep 18;10(9):e1004273. doi: 10.1371/journal.ppat.1004273. eCollection 2014 Sep.
 15. Dowse T, Soldati D. Host cell invasion by the apicomplexans: the significance of microneme protein proteolysis. *Curr Opin Microbiol.* 2004;7(4):388-396. doi: 10.1016/j.mib.2004.06.013.
 16. Hunter CA, Sibley LD. Modulation of innate immunity by *Toxoplasma gondii* virulence effectors. *Nat Rev Microbiol.* 2012;10(11):766-778. doi: 10.1038/nrmicro2858; 10.1038/nrmicro2858.
 17. Carey KL, Jongco AM, Kim K, Ward GE. The *Toxoplasma gondii* rhoptry protein ROP4 is secreted into the parasitophorous vacuole and becomes phosphorylated in infected cells. *Eukaryot Cell.* 2004;3(5):1320-30.
 18. Besteiro S, Michelin A, Poncet J, Dubremetz J, Lebrun M. Export of a *Toxoplasma gondii* Rhoptry Neck Protein Complex at the Host Cell Membrane to Form the Moving Junction during Invasion. *PLoS Pathog.* 2009;Feb;5(2):e1000309.

19. Etheridge RD, Alaganan A, Tang K, Lou HJ, Turk BE, Sibley LD. The *Toxoplasma* pseudokinase ROP5 forms complexes with ROP18 and ROP17 kinases that synergize to control acute virulence in mice. *Cell Host Microbe*. 2014 May 14;15(5):537-550.
20. Huynh MH, Carruthers VB. A *Toxoplasma gondii* Ortholog of Plasmodium GAMA Contributes to Parasite Attachment and Cell Invasion. *mSphere*. 2016;1(1):10.1128/mSphere.00012-16. eCollection 2016 Jan-Feb. doi: 10.1128/mSphere.00012-16 [doi].
21. Huynh MH, Boulanger MJ, Carruthers VB. A conserved apicomplexan microneme protein contributes to *Toxoplasma gondii* invasion and virulence. *Infect Immun*. 2014;82(10):4358-4368. doi: 10.1128/IAI.01877-14 [doi].
22. Sidik SM, Huet D, Ganesan SM, et al. A Genome-wide CRISPR Screen in *Toxoplasma* Identifies Essential Apicomplexan Genes. *Cell*. 2016;166(6):1423-1435.e12. doi: 10.1016/j.cell.2016.08.019 [doi].
23. Kafsack BF, Pena JD, Coppens I, Ravindran S, Boothroyd JC, Carruthers VB. Rapid membrane disruption by a perforin-like protein facilitates parasite exit from host cells. *Science*. 2009;323(5913):530-533. doi: 10.1126/science.1165740.
24. Guerin A, Corrales RM, Parker ML, et al. Efficient invasion by *Toxoplasma* depends on the subversion of host protein networks. *Nat Microbiol*. 2017;2(10):1358-1366. doi: 10.1038/s41564-017-0018-1 [doi].
25. Futter CE, Connolly CN, Cutler DF, Hopkins CR. Newly synthesized transferrin receptors can be detected in the endosome before they appear on the cell surface. *J Biol Chem*. 1995 May 5;270(18):10999-11003.
26. Margos G, Bannister LH, Dluzewski AR, Hopkins J, Williams IT, Mitchell GH. Correlation of structural development and differential expression of invasion-related molecules in schizonts of *Plasmodium falciparum*. *Parasitology*. 2004 Sep;129(Pt 3):273-287.
27. Hanssen E, Knoechel C, Dearnley M, et al. Soft X-ray microscopy analysis of cell volume and hemoglobin content in erythrocytes infected with asexual and sexual stages of *Plasmodium falciparum*. *J Struct Biol*. 2012;177(2):224-232. doi: 10.1016/j.jsb.2011.09.003 [doi].
28. Francis SE, Gluzman IY, Oksman A, et al. Molecular characterization and inhibition of a *Plasmodium falciparum* aspartic hemoglobinase. *EMBO J*. 1994 Jan 15;13(2):306-317.
29. Bakar NA, Klonis N, Hanssen E, Chan C, Tilley L. Digestive-vacuole genesis and endocytic processes in the early intraerythrocytic stages of *Plasmodium falciparum*. *J Cell Sci*. 2010;123:441-450; doi: 10.1242/jcs.061499.

30. Krugliak M, Zhang J, Ginsburg H. Intraerythrocytic *Plasmodium falciparum* utilizes only a fraction of the amino acids derived from the digestion of host cell cytosol for the biosynthesis of its proteins. *Mol Biochem Parasitol.* 2002;Feb;119(2):249-256.
31. Uemura T, Nakano A. Plant TGNs: dynamics and physiological functions. *Histochem Cell Biol.* 2013 Sep;140(3):341-345. doi: 10.1007/s00418-013-1116-7. Epub 2013 Jul 6.
32. Pfluger SL, Goodson HV, Moran JM, et al. Receptor for retrograde transport in the apicomplexan parasite *Toxoplasma gondii*. *Eukaryot Cell.* 2005;Feb 4(2):432-42.
33. Francia ME, Wicher S, Pace DA, Sullivan J, Moreno SNJ, Arrizabalaga G. A *Toxoplasma gondii* protein with homology to intracellular type Na⁺/H⁺ Exchangers is important for osmoregulation and invasion. *Exp Cell Res.* 2011 Jun 10;317(10):1382-1396.
34. Parussini F, Coppens I, Shah PP, Diamond SL, Carruthers VB. Cathepsin L occupies a vacuolar compartment and is a protein maturase within the endo/exocytic system of *Toxoplasma gondii*. *Mol Microbiol.* 2010;76(6):1340-1357. doi: 10.1111/j.1365-2958.2010.07181.x.
35. Uemura T, Suda Y, Ueda T, Nakano A. Dynamic Behavior of the trans-Golgi Network in Root Tissues of Arabidopsis Revealed by Super-Resolution Live Imaging. *Plant Cell Physiol.* . 2014 Apr;55(4):694-703. doi: 10.1093/pcp/pcu010. Epub 2014 Jan 18.
36. Sakura T, Sindikubwabo F, Oesterlin LK, et al. A Critical Role for *Toxoplasma gondii* Vacuolar Protein Sorting VPS9 in Secretory Organelle Biogenesis and Host Infection. *Sci Rep.* 2016 Dec 14;6:38842-doi: 10.1038/srep38842.
37. Radke JR, Striepen B, Guerini MN, Jerome ME, Roos DS, White MW. Defining the cell cycle for the tachyzoite stage of *Toxoplasma gondii*. *Mol Biochem Parasitol.* 2001;115(2):165-175.
38. Hu K, Johnson J, Florens L, et al. Cytoskeletal components of an invasion machine-the apical complex of *Toxoplasma gondii*. *PLoS Pathog.* 2006;Feb;2(2):e13:Epub. doi: 2006 Feb 24.
39. Lebrun M, Michelin A, El Hajj H, et al. The rhoptry neck protein RON4 re-localizes at the moving junction during *Toxoplasma gondii* invasion. *Cell Microbiol.* 2005;7(12):1823-1833. doi: 10.1111/j.1462-5822.2005.00646.x.
40. Radke JR, White MW. A cell cycle model for the tachyzoite of *Toxoplasma gondii* using the *Herpes simplex virus* thymidine kinase. *Mol Biochem Parasitol.* 1998;94(2):237-247.
41. Nishi M, Hu K, Murray JM, Roos DS. Organellar dynamics during the cell cycle of *Toxoplasma gondii*. *J Cell Sci.* 2008;121(Pt 9):1559-1568. doi: 10.1242/jcs.021089.

42. Gaji RY, Behnke MS, Lehmann MM, White MW, Carruthers VB. Cell cycle-dependent, intercellular transmission of *Toxoplasma gondii* is accompanied by marked changes in parasite gene expression. *Mol Microbiol*. 2011;79(1):192-204. doi: 10.1111/j.1365-2958.2010.07441.x; 10.1111/j.1365-2958.2010.07441.x.
43. Slomianny C. Three-dimensional reconstruction of the feeding process of the malaria parasite. *Blood Cells*. 1990;16(2-3):369-378.
44. Behnke MS, Wootton JC, Lehmann MM, et al. Coordinated progression through two subtranscriptomes underlies the tachyzoite cycle of *Toxoplasma gondii*. *PloS one*. 2010;(in press).
45. Subach FV, Subach OM, Gundorov IS, et al. Monomeric fluorescent timers that change color from blue to red report on cellular trafficking. *Nat Chem Biol*. 2009 Feb;5(2):118-126.
46. Khmelinskii A, Knop M. Analysis of protein dynamics with tandem fluorescent protein timers. *Methods Mol Biol*. 2014;1174:195-210. doi: 10.1007/978-1-4939-0944-5_13.
47. Agueta F, Upadhyayulab S, Gaudinb R, et al. Membrane dynamics of dividing cells imaged by lattice light-sheet microscopy. *Mol Biol Cell*. 2016 Nov 7;27(22):3418-3435. Epub 2016 Aug 17.
48. Tacheva-Grigorova SK, Santos AJ, Boucrot E, Kirchhausen T. Clathrin-mediated endocytosis persists during unperturbed mitosis. *Cell Rep*. 2013 Aug 29;4(4):659-668. doi: 10.1016/j.celrep.2013.07.017. Epub 2013 Aug 15.
49. Fielding AB, Royle SJ. Mitotic inhibition of clathrin-mediated endocytosis. *Cell Mol Life Sci*. 2013 Sep;70(18):3423-3433. doi: 10.1007/s00018-012-1250-8. Epub 2013 Jan 11.
50. Aikawa M, Hepler PK, Huff CG, Sprinz H. The feeding mechanism of avian malarial parasites. *J Cell Biol*. 1966;Feb;28(2):355-373.
51. Lobo CA, Rodriguez M, Hou G, Perkins M, Oskov Y, Lustigman S. Characterization of PfRhop148, a novel rhoptry protein of *Plasmodium falciparum*. *Mol Biochem Parasitol*. 2003 Apr 25;128(1):59-65.
52. Topolska AE, Lidgett A, Truman D, Fujioka H, Coppel RL. Characterization of a Membrane-associated Rhoptry Protein of *Plasmodium falciparum*. *J Biol Chem*. 2004 Feb 6;279(6):4648-4656. Epub 2003 Nov 12.
53. Nichols BA, Chiappino ML, Pavesio CE. Endocytosis at the micropore of *Toxoplasma gondii*. *Parasitol Res*. 1994;80(2):91-98.
54. Sibley LD, Niesman IR, Parmley SF, Cesbron-Delauw MF. Regulated secretion of multi-lamellar vesicles leads to formation of a tubulo-vesicular network in host-cell

- vacuoles occupied by *Toxoplasma gondii*. *J Cell Sci.* 1995;108 (Pt 4)(Pt 4):1669-1677.
55. Travier L, Mondragon R, Dubremetz JF, et al. Functional domains of the *Toxoplasma* GRA2 protein in the formation of the membranous nanotubular network of the parasitophorous vacuole. *Int J Parasitol.* 2008;38(7):757-773. doi: 10.1016/j.ijpara.2007.10.010.
 56. Wojczyk BS, Stwora-Wojczyk MM, Hagen FK, et al. cDNA cloning and expression of UDP-N-acetyl-D-galactosamine:polypeptide N-acetylgalactosaminyltransferase T1 from *Toxoplasma gondii*. *Mol Biochem Parasitol.* 2003;131(2):93-107.
 57. Zhao Y, Khaminets A, Hunn J, Howard J. Disruption of the *Toxoplasma gondii* parasitophorous vacuole by IFN γ -inducible immunity related GTPases (IRG proteins) triggers necrotic cell death. *PLoS Pathogens.* 2009;5(2):e1000288.
 58. Kafsack BF, Beckers C, Carruthers VB. Synchronous invasion of host cells by *Toxoplasma gondii*. *Mol Biochem Parasitol.* 2004;136(2):309-311.
 59. Larson ET, Parussini F, Huynh MH, et al. *Toxoplasma gondii* cathepsin L is the primary target of the invasion-inhibitory compound morpholinurea-leucyl-homophenyl-vinyl sulfone phenyl. *J Biol Chem.* 2009;284(39):26839-26850. doi: 10.1074/jbc.M109.003780.
 60. Dou Z, Coppens I, Carruthers VB. Non-canonical Maturation of Two Papain-family Proteases in *Toxoplasma gondii*. *J Biol Chem.* 2013;288(5):3523-3534. doi: 10.1074/jbc.M112.443697; 10.1074/jbc.M112.443697.
 61. Burg JL, Perlman D, Kasper LH, Ware PL, Boothroyd JC. Molecular analysis of the gene encoding the major surface antigen of *Toxoplasma gondii*. *J Immunol.* 1988;141:3584-3591.
 62. Mann T, Beckers C. Characterization of the subpellicular network, a filamentous membrane skeletal component in the parasite *Toxoplasma gondii*. *Mol Biochem Parasitol.* 2001;115(2):257-268.
 63. Huynh MH, Rabenau KE, Harper JM, Beatty WL, Sibley LD, V C. Rapid invasion of host cells by *Toxoplasma* requires secretion of the MIC2-M2AP adhesive protein complex. *Embo J.* 2003;22(9):2082-2090.

Chapter 3

T. gondii endocytosis does not require DrpB

3.1 Abstract

Ingested host proteins are taken up into *Toxoplasma gondii* and trafficked through the parasite's endosome-like compartments (ELCs) where endocytic trafficking of ingested protein intersects with exocytic trafficking to the parasite's specialized secretory organelles called the micronemes. Microneme proteins remain intact the rest of the way to the microneme organelles, while ingested proteins are further trafficked to a lysosome-like compartment called the VAC where they are degraded in a Cathepsin L (CPL)-dependent manner. Whether ingested host proteins are also trafficked through the trans-Golgi network (TGN) as in plants remains unclear since GalNac-YFP, typically used to specifically mark the TGN, colocalizes with ingested host proteins but labels both the TGN and ELCs. Moreover, the mechanisms that coordinate endocytosis of host cytosolic proteins into *T. gondii*, downstream trafficking to the VAC, and proper sorting of microneme versus ingested proteins remain unclear. In this study, the role of DrpB, a TGN-associated dynamin-related protein involved in secretory trafficking, in the *T. gondii* host protein ingestion pathway was determined. Using fluorescence microscopy and colocalization analysis, DrpB colocalized with ingested host proteins, however it also labeled both the TGN and ELCs, as observed for GalNac-YFP. Therefore, whether ingested proteins traffic through the TGN remains unclear. Further, expression of a dominant negative mutant of DrpB, ddFKBP-GFP-DrpB K72A, had no effect on the ability of *T. gondii* to internalize proteins from the host cell or to traffic ingested host proteins to the VAC. Taken together, this suggests that DrpB is not required for endocytic trafficking to the VAC, and is likely dedicated to exocytic trafficking only. This work provides the first glimpse into differentiating mechanisms for endocytic and exocytic trafficking in *T. gondii*.

3.2 Introduction

The obligate intracellular parasite *Toxoplasma gondii* lives in a parasitophorous vacuole (PV) where it consumes proteins from the host cell cytosol. In this endocytic pathway, host cytosolic proteins are taken up across the PV membrane (PVM) and parasite plasma membrane into endocytic vesicles in the parasite cytoplasm and trafficked to the parasite's lysosome-like organelle called the VAC for degradation. However, how endocytosed material is delivered to the VAC was unclear. Data in Chapter 2 showed that ingested protein colocalized significantly with the trans-Golgi network (TGN) marker GalNac-YFP¹, the endosomal-like compartment (ELC) marker/immature microneme protein proM2AP^{2, 3}, and the VAC marker cathepsin B (CPB).⁴ This suggested that endocytic trafficking in *T. gondii* could resemble plants with endocytosed material trafficking sequentially through the TGN, ELCs and finally to the lysosome.⁵ However, careful analysis of GalNac-YFP localization revealed that this marker is not restricted to the TGN and colocalizes with markers of the ELCs. Therefore, whether endocytic trafficking proceeds through the TGN as in plants is unclear. Further, colocalization with the immature microneme protein proM2AP indicated that endocytic trafficking to the VAC intersects with exocytic trafficking to the parasite's unique secretory organelles called micronemes (Figure 3-1). However, the mechanisms that govern endocytic trafficking and sorting of endocytic and exocytic cargoes in *T. gondii* are not known.

To further investigate if endocytic trafficking in *T. gondii* involves the TGN and to investigate the mechanisms that underlie this process, we determined the role of the

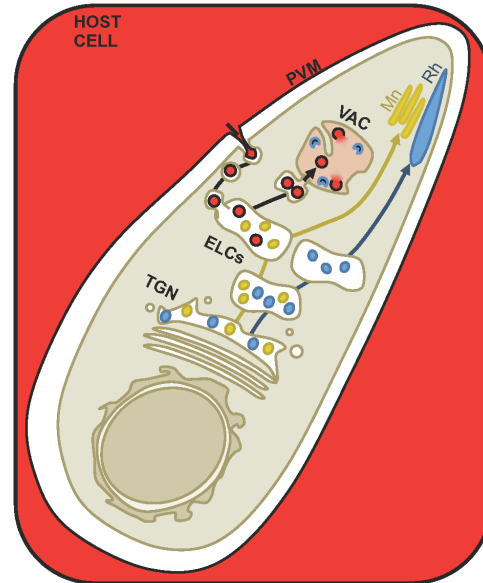


Figure 3-1. Recap of relevant findings from Chapter 2. Proteins from the host cell cytosol are endocytosed across the parasitophorous vacuole membrane (PVM) and parasite plasma membrane into endocytic vesicles in the *T. gondii* cytoplasm. Ingested proteins are then trafficked through endosome-like compartments but likely not the trans-Golgi network (TGN), and are delivered to the parasite's lysosome-like compartment (VAC) for degradation. Endocytic trafficking intersects with microneme trafficking, but mechanisms for sorting ingested proteins destined for degradation in the VAC from microneme proteins which must reach the microneme organelles intact remain unclear.

dynamamin-related protein DrpB. The dynamamin superfamily is a diverse set of GTPases that are perhaps best known for their highly conserved role in vesicle fission from the plasma membrane during endocytosis. Classical dynamamins consist of five domains, the N-terminal G domain for GTP binding and hydrolysis, the middle/stalk domain which mediates dimerization, the pleckstrin homology domain which mediates interaction with membranes in particular the lipid phosphatidylinositol bisphosphate (PI(4,5)P₂), the GTPase effector domain which assists in oligomerization and stimulates GTPase activity, and the proline-rich domain which mediates protein-protein interactions.⁶ Dynamamin-related proteins, including *T. gondii* DrpB and yeast Vps1 typically have only the G domain, the middle/stalk domain, and the GTPase effector domain.^{7, 8} Dynamamin-dependent vesicle scission during endocytosis is thought to involve assembly of dynamamin dimers into rings that form a collar around the forming vesicle neck, and GTP hydrolysis by the GTPase domain triggers a conformational change that results in constriction and fission of the vesicle membrane.⁶ Alternatively, dynamamin could participate in endocytosis indirectly through regulation of the actin cytoskeleton, as proposed for yeast.^{6, 9}

Other members the dynamamin family perform a similar function to promote maintenance of mitochondria or chloroplasts, cytokinesis, and trafficking from post-Golgi compartments including the trans-Golgi network (TGN) and endosomes.^{6, 10, 11} For example, the dynamamin-related proteins DRP3 in plants and Mgm1 in yeast are required for mitochondrial maintenance.^{12, 13} Plant DRP2 on the other hand, has been implicated in endocytosis at the plasma membrane, cell plate formation during cytokinesis and post-Golgi trafficking from the TGN and endosomes.¹⁴⁻¹⁷ DrpB in *T. gondii* is localized to the TGN and is required for exocytic trafficking to the microneme and rhoptry organelles, presumably through fission of microneme and rhoptry protein-containing vesicles from the TGN.^{7, 18} However, a role for DrpB in *T. gondii* endocytosis has not been tested.

If DrpB is indeed restricted to the TGN, it would serve as a suitable marker for determining if endocytic trafficking in *T. gondii* is plant-like. Further, DrpB could be predicted to play two possible roles in *T. gondii* endocytosis. First, DrpB could promote fission of endocytic vesicles at the parasite plasma membrane. Although DrpB has not been observed at the parasite plasma membrane^{7, 18}, dynamamin-dependent fission of endocytic vesicles at the plasma membrane is conserved in plants, mammals, fungi and

other protozoan parasites including the malaria parasite *Plasmodium spp.*^{6, 8, 10, 19, 20} Therefore, it is tempting to speculate that there could be transient populations of DrpB that are difficult to detect by traditional microscopy similar to the yeast dynamin-related protein Vps1.⁸ The second possible role would be in downstream trafficking of endocytosed material to the VAC potentially at the ELCs or TGN. To test these possibilities, a dominant negative mutant GTPase mutant of DrpB shown to interfere with dynamin function in *T. gondii* and other eukaryotes will be expressed.^{7, 21}

In this study, we find that ingested protein colocalizes with DrpB, but the localization of DrpB, like that of GalNac-YFP, is not restricted to the TGN. Therefore, it is still unclear whether endocytic trafficking of ingested protein proceeds through the TGN as in plants. DrpB is not required for trafficking of ingested host proteins across the parasite plasma membrane or for downstream trafficking to the VAC. Interestingly, expression of a dominant negative GTPase mutant of DrpB actually enhanced endocytosis in *T. gondii*. In contrast to wildtype DrpB, the dominant-negative mutant did not colocalize with ingested host protein and showed almost no colocalization with the ELCs or VAC, suggesting the observed enhancement of endocytosis is likely due to indirect effects such as decreased DrpB interaction with an effector protein that promotes endocytic trafficking or sequestration of a negative regulator of endocytic trafficking. Finally, these results provide functional distinction between exocytic and endocytic trafficking in *T. gondii*, with DrpB likely being directly devoted to exocytic trafficking only.

3.3 Results

3.3.1 DrpB localizes to the TGN and ELCs

Although GalNac-YFP is often used as a marker for the TGN, we found that GalNac-YFP was not restricted to the TGN and also localizes to the ELCs and potentially to the VAC (Figures 2-1, 2-4 and 2-6). Current literature suggests that DrpB is restricted to the TGN, and could serve as a suitable marker to determine if ingested proteins are trafficked through the TGN.^{7, 18} To determine this, the localization of DrpB was examined using RHΔhx ddFKBP-GFP-DrpB WT (ddGFP-DrpB WT) parasites.⁷ In addition to the endogenous copy of DrpB, these parasites express an ectopic copy of DrpB fused to GFP and a destabilization domain (dd), which allows for post-translational control of protein

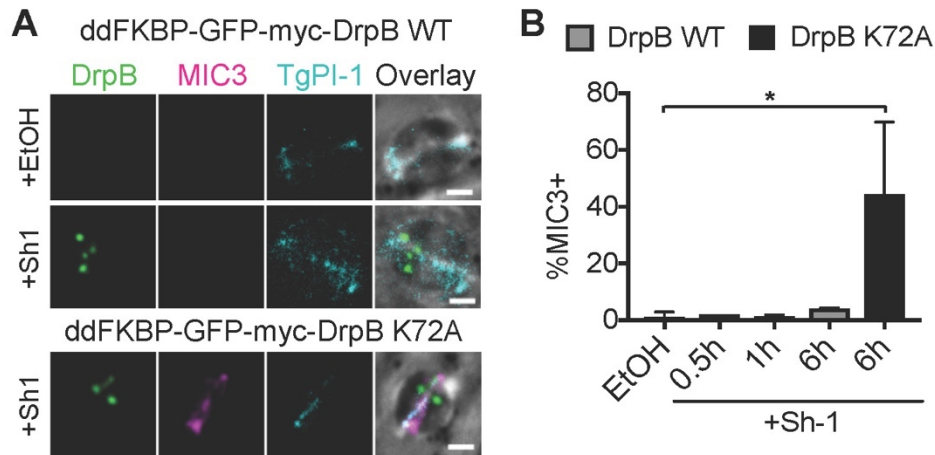


FIGURE 3-2 Expression of dominant negative, but not wildtype ddGFP-DrpB leads to MIC3 secretion into the PV lumen. A, Representative images for lack of aberrant secretion of MIC3 into the PV lumen in ddGFP-DrpB WT and ddGFP-DrpB K72A dominant negative mutant parasites. Synchronously-infected cells were treated with 1 μ M Sh-1 or the vehicle control ethanol (EtOH) for 6h, partially permeabilized with 0.02% saponin to allow staining of the PV lumen but not the parasite interior and stained with antibodies against MIC3 and as a positive control for PV lumen staining, TgPI-1. B, Quantitation of aberrant MIC3 secretion into the PV lumen in ddGFP-DrpB WT parasites treated with 1 μ M Sh-1 for the last 0.5, 1 or 6 h of infection or 6h with EtOH and fixed at 6 h post-invasion or ddGFP-DrpB K72A parasites treated with 1 μ M Sh-1 for 6h as a positive control. Shown is percentage of TgPI-1⁺ vacuoles that are MIC3⁺, at least 100 vacuoles scored in each of two biological replicates. One-way ANOVA with Dunnet's test for multiple comparisons to the EtOH control, only significant results shown. Bars represent means, error bars represent standard deviation, * p <0.05. All scale bars: 2 μ m.

expression upon addition of the stabilizing drug Shield-1. To minimize possible off-target effects due to DrpB overexpression, Shield-1 treatment was optimized to observe ddGFP-DrpB WT expression in the majority of parasites with minimal treatment: 0.8 μ M Shield-1 for 30 min. Secretion of microneme proteins is regulated such that they are only released during invasion and egress under normal conditions. However, *Breinich et al.* observed that overexpression of a dominant negative DrpB GTPase mutant, DrpB K72A, but not wildtype DrpB interfered with trafficking of microneme proteins such as MIC3 and led to their secretion into the PV lumen.⁷ As previously observed, ddGFP-DrpB WT overexpression under these conditions did not interfere with microneme trafficking (Figure 3-2).

Immunofluorescence staining of ddGFP-DrpB WT parasites revealed that ddGFP-DrpB WT showed little to no overlap with the VAC marker CPL or the residual chloroplast-like organelle called the apicoplast (Figure 3-3 top panels). However, ddGFP-DrpB WT did colocalize with ELC markers, most prominently with proM2AP (the immature proform of the micronemes protein M2AP) and partially with NHE3 (a vacuolar type Na⁺/H⁺ exchanger). This suggests that DrpB localizes to the ELCs in addition to the TGN but may

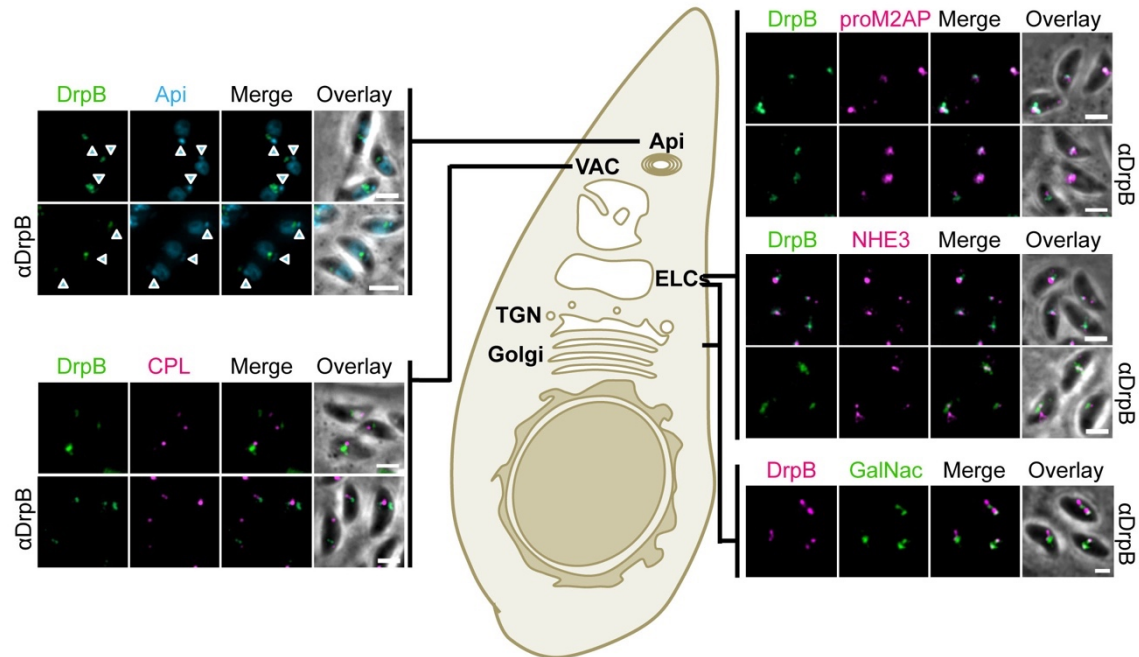


Figure 3-3. DrpB localizes to the TGN and ELCs. Representative images for localization of DrpB in RH Δ hx ddFKBP-GFP-DrpB WT and RH or RH GalNac-YFP parasites. Parasites were synchronously invaded into HFF cells and fixed at 3 h post-invasion. ddGFP-DrpB WT parasites were treated with 0.8 μ M Sh-1 for the last 30 min of infection, RH and RH GalNac-YFP (GalNac image only) parasites were stained with DrpB antibodies (α DrpB). Parasites were stained with DAPI to label the apicoplast (blue arrow heads) or antibodies to label CPL, NHE3 or proM2AP. Images are representative of two biological replicates for RH and RH GalNac-YFP and three biological replicates for ddGFP-DrpB parasites.

show a slightly different localization to GalNac-YFP, which most prominently colocalized with NHE3 (Figure 2-1). Consistent with this, DrpB showed dynamic interaction with the TGN/ELC marker GalNac-YFP, sometimes showing a high degree of colocalization and in other cases showing partial or no overlap (Figure 3-3). Colocalization of DrpB with ELCs was confirmed by antibody staining of endogenous DrpB in wildtype (RH) parasites, suggesting overexpression under these conditions also did not cause mislocalization of ddGFP-DrpB WT (Figure 3-3 bottom panels). Taken together, these findings suggest that ddGFP-DrpB WT is not restricted to the TGN and colocalization of ingested protein with ddGFP-DrpB WT cannot be used to conclusively determine if ingested protein traffics through the TGN. Nevertheless, a role for DrpB in *T. gondii* endocytic trafficking was investigated.

3.3.2 Ingested protein colocalizes with DrpB

To determine if DrpB plays a role in endocytic trafficking in *T. gondii*, we first investigated whether DrpB significantly colocalized with ingested host mCherry using the

host protein ingestion assay as depicted in Figure 3-4A. Chinese hamster ovary (CHO-K1) cells expressing cytosolic mCherry were synchronously infected with ddGFP-DrpB WT parasites to allow ingestion of host cytosol and then purified at 3 h post-invasion. The infected cells were treated with and 0.8 μ M Shield-1 to induce stabilization of ddGFP-DrpB WT or the vehicle ethanol (EtOH). Infected cells were also treated with morpholinurea-leucine-homophenylalanine-vinyl phenyl sulfone (LHVS) or the vehicle control DMSO. LHVS is an inhibitor of CPL, a VAC-localized protease that drives degradation of ingested host protein, to enhance detection of ingested protein.²² In samples where LHVS-

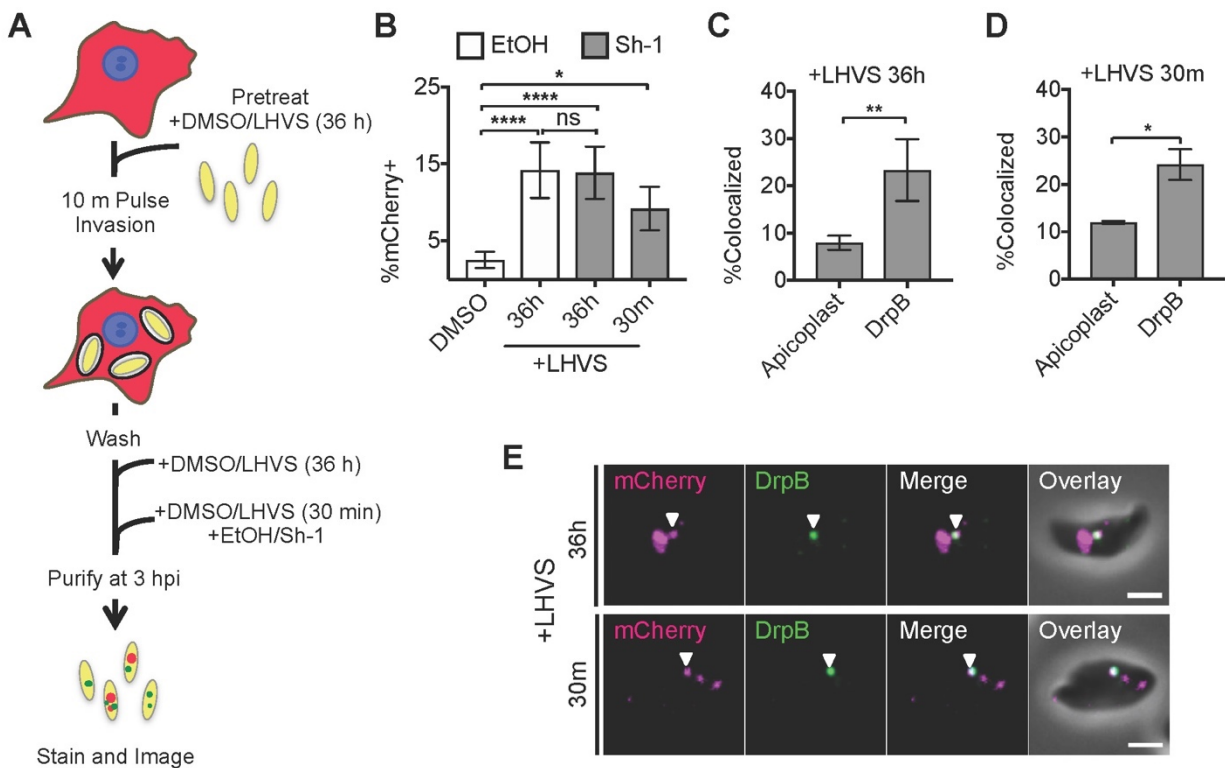


Figure 3-4. Ingested protein colocalizes with DrpB. A, Experimental design for detection and localization of ingested host cytosolic protein in ddGFP-DrpB WT parasites. CHO-K1 cells were transiently transfected with a plasmid encoding cytosolic mCherry fluorescent protein 18-24 h before synchronous invasion for 10 min, allowed to ingest host cytosol for 3 h, and purified before staining with DAPI to label the apicoplast and analysis by fluorescence microscopy. Parasites were treated with LHVS or DMSO for 36 h (pretreated with 1 μ M LHVS or the vehicle control DMSO for 36 h before infection and then for the entire 3 h infection period) or 30 min (50 μ M LHVS or 0.05% DMSO at 2.5h post-invasion) to enhance detection of ingested mCherry. Parasites were also treated with 0.8 μ M Sh-1 or EtOH at 2.5h post-invasion to induce stabilization of ddGFP-DrpB WT. B, Ingestion in ddGFP-DrpB WT parasites treated as in A. Shown is percentage of mCherry positive parasites, at least 200 parasites analyzed per condition for each of three biological replicates for 36 h LHVS treatment and 2 biological replicates for 30 min LHVS treatment, Dunnet's test for comparison of DMSO and LHVS treated samples, one-way ANOVA with Tukey's multiple comparisons for comparison of 36h DMSO and LHVS-treated samples. C and D, Quantitation of colocalization of ingested mCherry with ddGFP-DrpB WT or the apicoplast from LHVS/Sh-1 treated parasites in B. At least 30 ingested mCherry puncta per marker, unpaired two-sided t-test. E, Representative images for colocalization of ingested mCherry and ddGFP-DrpB WT in parasites analyzed in D (top) and E (bottom). All scale bars: 2 μ m, bars represent means, error bars represent standard deviation, * p <0.05 ** p <0.01, **** p <0.0001, ns is not significant.

dependent accumulation of host-derived mCherry is observed, ingestion is considered to be active and localization can be assessed. Colocalization of ingested proteins with the ELC marker proM2AP was examined with both prolonged LHVS treatment (+LHVS 36h: 36 h pre-treatment and 3 h treatment during the experimental infection with 1 μ M LHVS), which allows detection of both recently ingested and accumulated host protein and brief LHVS treatment (+LHVS 30 min: 50 μ M LHVS for the last 30 min of infection), which allows detection of only recently ingested host protein. The level of colocalization between ingested host protein and proM2AP was similar under both treatment conditions (36h in Figure 2-2D: $30.1\pm 8.2\%$ and 30 min in Figure 2-12D: $35.9\pm 1.3\%$), suggesting both methods are valid. Therefore, both LHVS treatment conditions were tested for DrpB colocalization. Following purification, the apicoplast, an apical organelle that is distinct from the endolysosomal system, was stained with DAPI as a negative control to test for random colocalization.

Ingestion was found to be active in the ddGFP-DrpB WT parasites, and the percentage of mCherry+ parasites was not significantly different when comparing ethanol and Shield-1 treatments indicating that overexpression of DrpB under these conditions did not interfere with ingestion (Figure 3-4B). Localization of ingested mCherry was determined as the percentage of ingested mCherry puncta overlapping with ddGFP-DrpB WT puncta or the apicoplast (%Colocalized). Ingested protein colocalized significantly with ddGFP-DrpB WT when compared to the apicoplast, and the level of colocalization was similar whether parasites were treated with LHVS for 36 h ($23.3\pm 6.5\%$) or 30 min ($24.2\pm 3.2\%$) (Figure 3-4 C through E). This suggests that DrpB could promote endocytic trafficking in *T. gondii* in addition to its role in promoting exocytic trafficking of a subset of microneme and rhoptry proteins.

3.3.3 DrpB is not required for endocytosis of host cytosol

To determine if DrpB plays a role in endocytic trafficking in *T. gondii*, we first investigated whether DrpB promotes fission of endocytic vesicles containing host cytosolic mCherry at the plasma membrane. If DrpB plays this role, then interfering with DrpB function should inhibit uptake of host cytosol across the parasite plasma membrane and reduce the percentage of mCherry+ parasites. To test this, an inducible dominant

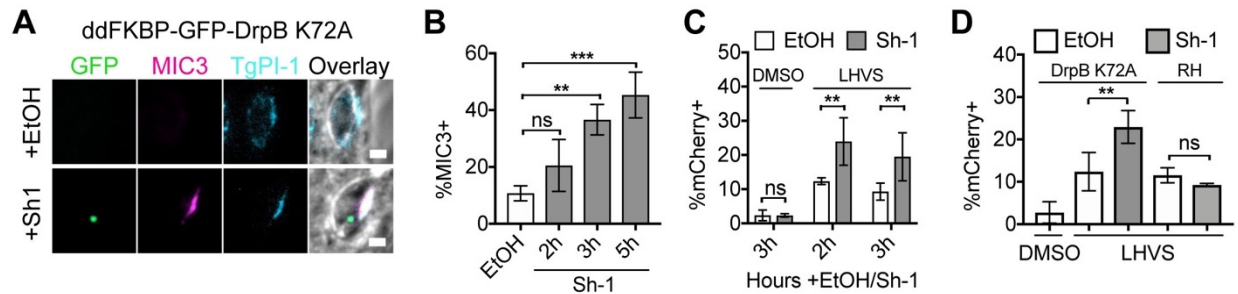


Figure 3-5. DrpB is not required for endocytosis of ingested protein. A, Representative images for aberrant secretion of MIC3 into the PV lumen in ddGFP-DrpB K72A parasites with the addition of Shield-1 (Sh-1), but not the vehicle control ethanol (EtOH). Synchronously-infected cells were treated with 1 μ M Sh-1 or EtOH for the last 5 h of infection, fixed at 6 h post-invasion, partially permeabilized with 0.02% saponin to allow staining of the PV lumen, and stained with antibodies against MIC3 and as a positive control for PV lumen staining, TgPI-1. Scale bars: 2 μ m. B, Quantitation of aberrant MIC3 secretion into the PV lumen in ddGFP-DrpB K72A parasites prepared as in A and treated with 1 μ M Shield-1 (Sh-1) for the last 2, 3 or 5 h of infection or 5 h for EtOH. Shown is percentage of TgPI-1⁺ vacuoles that are MIC3⁺, at least 100 vacuoles scored in each of 3 biological replicates. One-way ANOVA with Dunnet's test for multiple comparisons to the EtOH control. C and D, Quantitation of mCherry ingestion in ddGFP-DrpB K72A and RH parasites. Experiments were conducted as in Figure 3-2A, using CHO-K1 mCherry cells treated with 2 μ g/mL doxycycline for 96h. Infected cells were treated with 0.2% DMSO or 200 μ M LHVS for 30 min and 0.1% EtOH or 1 μ M Sh-1 for the indicated amounts of time in C, and 3 h in D. Shown is percentage of mCherry positive parasites, with at least 200 parasites analyzed for each of 2 biological replicates for DMSO+Shield-1 in C, and at least 3 biological replicates for all other samples. One-way ANOVA with Dunnet's test for multiple comparisons of LHVS+EtOH treated samples to the DMSO+EtOH treated control are not shown, but all comparisons are significant. Unpaired, two-sample t-tests for comparison of EtOH and Sh-1 treated samples shown. All bars represent means and error bars represent standard deviation. ** $p < 0.01$, *** $p < 0.001$, ns is not significant.

negative DrpB mutant was expressed to interfere with DrpB function using RH Δ hx ddFKBP-GFP-DrpB K72A (ddGFP-DrpB K72A) parasites. When treated with the vehicle control ethanol, these parasites are essentially wildtype, but addition of Shield-1 stabilizes ddGFP-DrpB K72A, a GTPase mutant shown to interfere with dynamin function in endocytosis in other organisms.²¹ Prolonged, overnight treatment with Shield-1 in this strain leads to aberrant secretion of microneme and rhoptry proteins into the PV lumen, depletion of microneme and rhoptry organelles and non-invasive parasites.⁷ To avoid issues with invasion for the ingestion assay, Shield-1 treatment was optimized to induce dominant negative effects in short periods of time using MIC3 secretion into the PV lumen as in Figure 3-2. A significant percentage of vacuoles were positive for MIC3 staining in the PV lumen within 3 but not 2 h of 1 μ M Shield-1 treatment when compared to the ethanol treated control (Figure 3-5A and B). Therefore, ingestion assays were performed with ddGFP-DrpB K72A parasites as in Figure 3-4A with 30 min LHVS treatment to observe recently ingested protein and Shield-1 treatment for up to 3 h to induce expression of ddGFP-DrpB K72A. Following harvest and fixation, the percentage of mCherry⁺ parasites was determined by fluorescence microscopy.

LHVS-dependent accumulation of mCherry was observed in the ethanol treated control parasites, confirming that ingestion is active in this parasite strain (Figure 3-5C). Interestingly, parasites treated with LHVS and Shield-1 showed a significant increase in the percentage of mCherry⁺ parasites compared to those treated with LHVS and ethanol (Figure 3-5C). A similar increase was not observed in DMSO-treated ddGFP-DrpB K72A parasites or in wildtype RH parasites treated with Shield-1, suggesting the increased accumulation of ingested protein was not due to defects in the turnover of ingested protein or off-target effects of Shield-1 itself (Figure 3-5C and D). Taken together, this suggests that DrpB is not required for fission of endocytic vesicles at the plasma membrane but may indirectly restrict the rate of ingested protein endocytosis.

3.3.4 DrpB is not required for downstream trafficking to the VAC

DrpB could also play a role in downstream trafficking of ingested proteins at the TGN or ELCs. In this case, interfering with DrpB function will interfere with delivery of ingested protein to the VAC, reducing colocalization of ingested mCherry with VAC markers and potentially preventing its degradation. Efficient turnover of ingested mCherry in parasites treated with DMSO and Shield-1 in Figure 3-5C suggested that endocytic trafficking to the VAC was not disturbed. To confirm this, the localization of ingested mCherry was determined in LHVS-treated parasites from Figure 3-5C. Following purification, parasites were stained with DAPI to label the apicoplast, with antibodies against proM2AP to label the ELCs, or with antibodies against CPL to label the VAC. As previously observed, ingested mCherry showed significant colocalization with proM2AP and CPL when compared to the apicoplast in ethanol-treated control samples (Figure 3-6A). When comparing ethanol and Shield-1 treated parasites, colocalization of ingested mCherry with proM2AP and the apicoplast was not affected, but surprisingly colocalization with the VAC marker CPL was significantly increased (Figure 3-6A). Localization of CPL relative to NHE3, proM2AP and CPB and the overall staining pattern of these markers was not altered under the same Shield-1 treatment conditions, excluding the possibility that increased colocalization of CPL with ingested mCherry was due to redistribution of CPL into multiple endocytic compartments, e.g. the VAC and ELCs (Figure 3-6B through D). Taken together, this suggests that DrpB is also not required for

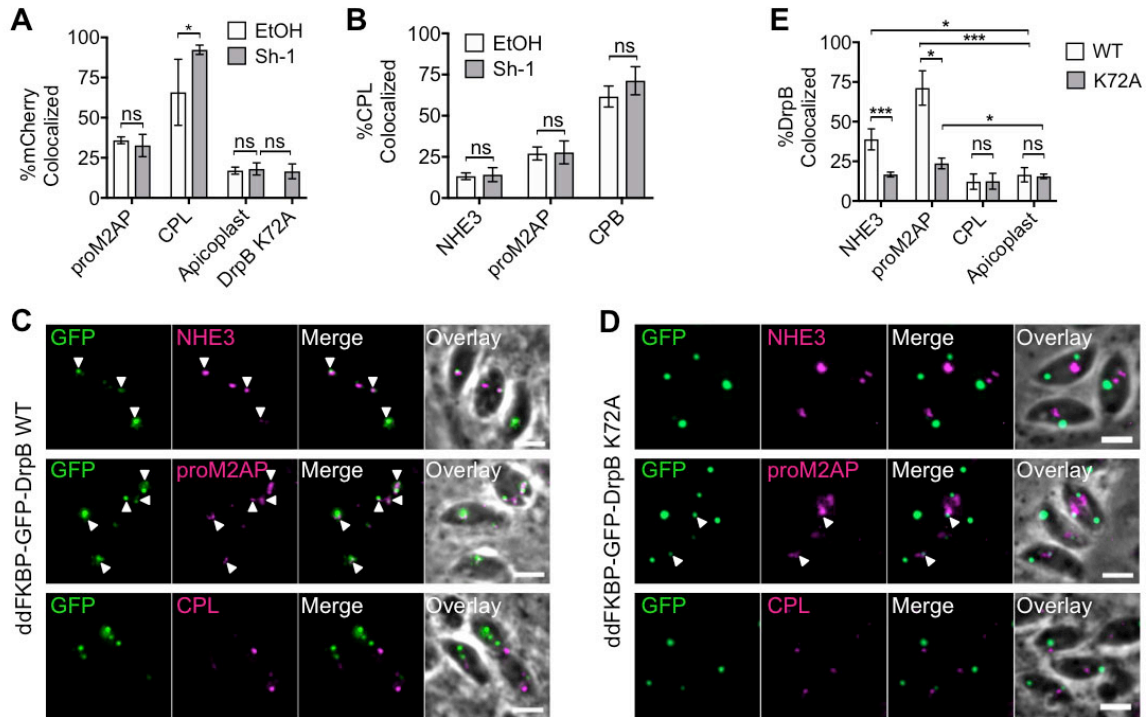


Figure 3-6. DrpB is not required for trafficking of ingested protein to the VAC. A, Quantitation of colocalization of ingested mCherry with GFP-DrpB K72A, proM2AP and CPL by antibody staining, or the apicoplast by DAPI staining in LHSV+Sh-1 treated ddGFP-DrpB K72A parasites from Figure 3-5C. At least 30 ingested mCherry puncta were analyzed per marker for each of 4 biological replicates for CPL and 3 biological replicates for all other markers. One-way ANOVA with Dunnet's test for multiple comparisons of EtOH treated samples to the apicoplast are not shown, but proM2AP and CPL comparisons are significant. Unpaired two-sample t-tests for comparison of EtOH and Sh-1 treated samples for each marker and comparison of the apicoplast and ddGFP-DrpB K72A in Sh-1 treated parasites shown. B, Quantitation of colocalization of CPL with the indicated markers by antibody staining in intracellular ddGFP-DrpB K72A parasites synchronously invaded into HFF cells, treated with 0.1% EtOH or 1 μ M Sh-1 for 3 h and fixed at 3 h post-invasion. At least 40 CPL puncta analyzed per marker for each of 3 biological replicates. Unpaired two-sample t-tests for comparison of EtOH and Sh-1 treated samples. C and D, Representative images for colocalization of ddGFP-DrpB WT or ddGFP-DrpB K72A with the indicated markers by antibody staining, quantitated in E. White arrows indicate regions of colocalization. Scale bars: 5 μ m. E, Quantitation of colocalization of Sh-1 treated ddGFP-DrpB WT or ddGFP-DrpB K72A with the indicated endolysosomal markers by antibody staining or the apicoplast by DAPI staining in intracellular parasites. ddGFP-DrpB WT parasites were treated with 0.8 μ M Sh-1 for 30 min and ddGFP-DrpB K72A parasites treated with 1.0 μ M Sh-1 for 3 h. At least 40 DrpB puncta analyzed per marker, per replicate for 3 biological replicates. One-way ANOVA with Dunnet's test for multiple comparisons of each marker to the apicoplast for each ddGFP-DrpB WT and ddGFP-DrpB K72A parasites, only significant results shown. Unpaired two-sample t-tests for comparison of localization in ddGFP-DrpB WT vs K72A. All bars represent means and error bars represent standard deviation. * p <0.05, *** p <0.001, ns is not significant.

downstream endocytic trafficking of ingested protein to the VAC or trafficking of CPL. Consistent with this, ddGFP-DrpB K72A showed almost no association with the endolysosomal system, maintaining reduced but significant localization with proM2AP, but not NHE3, and was not significantly associated with ingested mCherry or CPL (Figure 3-6A and C through E). This suggests that ddGFP-DrpB K72A may indirectly increase colocalization between ingested mCherry and CPL, potentially through enhancing the rate of endocytic trafficking to the VAC. Proposed mechanisms for these observations are

discussed below. Finally, these results provide functional distinction between exocytic and endocytic trafficking in *T. gondii*, with DrpB likely being devoted to exocytic trafficking only.

3.4 Discussion

3.4.1 Does endocytic traffic in *T. gondii* resemble traffic in plants?

Previous studies localized DrpB exclusively to the TGN, however, we find that DrpB also at least partially localizes to the ELCs. Therefore, colocalization of ingested protein with DrpB does not definitively indicate that endocytic trafficking in *T. gondii* involves the TGN as in plants. Extensive overlap DrpB with the ELC marker proM2AP and similar levels of colocalization of ingested protein with DrpB (~23-24%) and proM2AP (~30-35%) could suggest that DrpB colocalizes with ingested protein primarily in the ELCs. However, GalNac-YFP colocalized with ingested protein primarily in an ELC- or VAC-like compartment that was degradative in nature and contained CPB despite very little overall overlap between GalNac-YFP and VAC markers CPB or CPL (Figure 2-1). Whether DrpB colocalizes with ingested protein in a similar compartment was not determined but could prove valuable to better define if DrpB colocalizes with ingested proteins in the ELCs, TGN or elsewhere. Future studies will also greatly benefit from more specific markers of the TGN.

Expression of the dominant negative DrpB mutant, ddGFP-DrpB K72A, prevents delivery of microneme and rhoptry proteins to their respective organelles and leads to their secretion into the PV lumen, presumably by interfering with trafficking of microneme and rhoptry proteins out of the TGN.^{7, 18} In this study, we reproduce aberrant secretion of the microneme protein MIC3 in the presence of ddGFP-DrpB K72A, but find no defects in delivery of ingested proteins to the VAC. Therefore, if ingested protein is delivered to the TGN, then subsequent trafficking to the ELCs would occur in a DrpB-independent manner. In a model resembling plants, the TGN (and any contents that are not sorted away) is thought to mature into multivesicular endosomes that will fuse with the lysosome. Ingested host protein trafficking from the TGN to the VAC could resemble trafficking of soluble cargoes in plants, which are by default sent to the lysosome in the absence of sorting signals.²³⁻²⁶ Alternatively, ingested protein trafficking out of the TGN could require

vesicular trafficking like microneme and rhoptry proteins. Soluble microneme and rhoptry proteins bind to the sorting receptor TgSORTLR in the TGN lumen, and the AP1 adaptor complex is thought to interact with the cytosolic domains of TgSORTLR and transmembrane microneme and rhoptry proteins to mediate clathrin coated vesicle formation for trafficking to the ELCs.^{18, 27} Whether ingested host proteins traffic through the TGN, require sorting receptors like microneme and rhoptry proteins, or require clathrin- or AP1-dependent trafficking remains to be determined. However, whatever the mechanism, it is DrpB-independent, which distinguishes endocytic trafficking from exocytic trafficking.⁷

3.4.2 DrpB-independent does not necessarily mean dynamin-independent

Expression of a dominant negative DrpB did not interfere with ingestion of host mCherry or its trafficking to the VAC, suggesting that DrpB is not required for host mCherry endocytosis in *T. gondii*. However, this does not preclude the existence of DrpB-dependent endocytosis of other substrates. How host mCherry is taken up into endocytic vesicles in *T. gondii* is unclear. *T. gondii* expresses three dynamin-related proteins DrpA, B and C. DrpA localizes to a chloroplast-like organelle of *T. gondii* called the apicoplast, and is required for apicoplast maintenance.²⁸ The domain structure of DrpC, which contains only a GTPase domain, most closely resembles dynamins that are involved in maintenance of chloroplast division²⁹ and because DrpA maintains the apicoplast, DrpC is presumed to be involved in maintenance of mitochondria in *T. gondii*.¹⁸ However the localization and function of DrpC are unknown, leaving open the possibility that DrpC could drive dynamin-dependent endocytosis in *T. gondii*. Alternatively, endocytosis of host proteins could be dynamin-independent and involve BAR domain proteins or CtBP/BARS, which have established roles in membrane fission.³⁰

3.4.3 Expression of ddGFP-DrpB K72A enhances *T. gondii* endocytosis

Interestingly, expression of ddGFP-DrpB K72A enhanced endocytosis and delivery of ingested protein to the VAC. While this could indicate that DrpB directly inhibits endocytic trafficking, this enhancement is likely indirect given the lack of interaction of the dominant negative mutant ddGFP-DrpB K72A with ingested mCherry or the

endolysosomal system. ddGFP-DrpB K72A could sequester binding partners that are involved in DrpB-dependent exocytic trafficking along with liberating other partners. For example, blocking exocytic trafficking from the Golgi in mammalian cells leads to an increase in CLIC/GEEC endocytosis by freeing up the shared GTPase Arf1.³¹ Dynamin hydrolyzes GTP to GDP during membrane fission and GDP is exchanged for GTP to reactivate dynamin either spontaneously or through interaction with guanine nucleotide exchange factors.^{32, 33} ddGFP-DrpB K72A is defective in GTP binding and hydrolysis and should decrease pools of GDP-bound DrpB.^{7, 21} Therefore, ddGFP-DrpB K72A expression could lead to increased rates of endocytic trafficking by increasing free pools of guanine nucleotide exchange factors required for endocytic trafficking. Alternatively, both DrpB-dependent and DrpB-independent endocytosis could exist, and shutdown of DrpB-dependent endocytosis could lead to upregulation of DrpB-independent endocytosis. Consistent with this, knockdown of core structural proteins required for endocytosis via caveolae (a dynamin-dependent endocytic pathway) leads to upregulation of the dynamin-independent CLIC/GEEC endocytic pathway.³⁴ Understanding the mechanisms that underlie *T. gondii* endocytosis should be a key focus going forward, especially understanding mechanisms distinguishing exocytic and endocytic trafficking. This study provides the first glimpse into this aspect of *T. gondii* biology and suggests that DrpB is likely reserved for secretory trafficking only.

3.5 Materials and methods

Host Cell and Parasite Culture

Cells and parasites were maintained at 37°C with 5% CO₂ in a humidified incubator. CHO-K1 cells (ATCC® CCL-61™) were maintained in Ham's F12 supplemented with 10% Cosmic Calf serum, 20 mM HEPES, and 2 mM L-glutamine. CHO K1 cells expressing mCherry under a tetracycline-inducible promoter (CHO imCherry cells), were maintained in Ham's F12 supplemented with 10% Cosmic Calf serum, 20 mM HEPES, 2 mM L-glutamine, 200µg/mL hygromycin B (Invitrogen, Cat# 10687010) and 400 µg/mL geneticin (Invitrogen, Cat# 10131035). HFF cells (ATCC® CRL-1634™) were maintained in Dulbecco's modified Eagle's medium (DMEM) supplemented with 10% Cosmic Calf serum, 20 mM HEPES, 2 mM L-glutamine, and 50µg/ml penicillin/streptomycin.

Toxoplasma gondii parasites were maintained by serial passaging in HFF cells. *RHΔhx ddfFKBP-GFP-DrpB WT* and *RHΔhx ddfFKBP-GFP-DrpB K72A* parasites were kindly provided by Dr. Markus Meissner of University of Glasgow.⁷ *RHΔhx ddfFKBP-GFP-DrpB WT* parasites had lost transgene expression in a significant portion of the population and were subcloned by limiting dilution to obtain a 100% GFP⁺ population.

Chemicals and Reagents

Morpholine urea-leucyl-homophenyl-vinylsulfone phenyl (LHVS) was kindly provided by Dr. Matthew Bogyo at Stanford University. LHVS powder was dissolved in DMSO, and applied with a final DMSO concentration of 0.1-0.2%. Shield-1 was purchased from Clontech, resuspended in ethanol to a concentration of 1 μM and added to cultures with a final ethanol concentration of 0.08-0.1%.

Immunofluorescent Antibody Labeling

Purified parasites or chamberslides were fixed with 4% formaldehyde for 20 min, and washed 3 times with PBS for 5 min each. Slides were then permeabilized with 0.1% TritonX-100 for 10 min, rinsed three times in PBS, blocked with 10%FBS/0.01% Triton X-100/PBS, and incubated in primary antibodies diluted in wash buffer (1% FBS/1% NGS/0.01% Triton X-100/PBS) for 30 min to 1 h at room temperature. Primary antibodies used include affinity purified rabbit anti-CPL (1:100)³⁵, mouse anti-CPB (1:100)⁴, rat anti-DrpB (1:200) kindly provided by Dr. Peter Bradley at University of California Los Angeles⁷, affinity purified rabbit anti-proM2AP (1:400)², guinea pig anti-NHE3 (1:500) kindly provided by Gustavo Arrizabalaga³⁶, rabbit anti-TgPI-1 (1:500)³⁷, and mouse anti-MIC3 (1:500) kindly provided by Jean-Francois Dubremetz^{38, 39}. Slides were washed three times with wash buffer and incubated in Alex Fluor goat anti-mouse, anti-rabbit, anti-rat secondary antibody (1:1000) (Invitrogen Molecular Probes) in wash buffer for 1 h at room temperature. Slides were washed three times with wash buffer and mounted in Mowiol before imaging.

Transfection of CHO-K1 Cells

CHO-K1 cells that were 70-80% confluent, were transfected with 2 µg of pCMV mCherry N3 plasmid, kindly provided by Dr. Jonathan Howard Instituto Gulbenkian de Ciecía⁴⁰. The X-TREMEGENE 9 Transfection Reagent (Roche, Cat# 6365787001) was used at a 3:1 ratio of plasmid to transfection reagent in Opti-MEM (Gibco, Cat#31985062) in a total final volume of 200 µl. CHO-K1 cells were incubated with the transfection mixture overnight at 37°C and media was changed before infection at 18-24 h post-transfection.

Synchronized Invasion

The ENDO Buffer Method of invasion⁴¹ was used for synchronous infection with the following modifications. Briefly, parasite cultures were purified by scraping, syringing, and passing through a 3µm filter and then pelleted by spinning at 1000xg for 10 min. The pellet was then resuspended to 1-3x10⁷ parasites per 1 mL in ENDO Buffer (44.7 mM K₂SO₄, 10mM MgSO₄, 106mM sucrose, 5 mM glucose, 20 mM Tris-H₂SO₄, 3.5 mg/ml BSA, pH 8.2) for infection of 35 mm dishes, and 0.3-1x10⁷ parasites per 1 mL ENDO Buffer for infection of 8-well chamber slides. Host cells were rinsed once with ENDO Buffer, and then 1 mL of ENDO Buffer-parasite suspension was added to each 35 mm dish or 100µl of ENDO Buffer-parasite suspension was added to each chamber of an 8-well chamber slide. Parasites were allowed to settle at 37°C for 10 min before the ENDO Buffer was gently removed and replaced with twice the volume of Invasion Media (Ham's F12/3% Cosmic Calf Serum/20 µM HEPES). Parasites were allowed to invade at 37°C for 10 min before washing three times with warm media to remove uninvaded parasites. Infected cells were incubated at 37°C until ready for purification or fixation.

Protease Protection Assay

Protease protection assay was performed as in Dou et al.²² Briefly, purified parasites were pelleted for 10 min at 1000xg at 4°C, supernatant was aspirated, and the pellet resuspended in 250 µl of freshly prepared 1 mg/mL Pronase (Roche, Cat# 10165921001)/0.01% Saponin/PBS and incubated at 12°C for 1 h. 5 mL ice cold PBS was added to stop the reaction.

Intracellular Fluorescent Protein Acquisition Assay

Host cells expressing cytosolic mCherry were obtained by with transiently transfecting CHO-K1 cells with pCVM mCherry N3 plasmid or treating CHO-K1 imCh cells with 2 µg/mL doxycycline (Clontech, Cat# 63111) for 96 h. Cytosolic mCherry expressing cells were then synchronously invaded with *T. gondii* parasites by the ENDO Buffer method, treated with LHVS or equal volume of DMSO for the indicated time prior to harvest, and purified at the indicated times post-invasion as previously described.²² For ddGFP-DrpB strains, EtOH or Shield-1 was added for the indicated amounts of time prior to harvest to induce DrpB WT or K72A expression. All subsequent harvesting steps are performed on ice or at 4°C unless otherwise noted. Infected cells were washed twice with ice-cold PBS to remove any extracellular parasites, and intracellular parasites were liberated and purified by scraping and syringing with a 5/8" 25g needle before passing through a 3 µm filter. Parasites were then subjected to the protease protection assay, pelleted by spinning at 1000xg for 10 min and washed three times in ice cold PBS before depositing on Cell-Tak (Corning, Cat# 354240) coated chamber slides. Parasites were fixed and stained with the indicated antibodies.

Assessment of ingestion and localization

Imaging was performed at 63x with an AxioCAM MRm camera-equipped Zeiss Axiovert Observer Z1 inverted fluorescence microscope. Ingestion of host mCherry was scored manually as mCherry-positive or mCherry-negative. Colocalization of ingested mCherry and endolysosomal markers was scored manually with each individual puncta of ingested mCherry or endolysosomal marker signal being scored using a binary measure of colocalized or not. This gives a readout of percent puncta colocalized with a given endolysosomal marker within each experiment. Ingested mCherry or endolysosomal marker puncta were scored as colocalized if they showed any overlap, and there was no differentiation between complete or partial colocalization.

Detection of MIC3 Secretion into the PV

HFF chamber slides were synchronously invaded with ddFKBP-GFP-DrpB WT or K72A parasites by the ENDO Buffer Method and treated with ethanol or Shield-1 for the

indicated amounts of time immediately prior to fixation at 6 h post-invasion. Chamber slides were fixed and stained for MIC3 and TgPI-1 as described above, except cells were partially permeabilized with 0.02% w/v saponin for staining of the PV lumen but not the parasite interior. Cells were then blocked with 10%FBS/PBS, and incubated in primary and secondary antibodies diluted in wash buffer without detergent (1% FBS/1% NGS/PBS) to stain MIC3 as a representative microneme protein and the dense granule protein TgPI-1 as a control stain for the PV lumen. %MIC3+ vacuoles were determined by scoring of TgPI-1+ vacuoles for MIC3 staining.

3.6 Notes and notable contributions

Data in this chapter was published in *Traffic*:

McGovern OL, Rivera-Cuevas Y, Kannan G, Narwold A,Jr, Carruthers VB. Intersection of Endocytic and Exocytic Systems in *Toxoplasma gondii*. *Traffic*. 2018. doi: 10.1111/tra.12556 [doi].

Author contributions are as follows. Experiments were designed by Olivia McGovern and Vern Carruthers. The CHO-K1 imCherry cell line used to generate data in Figures 3-5 and 3-6 in this study was created by Geetha Kannan. Data for all figures was collected and analyzed by Olivia McGovern.

Other contributions are as follows. The ingestion assay used in this study was originally designed by Zhicheng Dou and modified by Olivia McGovern to include synchronized invasion and reduced LHVS treatment times. A special thank you to Ronald Holz for his suggestion to reduce LHVS treatment to more accurately measure when host protein ingestion is occurring, which made experiments in Figure 3-5 and 3-6 possible. We gratefully acknowledge funding to support this work including NIH T32 Molecular Mechanisms of Microbial Pathogenesis (5T32AI007528 to Olivia McGovern), NIH Ruth L. Kirschstein F31-Diversity (1F31AI118274-01 to Olivia McGovern), and ASM Robert D. Watkins Graduate Research Fellowship (to Olivia McGovern) and an NIH operating grant (R01AI120607 to Vern Carruthers). We thank our colleagues for the generous contribution of reagents essential for this study including Markus Meissner, David Roos,

Matthew Bogyo, Jonathan Howard, Peter Bradley, Jean-Francois Dubremetz, and Gustavo Arrizabalaga.

3.7 References

1. Pfluger SL, Goodson HV, Moran JM, et al. Receptor for retrograde transport in the apicomplexan parasite *Toxoplasma gondii*. *Eukaryot Cell*. 2005;Feb 4(2):432--42.
2. Harper JM, Huynh MH, Coppens I, Parussini F, Moreno S, Carruthers VB. A cleavable propeptide influences *Toxoplasma* infection by facilitating the trafficking and secretion of the TgMIC2-M2AP invasion complex. *Mol Biol Cell*. 2006;17(10):4551-4563. doi: E06-01-0064 [pii]; 10.1091/mbc.E06-01-0064 [doi].
3. Parussini F, Coppens I, Shah PP, Diamond SL, Carruthers VB. Cathepsin L occupies a vacuolar compartment and is a protein maturase within the endo/exocytic system of *Toxoplasma gondii*. *Mol Microbiol*. 2010;76(6):1340-1357. doi: 10.1111/j.1365-2958.2010.07181.x.
4. Dou Z, Coppens I, Carruthers VB. Non-canonical Maturation of Two Papain-family Proteases in *Toxoplasma gondii*. *J Biol Chem*. 2013;288(5):3523-3534. doi: 10.1074/jbc.M112.443697; 10.1074/jbc.M112.443697.
5. Dettmer J, Hong-Hermesdorf A, Stierhof Y, Schumacher K. Vacuolar H⁺-ATPase activity is required for endocytic and secretory trafficking in Arabidopsis. *Plant Cell*. 2006;18:715-730.
6. Ferguson SM, De Camilli P. Dynamin, a membrane-remodelling GTPase. *Nat Rev Mol Cell Biol*. 2012;13(2):75-88. doi: 10.1038/nrm3266 [doi].
7. Breinich MS, Ferguson DJ, Foth BJ, et al. A dynamin is required for the biogenesis of secretory organelles in *Toxoplasma gondii*. *Curr Biol*. 2009;19(4):277-286. doi: 10.1016/j.cub.2009.01.039.
8. Smaczynska-de R, II, Allwood EG, Aghamohammadzadeh S, Hetteema EH, Goldberg MW, Ayscough KR. A role for the dynamin-like protein Vps1 during endocytosis in yeast. *J Cell Sci*. 2010;123(Pt 20):3496-3506. doi: 10.1242/jcs.070508 [doi].
9. Weinberg J, Drubin DG. Clathrin-mediated endocytosis in budding yeast. *Trends Cell Biol*. 2012;22(1):1-13. doi: 10.1016/j.tcb.2011.09.001 [doi].
10. Fujimoto M, Tsutsumi N. Dynamin-related proteins in plant post-Golgi traffic. *Front Plant Sci*. 2014;5:408. doi: 10.3389/fpls.2014.00408 [doi].
11. Praefcke GJ, McMahon HT. The dynamin superfamily: universal membrane tubulation and fission molecules?. *Nat Rev Mol Cell Biol*. 2004;5(2):133-147. doi: 10.1038/nrm1313 [doi].

12. Fujimoto M, Arimura S, Mano S, et al. *Arabidopsis* dynamin-related proteins DRP3A and DRP3B are functionally redundant in mitochondrial fission, but have distinct roles in peroxisomal fission. *Plant J*. 2009;58(3):388-400. doi: 10.1111/j.1365-313X.2009.03786.x [doi].
13. Wong ED, Wagner JA, Scott SV, et al. The intramitochondrial dynamin-related GTPase, Mgm1p, is a component of a protein complex that mediates mitochondrial fusion. *J Cell Biol*. 2003;160(3):303-311. doi: 10.1083/jcb.200209015 [doi].
14. Jin JB, Kim YA, Kim SJ, et al. A new dynamin-like protein, ADL6, is involved in trafficking from the trans-Golgi network to the central vacuole in *Arabidopsis*. *Plant Cell*. 2001;13(7):1511-1526.
15. Lam BC, Sage TL, Bianchi F, Blumwald E. Regulation of ADL6 activity by its associated molecular network. *Plant J*. 2002;31(5):565-576. doi: 1377 [pii].
16. Fujimoto M, Arimura S, Nakazono M, Tsutsumi N. *Arabidopsis* dynamin-related protein DRP2B is co-localized with DRP1A on the leading edge of the forming cell plate. *Plant Cell Rep*. 2008;27(10):1581-1586. doi: 10.1007/s00299-008-0583-0 [doi].
17. Taylor NG. A role for *Arabidopsis* dynamin related proteins DRP2A/B in endocytosis; DRP2 function is essential for plant growth. *Plant Mol Biol*. 2011;76(1-2):117-129. doi: 10.1007/s11103-011-9773-1 [doi].
18. Pieperhoff MS, Schmitt M, Ferguson DJ, Meissner M. The role of clathrin in post-Golgi trafficking in *Toxoplasma gondii*. *PLoS One*. 2013;8(10):e77620. doi: 10.1371/journal.pone.0077620 [doi].
19. Hinshaw JE. Dynamin and its role in membrane fission. *Annu Rev Cell Dev Biol*. 2000;16:483-519. doi: 10.1146/annurev.cellbio.16.1.483 [doi].
20. Milani KJ, Schneider TG, Taraschi TF. Defining the Morphology and Mechanism of the Hemoglobin Transport Pathway in *Plasmodium falciparum* Infected Erythrocytes. *Eukaryot Cell*. 2015. doi: EC.00267-14 [pii].
21. Damke H, Baba T, Warnock DE, Schmid SL. Induction of mutant dynamin specifically blocks endocytic coated vesicle formation. *J Cell Biol*. 1994;127(4):915-934.
22. Dou Z, McGovern O, Di Cristina M, Carruthers V. *Toxoplasma gondii* ingests and digests host cytosolic proteins. *mBio*. 2014;5(4):e01188-14.
23. Brillada C, Rojas-Pierce M. Vacuolar trafficking and biogenesis: a maturation in the field. *Curr Opin Plant Biol*. 2017 Aug 31;40:77-81. doi: 10.1016/j.pbi.2017.08.005. [Epub ahead of print].

24. Kunzl F, Fruholz S, Fassler F, Li B, Pimpl P. Receptor-mediated sorting of soluble vacuolar proteins ends at the trans-Golgi network/early endosome. *Nat Plants*. 2016;2:16017. doi: 10.1038/nplants.2016.17 [doi].
25. Cui Y, Shen J, Gao C, Zhuang X, Wang J, Jiang L. Biogenesis of Plant Prevacuolar Multivesicular Bodies. *Mol Plant*. 2016;9(6):774-786. doi: 10.1016/j.molp.2016.01.011 [doi].
26. Scheuring D, Viotti C, Kruger F, et al. Multivesicular bodies mature from the trans-Golgi network/early endosome in Arabidopsis. *Plant Cell*. 2011;23(9):3463-3481. doi: 10.1105/tpc.111.086918 [doi].
27. Venugopal K, Werkmeister E, Barois N, et al. Dual role of the *Toxoplasma gondii* clathrin adaptor AP1 in the sorting of rhoptry and microneme proteins and in parasite division. *PLoS Pathog*. 2017 Apr 21;13(4):e1006331.
28. van Dooren GG, Reiff SB, Tomova C, Meissner M, Humbel BM, Striepen B. A novel dynamin-related protein has been recruited for apicoplast fission in *Toxoplasma gondii*. *Curr Biol*. 2009;19(4):267-276. doi: 10.1016/j.cub.2008.12.048.
29. Gao H, Kadirjan-Kalbach D, Froehlich JE, Osteryoung KW. ARC5, a cytosolic dynamin-like protein from plants, is part of the chloroplast division machinery. *Proc Natl Acad Sci U S A*. 2003;100(7):4328-4333. doi: 10.1073/pnas.0530206100 [doi].
30. Renard HF, Johannes L, Morsomme P. Increasing Diversity of Biological Membrane Fission Mechanisms. *Trends Cell Biol*. 2018. doi: S0962-8924(17)30234-9 [pii].
31. Kumari S, Mayor S. ARF1 is directly involved in dynamin-independent endocytosis. *Nat Cell Biol*. 2008;10(1):30-41. doi: ncb1666 [pii].
32. Choi JH, Park JB, Bae SS, et al. Phospholipase C-gamma1 is a guanine nucleotide exchange factor for dynamin-1 and enhances dynamin-1-dependent epidermal growth factor receptor endocytosis. *J Cell Sci*. 2004;117(Pt 17):3785-3795. doi: 10.1242/jcs.01220 [doi].
33. Pucadyil TJ, Schmid SL. Conserved functions of membrane active GTPases in coated vesicle formation. *Science*. 2009;325(5945):1217-1220. doi: 10.1126/science.1171004 [doi].
34. Chaudhary N, Gomez GA, Howes MT, et al. Endocytic crosstalk: cavins, caveolins, and caveolae regulate clathrin-independent endocytosis. *PLoS Biol*. 2014;12(4):e1001832. doi: 10.1371/journal.pbio.1001832 [doi].
35. Larson ET, Parussini F, Huynh MH, et al. *Toxoplasma gondii* cathepsin L is the primary target of the invasion-inhibitory compound morpholinurea-leucyl-homophenyl-vinyl sulfone phenyl. *J Biol Chem*. 2009;284(39):26839-26850. doi: 10.1074/jbc.M109.003780.

36. Francia ME, Wicher S, Pace DA, Sullivan J, Moreno SNJ, Arrizabalaga G. A *Toxoplasma gondii* protein with homology to intracellular type Na⁺/H⁺ Exchangers is important for osmoregulation and invasion. *Exp Cell Res*. 2011 Jun 10;317(10):1382–1396.
37. Morris MT, Coppin A, Tomavo S, V C. Functional analysis of *Toxoplasma gondii* protease inhibitor 1. *J Biol Chem*. 2002;277(47):45259-66.
38. Lebrun M, Michelin A, El Hajj H, et al. The rhoptry neck protein RON4 re-localizes at the moving junction during *Toxoplasma gondii* invasion. *Cell Microbiol*. 2005;7(12):1823-1833. doi: 10.1111/j.1462-5822.2005.00646.x.
39. Achbarou A, Mercereau-Puijalon O, Autheman JM, Fortier B, Camus D, Dubremetz JF. Characterization of microneme proteins of *Toxoplasma gondii*. *Mol Biochem Parasitol*. 1991;47(2):223-233. doi: 0166-6851(91)90182-6 [pii].
40. Zhao Y, Khaminets A, Hunn J, Howard J. Disruption of the *Toxoplasma gondii* parasitophorous vacuole by IFN γ -inducible immunity related GTPases (IRG proteins) triggers necrotic cell death. *PLoS Pathogens*. 2009;5(2):e1000288.
41. Kafsack BF, Beckers C, Carruthers VB. Synchronous invasion of host cells by *Toxoplasma gondii*. *Mol Biochem Parasitol*. 2004;136(2):309-311.

Chapter 4

Discussion

4.1 Overview

Cathepsin L (CPL)-deficient parasites exhibit virulence defects in both the acute and chronic stages of infection.^{1,2} While we do not understand the exact contribution of host protein ingestion to virulence since CPL contributes to degradation of both proteins acquired from the host cell and parasite-derived proteins, these virulence defects suggest that ingestion pathway could be an important source of novel drug targets. Further, *Plasmodium spp.* have an analogous endocytic pathway for ingestion of host cytosol that is essential for scavenging of amino acids, but the mechanisms of this pathway are poorly understood.³ Therefore, a better understanding of the *T. gondii* ingestion pathway could be useful for development of novel therapeutics for toxoplasmosis and could serve as a model to understand host protein ingestion in *Plasmodium spp.*

Prior to these studies, we knew that proteins from the host cell cytosol were taken up into *T. gondii* and degraded in the lysosome-like VAC. Acquisition of host proteins required GRA2, a structural component to the intravacuolar network (IVN), and degradation of the ingested protein required the VAC-localized protease CPL.² Our hypothetical model can now be updated based on data in Chapters 2 and 3 (Figure 4-1). First, host proteins are rapidly ingested within 7 minutes post-infection, when IVN tubules are not yet established, suggesting IVN is not required for ingestion. Once taken up into the parasite, ingested host proteins are trafficked through the endosome-like compartments (ELCs), where they intersect with exocytic trafficking to the micronemes, and reach the VAC within 30 minutes for degradation. Whether endocytic cargoes are also trafficked through the trans-Golgi network (TGN) as in plants remains unclear since typical TGN markers in the field, GalNac and DrpB, localized to both the TGN and ELCs. Definitive mechanistic insight is still elusive, but DrpB is not required for endocytic

trafficking across the parasitophorous vacuole membrane (PVM) and parasite plasma membrane or for downstream trafficking to the VAC.

Remaining gaps in our hypothetical model that should be addressed in future work will be discussed in this chapter (Figure 4-1). Phenotype scores from a CRISPR-based screen knocking out every gene in the *T. gondii* genome will also be discussed as a guide for which targets could be particularly fruitful (Table 4-1).⁴ Phenotype scores indicate the relative contribution of a gene to parasite fitness under normal growth conditions *in vitro*. A negative score indicates that loss of the gene decreases fitness, and a positive score indicates that loss of the gene confers an advantage relative to the entire population of knockouts. Although the fitness scores do not indicate involvement in *T. gondii* endocytosis, from a practical point of view, genes that are most important for parasite survival would be most likely to lead to discovery of druggable targets. Clathrin, DrpB, Rab5A and Rab5C are required for microneme and rhoptry organelle biogenesis and are therefore essential. For reference, they have phenotype scores of -4 to -5 (Table 4-1).⁴⁻⁷

Trafficking across the PVM and parasite plasma membrane

Section 4.2

- ① Role of the IVN and Host ESCRT?

Section 4.3

- ② Clathrin-mediated endocytosis or not?

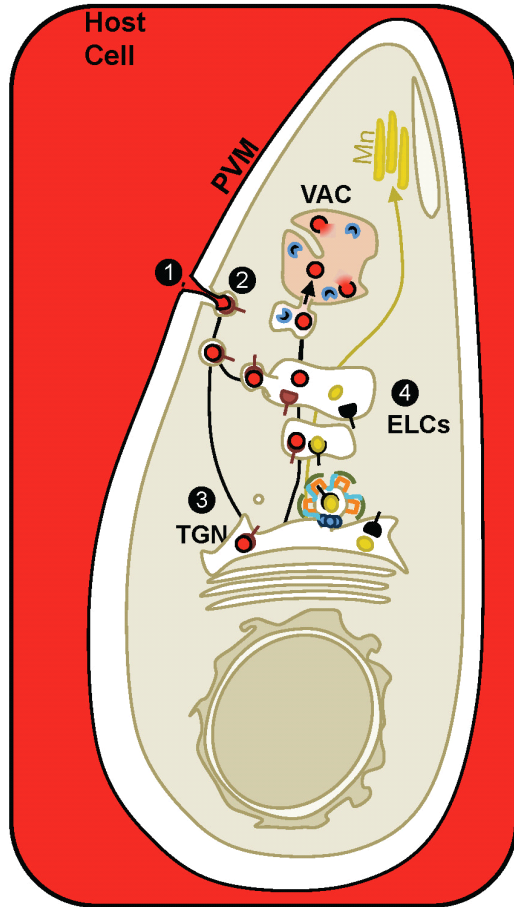
Downstream trafficking to the VAC

Section 4.4

- ③ Endocytic trafficking through the TGN?

- ④ Role for Rab5, Rab7, Mon1-Ccz1, CORVET or HOPS?

- ⑤ Are TgSORTLR or VSRs endocytic sorting receptors?



- Ingested host protein
- Microneme (Mn) protein
- TgSORTLR
- Putative Ingestion Receptor
- AP1
- ┌ TgEpsL
- └ Clathrin
- Dynamin

Figure 4-1. Working model for host protein ingestion and overview of Chapter 4 discussion of ongoing work and future directions. Note Section 4.6 and 4.7 are not included in this figure. Section 4.6 will address tools to be used and/or developed for studying the targets discussed in Sections 4.2-4.5. Section 4.7 will address the possible roles of the endocytosis in *T. gondii*.

Table 4-1. Phenotype scores for genes potentially involved in *T. gondii* endocytosis.

GeneID	Protein Name	Domain/Complex	Predicted (?)/Known Function	Phenotype Score ⁴
TgGT1_290950	Clathrin	Heavy Chain	Interacts with AP-1 mu1 at TGN ⁸ , promotes microneme and rhoptry trafficking at the TGN ⁵	- 4.77
TgGT1_221940	AP2	alpha subunit	Clathrin adaptor for endocytosis? ⁹	- 4.32
TgGT1_240870		beta2 subunit		- 2.83
TgGT1_230920		mu2 subunit		- 1.60
TgGT1_313450		sigma-1 subunit		- 2.88
TgGT1_320760	Hypothetical	BAR/IMD-like Domain	Promote membrane curvature?	0.56
TgGT1_259720	Hypothetical	BAR/IMD-like Domain	Promote membrane curvature?	- 4.55
TgGT1_216030A	Hypothetical	ENTH/VHS Domain	Promote membrane curvature, clathrin adaptor protein?	- 0.67
TgGT1_227800	TgEPS15	Eps15 Homology Domain	Clathrin-mediated endocytosis nucleation/scaffold protein?	-3.19
TgGT1_214180	TgEpsL	ENTH Domain	Interacts with TgAP-1 at TGN but likely not AP-2, formation of clathrin coated vesicles in secretory trafficking ⁸	-0.52
TgGT1_213370	Frm3	Actin-binding	Actin nucleation during endocytosis? ¹⁰	-2.79
TgGT1_267045	Hypothetical	Ras superfamily/Rho GTPase	Regulation of actin during endocytosis?	0.81
TgGT1_249170	Hypothetical	Ras superfamily/Rho GTPase	Regulation of actin during endocytosis?	-0.79
TgGT1_233300	Hypothetical	RhoGAP	Regulation of actin during endocytosis?	1.52
TGGT1_321620	DrpB	GTPase	Microneme and rhoptry trafficking at the TGN ⁶	-4.91
TgGT1_270690	DrpC	GTPase	Mitochondrial maintenance? ⁵	-4.54
TgGT1_267810	Rab5A	GTPase	Microneme and rhoptry trafficking at the TGN/ELCs ⁷	-4.48
TgGT1_207460B [†]	Rab5B	GTPase	Undefined ⁷ , recycling to plasma membrane?	0.55
TgGT1_207460A [†]	Rab5B	GTPase	Undefined ⁷ , recycling to plasma membrane?	-1.35
TgGT1_219720	Rab5C	GTPase	Microneme and rhoptry trafficking at the TGN/ELCs ⁷	-4.24
TgGT1_248880	Rab7	GTPase	Undefined ⁷ , fusion with the lysosome?	-2.67
TgGT1_230220	Vps11	CORVET/HOPS	Exocytic trafficking to the micronemes and rhoptries ¹¹ , biogenesis of the VAC ¹¹ , endocytic trafficking through Rab5 and Rab7 compartments to the VAC?	-4.09

GeneID	Protein Name	Domain/Complex	Predicted (?)/Known Function	Phenotype Score ⁴
TgGT1_320670	Vps16	CORVET/HOPS	Exocytic trafficking to the micronemes and rhoptries? Endocytic trafficking through Rab5 and Rab7 compartments to the VAC?	-4.82
TgGT1_289730	Vps18	CORVET/HOPS	Exocytic trafficking to the micronemes and rhoptries ¹¹ , endocytic trafficking through Rab5 and Rab7 compartments to the VAC?	-3.24
TgGT1_295000	Vps33	CORVET/HOPS	Exocytic trafficking to the micronemes and rhoptries? Endocytic trafficking through Rab5 and Rab7 compartments to the VAC?	-4.78
TgGT1_224270	Vps41	HOPS	Exocytic trafficking to the micronemes and rhoptries? Endocytic trafficking through Rab5 and Rab7 compartments to the VAC?	-3.75
TgGT1_315530	Vps39	HOPS	Exocytic trafficking to the micronemes and rhoptries ¹¹ , endocytic trafficking through Rab5 and Rab7 compartments to the VAC?	-4.18
TgGT1_291120	Mon1	SAND1/Mon1-Ccz1	Rab7 GEF? Exocytic trafficking to the micronemes and rhoptries ¹¹ , endocytic trafficking through Rab5 and Rab7 compartments to the VAC?	-4.42
TgGT1_207960	Ccz1	SAND1/Mon1-Ccz1	Rab7Gef? Exocytic trafficking to the micronemes and rhoptries? Endocytic trafficking through Rab5 and Rab7 compartments to the VAC?	-3.96
TgGT1_224710	VSR1	PA domain	Undefined(unpublished data), cargo recognition for sorting to the VAC?	-0.90
TgGT1_312860	VSR2	PA domain	Undefined(unpublished data), cargo recognition for sorting to the VAC?	-0.09

Note: phenotype scores are color coded from dark red (most essential) to blue (least essential), and hypothetical proteins were found based on Interpro search terms. [†]There are two, separate annotated Rab5B-like genes found in the GT1 genome, which is the strain that guide RNAs for the genome-wide CRISPR screen was designed against. These genes are TgGT1_207460A and TgGT1_207460B, and neighbor each other on chromosome 1b. This appears to be an incorrect annotation in the ToxoDB database, and these likely correspond to the 5' and 3' ends of a single Rab5B gene.

4.2 Ongoing and future work for mechanisms of trafficking across the PVM

The 40% reduction in ingestion observed in overnight replicated GRA2 knockout parasites could be explained by the IVN contributing directly, e.g. ingestion of IVN tubules or vesicles derived from the IVN, or indirectly through the role of the IVN in organizing parasites in the PV.^{2, 12} Data in Chapter 2 showed that ingestion begins within 7 minutes post-invasion. Since IVN tubules are not generated until about 1 h post-invasion, this suggests that the IVN is not directly required for ingestion.¹³ Consistent with this, preliminary studies show that GRA2 is not required for ingestion during the first hour of infection before IVN tubules are generated or even at 3 hours post-invasion when IVN tubules are generated, but vacuoles are not disorganized (Figure 4-2A). This suggests

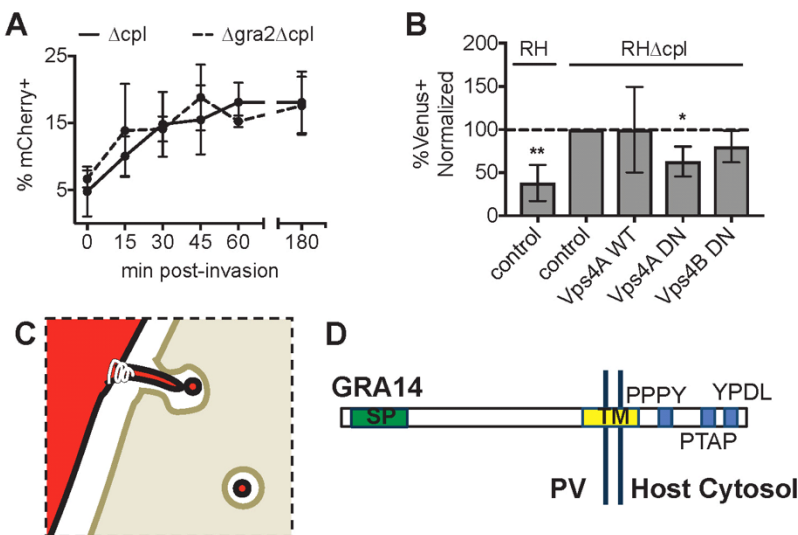


Figure 4-2. Host ESCRT may contribute to ingestion. **A.** Ingestion of host cytosolic mCherry in CPL knockout parasites that are wildtype (Δcpl) or knocked out for GRA2 ($\Delta cpl\Delta gra2$). Ingestion assay performed as in Figure 2-2. Shown is percentage of parasites with ingested mCherry, at least 200 parasites analyzed per strain per time point for three biological replicates. Paired t-test to compare Δcpl vs. $\Delta cpl\Delta gra2$ parasites for each time point. No significant differences. Performed and analyzed by Olivia McGovern. **B.** Ingestion of host cytosolic Venus in cells expressing wildtype or dominant negative Vps4 on ingestion of host Venus. CHO cells were transfected with Venus alone (control) or cotransfected with plasmids expressing wildtype Vps4A or dominant negative mutants of Vps4A or Vps4B, infected with RH or Δcpl parasites and harvested at 3 h post-infection. Shown is percent parasites with ingested Venus normalized to the cpl knockout control. At least 200 parasites analyzed per condition for three biological replicates. One sample t-test to test if values are less than 100, only significant results shown. * $p < 0.05$, ** $p < 0.01$. Performed and analyzed by Anna-Lisa Lawrence. **C.** Model for ingestion across the PVM and parasite plasma membrane depicting a role for ESCRT in PVM scission. **D.** GRA14 schematic. SP is signal peptide, TM is transmembrane domain. Blue rectangles indicate location of PPPY, PTAP, and YPDL motifs for ESCRT recruitment in retroviruses. Bioinformatic analysis performed by Dr. Vern Carruthers.

that IVN contributes to ingestion indirectly by organizing parasites within the PV, and host protein-containing vesicles are likely derived from the PVM rather than the IVN.

The hypothetical model proposed in Chapter 1 also suggested that proteins in the host cell like the Endosomal Sorting Complex Required for Transport (ESCRT) complex, which drives intraluminal vesicle formation on host endosomes, could aid in endocytic trafficking across the PVM. The complexes of the ESCRT machinery, ESCRT-0, -I, -II, -III are

sequentially recruited to bend endosomal membranes away from the cytosol, and Vps4 hydrolyzes ATP to recycle the ESCRT machinery back to the cytosol and to drive scission and release of vesicles into the lumen of the endosome.¹⁴ We propose that host ESCRT could be recruited to the PVM, where it would promote scission of vesicles into the PV lumen. Consistent with this, expression of a dominant negative Vps4 mutant in infected host cells, which cannot hydrolyze ATP or form intraluminal vesicles, reduces ingestion by 40% (Figure 4-2B).¹⁵ This suggests that host ESCRT is required for endocytosis (Figure 4-2C). It is unclear whether reduction in endocytosis is due to requirement of Vps4 and/or other ESCRT components since Vps4 drives membrane scission and ESCRT recycling. Future studies will include interference with additional ESCRT components through expression of dominant negative mutants or siRNA knockdown.

How ESCRT could be hijacked by *T. gondii* is also being explored. Presence of the lipid phosphatidylinositol-3-phosphate (PI3P) in endosomal membranes and ubiquitinated proteins are responsible for recruiting ESCRT machinery.¹⁴ PI3P does not appear to be abundant on the PVM and ubiquitinated proteins are not abundantly present without interferon gamma stimulation, which is not a necessary condition for ingestion.¹⁶ However, enveloped viruses can bypass these requirements and use ESCRT machinery to bud out of the host cell.¹⁷ PT/SAP and YPXL motifs in the cytosolic portion of HIV GAG directly recruit Tsg101 of ESCRT-I and the ESCRT-associated protein Alix.¹⁸ Alix binds to HIV Gag, Tsg101 and CHMP4 of ESCRT-III.¹⁸ The rest of the ESCRT-III complex is assembled and recruits Vps4 to mediate scission of HIV particles out of the cell.¹⁸ Additionally, PPXY motifs in the Gag of retroviruses like Rous Sarcoma Virus recruit Nedd4 family ubiquitin ligases.^{18, 19} How these Nedd4 ubiquitin ligases connect retroviral budding with the ESCRT machinery is not well established, but ubiquitination of Gag could provide a scaffold for ESCRT assembly at the viral budding site. Alix and the ESCRT-I complex both bind to ubiquitin, and mutation of the Alix ubiquitin binding sites impairs HIV and EIAV budding.^{14, 20} Conjugation of ubiquitin to EIAV, which lacks a PPXY motif, rescues budding of viruses lacking their YDXL motif in an Alix- and Tsg101-dependent manner.²¹ Alternatively, arrestin-related-trafficking proteins (ARTs) may link Nedd4 ubiquitin ligases to ESCRT machinery. ARTs are recruited to budding sites for Murine Leukemia Virus, they interact with Nedd4 ubiquitin ligases, Alix and Tsg101, and

their overexpression inhibits viral budding.²² Interestingly, the dense granule protein GRA14 is an integral membrane protein in the IVN and PVM of *T. gondii*, and the C-terminal domain, which is exposed to the host cytosol, contains all three of these motifs (Figure 4-2D).²³ It will be interesting to know if GRA14 is required for ingestion of host cytosol and hijacking host ESCRT. Given the roles of the PTAP, YPDL and PPPY motifs in retroviruses, Alix, Tsg101, CHMP4 and ARTs should be priorities for dominant negative interference and siRNA knockdown experiments to test the role of ESCRT.

4.3 Ongoing and future work for mechanisms of trafficking across the parasite plasma membrane

The proposed site of endocytosis is the micropore, which sometimes shows a proteinaceous coat by electron microscopy.²⁴ Since *T. gondii* lacks caveolins/cavins, this coat is likely clathrin, suggesting that clathrin-mediated endocytosis may occur in *T. gondii*.^{5, 25} However, a bioinformatics search for homologs of genes in the yeast clathrin interactome revealed a paucity of effectors required for endocytosis. Clathrin, dynamin, actin and an epsin-like protein (TgEpsL) are expressed in *T. gondii*, and the bioinformatic search found homologs for the scaffolding protein EPS15 and the clathrin adaptor complex AP2.⁵ However, there were no obvious homologs for the nucleator intersectin, adaptors AP180 or epsin, actin polymerizing and branching proteins N-WASP and Arp2/3, Hip1R which links actin to the clathrin coat, or uncoating proteins related to auxillin.⁵ It should be noted that the F-BAR nucleator FCHO1/2 and N-BAR proteins endophilin and amphiphysin were not included in this search. Given that clathrin also has not been localized to the plasma membrane, this could suggest that clathrin-mediated endocytosis does not occur in *T. gondii*.⁵

However, other parasite proteins could substitute for these missing players. Additional searching revealed *T. gondii* encodes two hypothetical BAR domain proteins (TgGT1_259720 and TgGT1_320760) and a hypothetical ENTH-domain containing protein (TgGT1_216030A) that could participate in membrane bending or nucleation or endocytosis like FCHO1/2 (Table 4-1). A recent study in yeast also discovered a clathrin-independent endocytic pathway that does not require Arp2/3 and instead relies on formin and RhoA GTPase.²⁶ *T. gondii* expresses three formin (Frm) proteins capable of

polymerizing actin. *T. gondii* Frm1 and Frm2 promote parasite motility during invasion.²⁷ Frm3 is not required for invasion and localizes to a discrete, unidentified structure at the apical end of the parasite.¹⁰ Frm3 seems like the best candidate given that this localization is consistent with the micropore (Table 4-1). Alternatively, *T. gondii* may not require these missing effectors or may have evolved novel effector proteins of its own. For example, another protozoan parasite, *Trypanosoma brucei*, undergoes clathrin-mediated endocytosis despite lacking AP2 and encoding a single dynamin that is devoted to mitochondrial maintenance but not endocytosis.^{28, 29} Plants have evolved a unique nucleator complex for clathrin-mediated endocytosis called the TPLATE complex.³⁰ Protein BLAST searches did not reveal homologs of any TPLATE complex members in the *T. gondii* genome, but other yet to be discovered parasite-specific effectors could exist and coordinate clathrin-mediated endocytosis.

It is also possible that ingestion of host proteins by *T. gondii* could resemble clathrin-independent mechanisms and require actin, regulatory Rho family GTPases, and/or BAR-domain containing proteins as in the RhoA GTPase-dependent IL-2 receptor endocytosis pathway, CLIC/GEEC, or FEME (Figure 4-3B).³¹⁻³³ Actin could be nucleated by a protein like Frm3, and *T. gondii* has two hypothetical Rho-like GTPases and a hypothetical RHOGAP-like protein, TgGT1_267045, TgGT1_249170 and TgGT1_233300 respectively (Table 4-1). Alternatively, N-BAR or ENTH domain proteins that have amphipathic helices may act independently in membrane scission. The N-BAR domains of endophilin and amphiphysin and the ENTH domain of epsin have amphipathic helices and are capable of vesiculating liposomes *in vitro*.^{34, 35} Also, overexpression of epsin can rescue scission of clathrin-coated vesicles when dynamin is knocked down.³⁵

Whatever mechanism drives endocytosis across the PVM and parasite plasma membrane, data in Chapter 3 shows that it does not require DrpB, but host protein ingestion could still require dynamin. *Toxoplasma* expresses two more dynamins-related proteins, DrpA and DrpC, which have not been tested in endocytosis. DrpA is responsible for the maintenance of the chloroplast-like organelle of the parasite, the apicoplast. DrpC is presumed to function in mitochondrial maintenance, but its localization and function are undefined and could possibly drive endocytic vesicle fission (Figure 4-3A).^{7, 36}

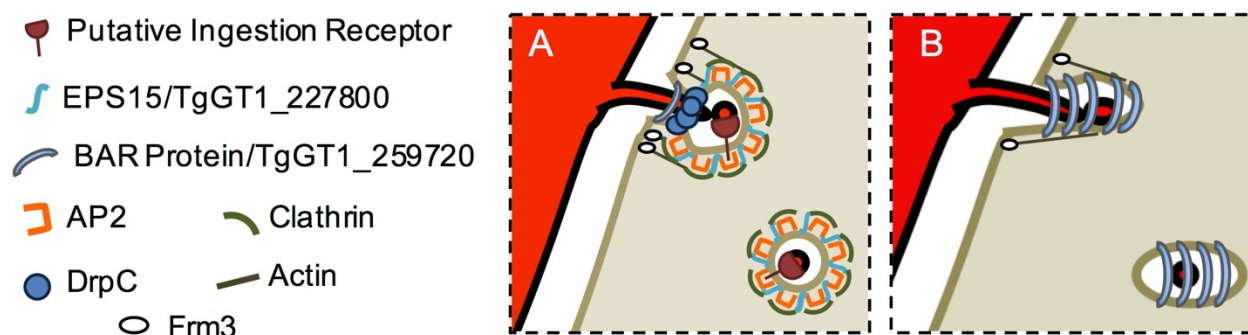


Figure 4-3. Hypothetical models for mechanisms of endocytosis. **A.** Clathrin-mediated endocytosis or **B.** clathrin-independent CLIC/GEEC-like mechanism of endocytosis, driven by BAR-domain containing proteins and actin. Favored proteins, based on phenotype score or proposed function, are inserted into their potentially appropriate places as indicated by the legend to the left. Note that actin filaments are depicted as linear and orthogonal to the plasma membrane depicting the mechanisms for actin polymerization by formin versus N-WASP and Arp2/3, which promotes branched actin.

Future studies will include more comprehensive bioinformatic searches for homologs of characterized endocytic players. To differentiate between clathrin-dependent and -independent mechanisms, clathrin, AP2 and actin should be targeted. DrpC, the hypothetical BAR-domain containing protein TgGT1_259720, and the putative EPS15 homolog TgGT1_227800 could be interesting given their phenotype scores are -4.54, -4.55, and -3.19 respectively (Table 4-1), indicating they are particularly important to parasite survival. Finally, studying these proteins should also give insight into the site of endocytosis in *T. gondii*. We predict that endocytosis occurs at the micropore, but to date there are no known markers associated with this elusive structure. Frm3 or AP2 could be particularly interesting from this point of view given Frm3's peculiar localization and that AP2 is expected to be exclusively dedicated to endocytosis at the plasma membrane.³⁷

4.4 Ongoing and future work for mechanisms of trafficking to the VAC

Localization of GalNac and DrpB to the TGN and ELCs prevented us from determining if ingested protein trafficked through the TGN. Future studies will benefit from discovery of markers that are restricted exclusively to the TGN. Alternatively, ingested protein trafficking could be tracked using correlative light and electron microscopy (CLEM), which allows electron microscopy of structures of interest that are identified by fluorescence microscopy on a defined grid.³⁸ MiniSOG is a small green fluorescent

protein that generates reactive oxygen species when exposed to 488nm light, and in the presence of diaminobenzidine, will create electron dense deposits that can be detected by osmium tetroxide staining by electron microscopy.³⁸ Parasites allowed to ingest miniSOG from host cells in a time course like in Chapter 2 could be imaged in this way to define the ultrastructural morphology of compartments that contain ingested proteins. For example, is the non-digestive compartment occupied at 7 minutes post-invasion really a double membrane vesicle like in *Plasmodium spp.*? Are ingested proteins associated with Golgi or TGN-like structures at a later time point? This method could also be coupled with immunogold labeling of Rab5, Rab7, or a specific TGN marker to identify specific endocytic compartments.

If ingested host proteins are trafficked through the TGN, it will be interesting to identify the mechanism of downstream trafficking to the VAC is. Knockdown of a component of the ESCRT-II complex in plants blocks maturation of the TGN into Rab5 endosomes.³⁹ *T. gondii* lacks most components of ESCRT, and only expresses the ATPase Vps4 and one subunit of ESCRT-III.⁹ If the TGN is involved in endocytic trafficking, subsequent trafficking could involve clathrin coated vesicles as proposed for exocytic trafficking to the micronemes and rhoptries. Albeit this would occur in a DrpB-independent manner as indicated in Chapter 3.

The roles of Rab5 and Rab7 in endocytic trafficking to the VAC also remain untested. Like plants and *Plasmodium spp.*, *T. gondii* expresses two C-terminally geranylated, conventional Rab5s, Rab5A and Rab5C, and one plant-specific, N-terminally myristoylated Rab5, Rab5B.^{7, 40, 41} As in plants, the conventional Rab5s show nearly perfect colocalization, whereas plant-like Rab5B only partial colocalizes with RabA and Rab5C, and also shows surface localization.^{7, 41} In plants, the conventional Rab5s promote endocytic trafficking to the lysosome, whereas the plant-specific Rab5 promotes trafficking from a late endosomal compartment to the plasma membrane.⁴¹ Rab5A and C but not Rab5B promote exocytic trafficking to the micronemes and rhoptries.^{7, 42} The function of Rab5B remains unknown.⁷ Rab5A and RabC could play dual roles in endocytic and exocytic trafficking. Alternatively, Rab5B localization could be consistent with a conserved role in recycling to the plasma membrane or endocytic trafficking from the

plasma membrane to the ELCs. In this case, Rab5A and Rab5C could be dedicated to exocytic trafficking, while Rab5B, could be devoted to endocytic trafficking.

Based on model systems, subsequent trafficking to the VAC would involve a Rab5 to Rab7 switch mediated by recruitment of the Rab7 GEF SAND1/Mon1-Ccz1 and conversion of the CORVET complex to the HOPS complex.^{30, 43, 44} *T. gondii* expresses the core subunits shared by the CORVET and HOPS complexes (Vps11, Vps16, Vps18, Vps33) and the two HOPS-specific subunits (Vps39, Vps41), but not the CORVET-specific subunits (Vps3, Vps8).¹¹ Therefore, whether CORVET functions in *T. gondii* is uncertain. Expression of dominant negative Rab7 does not interrupt microneme and rhoptry biogenesis, implying that it is not involved in this exocytic trafficking route.⁷ Consistent with a role for CORVET and/or HOPS in trafficking to the VAC, Vps11 knockdown resulted loss of Rab7 association with endosomes also the absence of CPL staining, indicating disruption of the VAC.¹¹ However, in contrast to Rab7, the putative Rab7 GEF Mon1 and HOPS-specific subunit Vps39 are required for microneme and rhoptry biogenesis.¹¹ It would be interesting to know if Rab7 and Mon1 or HOPS have different effects on endocytic trafficking as well.

Future studies should resolve colocalization with ELCs, which refers to both the Rab5 and Rab7 endosomes, by using Rab5 and Rab7 as specific markers. Testing Rab5B function would be particularly interesting given its localization and the prospect for identifying plant-like features of *T. gondii* and potentially *Plasmodium spp.* Finally, studies of Rab7 would also be interesting given its phenotype score (-2.67) and possible lack of a role in exocytic trafficking to the micronemes and rhoptries.

4.5 Sorting receptors for endocytic cargo

Data in Chapter 2 showed that endocytic trafficking of ingested proteins and exocytic trafficking of microneme proteins intersects in the ELCs and potentially the TGN if ingested proteins transit there. How these cargoes are properly sorted to ensure that ingested cargo is sent to the VAC for degradation and microneme proteins are delivered intact to the micronemes is not clear but sorting mechanisms will be required. In future studies, it will be interesting to determine if ingested host proteins require sorting to reach the VAC. Endocytic trafficking through TGN and/or ELCs to the VAC could occur by bulk

flow like endocytosed solutes or receptor ligands released in the lumen of endosomes in mammalian cells.⁴⁵ This could even occur from the TGN since endocytosed RFP is delivered to the TGN in plants, where it mixes with exocytic cargoes, and is delivered to the lysosome without any sorting signal or receptors.^{46, 47} However, secretion of soluble proteins into the PV lumen via dense granules is considered to be the default pathway in *T. gondii*.^{48, 49} Whether this occurs from the Golgi or TGN is unclear, but the TGN is likely give that interference with trafficking of microneme and rhoptry proteins from the TGN, e.g. interfering with clathrin or DrpB, leads to their secretion into the PV lumen, presumably via dense granules.^{5, 6, 8, 50} Unless this default secretion occurs from the Golgi due to downstream blockage in the secretory pathway, unguided transport to the VAC would more likely start in the ELCs.

On the other hand, endocytic trafficking could require receptors and sorting machinery. Receptors at the parasite plasma membrane could recognize parasite proteins embedded in the PV-derived membrane of host protein-containing vesicles, which would be difficult to identify using a candidate-based approach. Receptors could also recognize ingested host protein-containing vesicles in endosomal compartments like the TGN or ELCs to assist with sorting to lysosomes. In this case we can look to mannose-6 phosphate receptor, sortilin and the plant-like vacuolar sorting receptors (VSRs), which are the best studied receptors for sorting proteases to the lysosome.

T. gondii does not have a mannose-6-phosphate receptor but does express sortilin (TgSORTLR) and two plant-like VSRs, VSR1 and VSR2 (Table 4-1). TgSORTLR sorts microneme and rhoptry proteins from the TGN to the ELCs on their way to their respective organelles.⁵⁰ The role of TgSORTLR in endocytic trafficking to the VAC has not been tested, so it is possible that it could act as a sorting receptor that co-transportes ingested protein vesicles, microneme proteins and rhoptry proteins from the TGN to the ELCs. However, this seems unlikely given the lack of colocalization between ingested host protein and immature rhoptry proteins, described in Chapter 2.

VSR1 and VSR2 could be interesting candidates. VSRs are thought to bind soluble lysosomal proteases in endoplasmic reticulum via its luminal protease associated (PA) domain and escorts them to the TGN where they are released for bulk flow trafficking to the lysosome.^{47, 51} From there the VSRs are trafficked to Rab5 endosomes, where many predominantly localize, and are recycled back to the endoplasmic reticulum or Golgi for another round sorting.^{47, 51, 52} VSRs also have epidermal growth factor repeats that can bind calcium, and cargo binding is thought to depend on both calcium and pH.⁵¹ One study found that optimal cargo binding for BP-80 occurred at pH 6.0 when performed in the presence of low calcium, and in another study high concentrations of calcium stabilized cargo binding at pH as low as 4.0 whereas calcium depletion can trigger cargo release independent of pH.^{53, 54} Interestingly, like mannose-6-phosphate receptor and some sortillins, the VSR BP80 also localizes partially to the plasma membrane where it participates in endocytosis.⁵⁵⁻⁵⁷

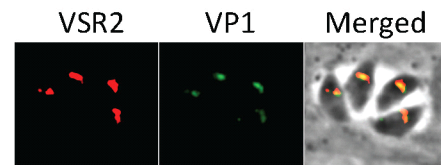


Figure 4-4. VSR2 colocalizes with VP1, an ELC marker. Endogenously myc-tagged VSR2 parasite strain was generated by Raj Gaji, allowed to replicate overnight in HFF cells, fixed and stained with anti-myc and anti-VP1 antibodies as described in Chapters 2 and 3.

T. gondii VSR1 and VSR2 do not play roles in trafficking to the micronemes and rhoptries (data not shown), and VSR2 predominantly colocalizes with ELCs of *T. gondii* (Figure 4-4).^{50, 58, 59} The localization of VSR1 is not known. VSR1 and VSR2 are not likely to participate in endocytic trafficking if they work the same way in plants, but they may be regulated differently since they each have a PA domain but do not appear to have EGF domains. How cargo binding and release could work is also difficult to predict given that the gradients of calcium concentration and pH within the *T. gondii* endolysosomal system have not been defined. Knockouts of VSR1 and VSR2 are in hand and could be tested for defects in ingested protein uptake and downstream trafficking to the VAC. However, an unbiased approach to discovering possible receptors for endocytic trafficking may be more productive and is described in the next section.

4.6 Tools for testing predictable and unpredictable targets

Predictions so far are based on what we know about model systems. However, discovery of parasite-specific proteins that we cannot predict a role for will be even more

interesting. Developing a strategy to find these proteins in an unbiased way will be important for future work. If studies of roles for conserved endocytic players are confirmed, they could be used as handles a proximity-based labelling approaches to identify binding partners in live or fixed cells. In proximity labeling using Ascorbate Peroxidase (APEX), proteins of interest are fused to ascorbate peroxidase, which in the presence of biotin-phenol and hydrogen peroxide, generates biotin-phenoxy radicals that can covalently bind to tyrosine, tryptophan, cysteine, and histidine amino acids of proteins within 20 nm.⁶⁰ Alternatively, if tagging is an issue, biotinylation by antibody recognition method (BAR) can be applied in fixed cells.⁶¹ In this method, fixed cells are stained with antibodies against the protein of interest and secondary antibodies conjugated to horseradish peroxidase. In the presence of hydrogen peroxide and biotin-tyramide, horseradish peroxidase creates biotin-phenoxy radicals that can covalently bind to fixed proteins in proximity to the antibody-stained protein of interest. Proximity labeling by these techniques can be performed in minutes, which should minimize non-specific labeling, and biotinylated proteins can then be pulled down using Streptavidin and identified by mass spectrometry. For example, players in endocytosis at the parasite plasma membrane could be used to identify micropore markers if it is the site of endocytosis, some of which may be endocytic receptors. If AP2 is involved in host protein endocytosis, it would be expected to bind to endocytosed transmembrane proteins, which would be good candidates for endocytic receptors.

The roles of proteins of interest could be tested using the ddfFKBP/Shield-1 system as described in Chapter 3 for determining the role of DrpB. Briefly, proteins of interest are fused to the ddfFKBP destabilization domain, which leads to protein destabilization, ubiquitination and proteasomal degradation unless treated with the stabilizing drug Shield-1.^{62, 63} This allows for conditional, rapid, reversible post-translational induction of dominant negative mutants. We are also preparing to use the newly developed auxin-inducible degradation (AID) for conditional protein knockdown. In this system, proteins of interest are fused to the auxin-inducible degron peptide, which mediates ubiquitination and proteasomal degradation of the protein of interest in response to the plant hormone auxin. This allows for conditional, rapid, reversible protein knockdown.^{64, 65} These approaches are advantageous due to their ability to induce protein expression or

degradation within a period of hours, which will be especially important for essential genes that cannot be knocked out like clathrin and for potentially preventing compensatory mechanisms from taking over. They will work well as complementary approaches to demonstrate the roles of potential endocytic players in future work.

4.7 The importance of host protein ingestion

Host cytosol ingestion in *Plasmodium spp.* parasites is essential for acquisition of amino acids.³ Targeting this pathway has been a successful therapeutic strategy.^{66, 67} *T. gondii* could gain access to arginine, tryptophan and tyrosine via the GRA17/GRA23 hypothetical nutrient pore, but in the context of the immune response ingestion could be required to scavenge these essential amino acids. Interferon gamma, the main driver of the immune response against *T. gondii*, induces expression of indoleamine-dioxygenase, which degrades and starves the parasite of tryptophan.⁶⁸ Further, macrophages infected with certain strains of *T. gondii* undergo parasite-driven activation of the arginine-degrading enzyme arginase-1, which limits the growth of the parasite.⁶⁹ In this context, the main source of arginine and tryptophan will be bound up in host proteins, which could be liberated via ingestion.

Beyond nutrient acquisition from the host cell, endocytosis could be important for cell signaling, membrane turnover, or specifically in the case of *T. gondii* sensing the host cell environment or controlling the immune response.⁷⁰ Interestingly, the virulence defect of cathepsin L (CPL) knockout parasites is completely rescued in the absence of the interferon gamma receptor, suggesting that protein degradation in the VAC is somehow involved in immune evasion.² This could be explained by the ingestion pathway providing access to essential amino acids like arginine or tryptophan through CPL-dependent degradation of ingested proteins when arginase and indoleamine-dioxygenase are upregulated during the immune response. Could the parasite sample the host cytosol to sense when it is in danger? Ingestion of mCherry from the host cytosol is expected to occur by a non-specific bulk flow-like mechanism since *T. gondii* is not expected to have receptors on the PVM that recognize fluorescent proteins. However, the parasite could have receptors on the PVM that bind to specific host immune effectors. For example, rhoptry proteins on the host cytosolic face of the PVM bind to and inactivate immunity

related GTPases and guanylate-binding proteins, interferon-gamma induced immune effectors that vesiculate and strip away the PVM, leading to autophagic death of the parasite.⁷¹⁻⁷³

Finally, host cytosol ingestion has been demonstrated in acute stage parasites, but whether this process also occurs in chronic stage parasites is unclear. Parasites lacking CPL can differentiate into cysts normally, but eventually accumulate autophagosomes and die.¹ Chronic stage parasites are thought to persist for the lifetime of the host, but are not completely dormant and continue to divide.⁷⁴ Whether autophagosomes accumulate because they are not being turned over or are induced in response to starvation for host-derived nutrients like amino acids is unclear. Current work aims to determine if ingestion also occurs in chronic cyst stage parasites.

4.8 Conclusion

The work in this dissertation has expanded our understanding of endocytosis in *Toxoplasma gondii*, but there is much more to be discovered. As a cell biologist, the paucity of conserved endocytic players and the fact that *T. gondii* performs endocytosis across two membranes presents an exciting opportunity to discover potentially novel aspects of endocytosis. The analogous endocytic pathway for ingestion of red blood cell cytosol in *Plasmodium spp.* has been a successful therapeutic strategy, but drug resistance to nearly every antimalarial treatment is emerging.^{3, 66, 67, 75} However, very little is known about how this pathway works either. It is also not known if other Apicomplexan parasites have analogous ingestion pathways, including *Cryptosporidium* which causes serious diarrheal illness that is often not curable in immunocompromised individuals.⁷⁶ *T. gondii* could serve as a model for understanding these and other apicomplexan parasites as well as for the eventual discovery of druggable targets for toxoplasmosis other apicomplexan infections.

4.9 References

1. Di Cristina M, Dou Z, Lunghi M, et al. Toxoplasma depends on lysosomal consumption of autophagosomes for persistent infection. *Nat Microbiol.* 2017;2:17096. doi: 10.1038/nmicrobiol.2017.96 [doi].

2. Dou Z, McGovern O, Di Cristina M, Carruthers V. *Toxoplasma gondii* ingests and digests host cytosolic proteins. . *mBio*. 2014;5(4):e01188-14.
3. Liu J, Istvan ES, Gluzman IY, Gross J, Goldberg DE. Plasmodium falciparum ensures its amino acid supply with multiple acquisition pathways and redundant proteolytic enzyme systems. *Proc Natl Acad Sci U S A*. 2006;103(23):8840-8845. doi: 0601876103 [pii].
4. Sidik SM, Huet D, Ganesan SM, et al. A Genome-wide CRISPR Screen in *Toxoplasma* Identifies Essential Apicomplexan Genes. *Cell*. 2016;166(6):1423-1435.e12. doi: 10.1016/j.cell.2016.08.019 [doi].
5. Pieperhoff MS, Schmitt M, Ferguson DJ, Meissner M. The role of clathrin in post-Golgi trafficking in *Toxoplasma gondii*. *PLoS One*. 2013;8(10):e77620. doi: 10.1371/journal.pone.0077620 [doi].
6. Breinich MS, Ferguson DJ, Foth BJ, et al. A dynamin is required for the biogenesis of secretory organelles in *Toxoplasma gondii*. *Curr Biol*. 2009;19(4):277-286. doi: 10.1016/j.cub.2009.01.039.
7. Kremer K, Kamin D, Rittweger E, et al. An Overexpression Screen of *Toxoplasma gondii* Rab-GTPases Reveals Distinct Transport Routes to the Micronemes. *PLoS Pathog*. 2013;9(3):e1003213. doi: 10.1371/journal.ppat.1003213; 10.1371/journal.ppat.1003213.
8. Venugopal K, Werkmeister E, Barois N, et al. Dual role of the *Toxoplasma gondii* clathrin adaptor AP1 in the sorting of rhoptry and microneme proteins and in parasite division. *PLoS Pathog*. 2017 Apr 21;13(4):e1006331.
9. Tomavo S, Slomianny C, Meissner M, Carruthers VB. Protein trafficking through the endosomal system prepares intracellular parasites for a home invasion. *PLoS Pathog*. 2013;9(10):e1003629. doi: 10.1371/journal.ppat.1003629 [doi].
10. Daher W, Klages N, Carlier MF, Soldati-Favre D. Molecular characterization of *Toxoplasma gondii* formin 3, an actin nucleator dispensable for tachyzoite growth and motility. *Eukaryot Cell*. 2012;11(3):343-352. doi: 10.1128/EC.05192-11; 10.1128/EC.05192-11.
11. Morlon-Guyot J, Pastore S, Berry L, Lebrun M, Daher W. *Toxoplasma gondii* Vps11, a subunit of HOPS and CORVET tethering complexes, is essential for the biogenesis of secretory organelles. *Cell Microbiol*. 2015;17(8):1157-1178. doi: 10.1111/cmi.12426 [doi].
12. Travier L, Mondragon R, Dubremetz JF, et al. Functional domains of the *Toxoplasma* GRA2 protein in the formation of the membranous nanotubular network of the parasitophorous vacuole. *Int J Parasitol*. 2008;38(7):757-773. doi: 10.1016/j.ijpara.2007.10.010.

13. Sibley LD, Niesman IR, Parmley SF, Cesbron-Delauw MF. Regulated secretion of multi-lamellar vesicles leads to formation of a tubulo-vesicular network in host-cell vacuoles occupied by *Toxoplasma gondii*. *J Cell Sci.* 1995;108 (Pt 4)(Pt 4):1669-1677.
14. Schmidt O, Teis D. The ESCRT machinery. *Curr Biol.* 2012;22(4):R116-20. doi: 10.1016/j.cub.2012.01.028 [doi].
15. Babst M, Wendland B, Estepa EJ, Emr SD. The Vps4p AAA ATPase regulates membrane association of a Vps protein complex required for normal endosome function. *EMBO J.* 1998;17(11):2982-2993. doi: 10.1093/emboj/17.11.2982 [doi].
16. Wang Y, Weiss LM, Orlofsky A. Host cell autophagy is induced by *Toxoplasma gondii* and contributes to parasite growth. *J Biol Chem.* 2009;284(3):1694-1701. doi: 10.1074/jbc.M807890200 [doi].
17. Coers J, Haldar AK. Ubiquitination of pathogen-containing vacuoles promotes host defense to *Chlamydia trachomatis* and *Toxoplasma gondii*. *Commun Integr Biol.* 2015;8(6):e1115163. doi: 10.1080/19420889.2015.1115163 [doi].
18. Fujii K, Hurley JH, Freed EO. Beyond Tsg101: the role of Alix in 'ESCRTing' HIV-1. *Nat Rev Microbiol.* 2007;5(12):912-916. doi: nrmicro1790 [pii].
19. Votteler J, Sundquist WI. Virus budding and the ESCRT pathway. *Cell Host Microbe.* 2013;14(3):232-241. doi: 10.1016/j.chom.2013.08.012 [doi].
20. Dowlatshahi DP, Sandrin V, Vivona S, et al. ALIX is a Lys63-specific polyubiquitin binding protein that functions in retrovirus budding. *Dev Cell.* 2012;23(6):1247-1254. doi: 10.1016/j.devcel.2012.10.023 [doi].
21. Joshi A, Munshi U, Ablan SD, Nagashima K, Freed EO. Functional replacement of a retroviral late domain by ubiquitin fusion. *Traffic.* 2008;9(11):1972-1983. doi: 10.1111/j.1600-0854.2008.00817.x [doi].
22. Rauch S, Martin-Serrano J. Multiple interactions between the ESCRT machinery and arrestin-related proteins: implications for PPXY-dependent budding. *J Virol.* 2011;85(7):3546-3556. doi: 10.1128/JVI.02045-10 [doi].
23. Rome ME, Beck JR, Turetzky JM, Webster P, Bradley PJ. Intervacuolar transport and unique topology of GRA14, a novel dense granule protein in *Toxoplasma gondii*. *Infect Immun.* 2008;76(11):4865-4875. doi: 10.1128/IAI.00782-08 [doi].
24. Nichols BA, Chiappino ML, Pavesio CE. Endocytosis at the micropore of *Toxoplasma gondii*. *Parasitol Res.* 1994;80(2):91-98.
25. Lige B, Romano JD, Sampels V, Sonda S, Joiner KA, Coppens I. Introduction of caveolae structural proteins into the protozoan *Toxoplasma* results in the formation

- of heterologous caveolae but not caveolar endocytosis. *PLoS One*. 2012;7(12):e51773. doi: 10.1371/journal.pone.0051773 [doi].
26. Prosser DC, Drivas TG, Maldonado-Baez L, Wendland B. Existence of a novel clathrin-independent endocytic pathway in yeast that depends on Rho1 and formin. *J Cell Biol*. 2011;195(4):657-671. doi: 10.1083/jcb.201104045 [doi].
 27. Daher W, Plattner F, Carlier MF, Soldati-Favre D. Concerted action of two formins in gliding motility and host cell invasion by *Toxoplasma gondii*. *PLoS Pathog*. 2010;6(10):e1001132. doi: 10.1371/journal.ppat.1001132; 10.1371/journal.ppat.1001132.
 28. Allen CL, Goulding D, Field MC. Clathrin-mediated endocytosis is essential in *Trypanosoma brucei*. *EMBO J*. 2003;22(19):4991-5002. doi: 10.1093/emboj/cdg481 [doi].
 29. Gabernet-Castello C, Dacks JB, Field MC. The single ENTH-domain protein of trypanosomes; endocytic functions and evolutionary relationship with epsin. *Traffic*. 2009;10(7):894-911. doi: 10.1111/j.1600-0854.2009.00910.x [doi].
 30. Paez Valencia J, Goodman K, Otegui MS. Endocytosis and Endosomal Trafficking in Plants. *Annu Rev Plant Biol*. 2016;67:309-335. doi: 10.1146/annurev-arplant-043015-112242 [doi].
 31. Mayor S, Parton RG, Donaldson JG. Clathrin-independent pathways of endocytosis. *Cold Spring Harb Perspect Biol*. 2014;6(6):10.1101/cshperspect.a016758. doi: 10.1101/cshperspect.a016758 [doi].
 32. Ferreira APA, Boucrot E. Mechanisms of Carrier Formation during Clathrin-Independent Endocytosis. *Trends Cell Biol*. 2018;28(3):188-200. doi: S0962-8924(17)30208-8 [pii].
 33. Marques PE, Grinstein S, Freeman SA. SnapShot:Macropinocytosis. *Cell*. 2017;169(4):766-766.e1. doi: S0092-8674(17)30485-3 [pii].
 34. Ford MG, Mills IG, Peter BJ, et al. Curvature of clathrin-coated pits driven by epsin. *Nature*. 2002;419(6905):361-366. doi: 10.1038/nature01020 [doi].
 35. Boucrot E, Pick A, Camdere G, et al. Membrane fission is promoted by insertion of amphipathic helices and is restricted by crescent BAR domains. *Cell*. 2012;149(1):124-136. doi: 10.1016/j.cell.2012.01.047 [doi].
 36. van Dooren GG, Reiff SB, Tomova C, Meissner M, Humbel BM, Striepen B. A novel dynamin-related protein has been recruited for apicoplast fission in *Toxoplasma gondii*. *Curr Biol*. 2009;19(4):267-276. doi: 10.1016/j.cub.2008.12.048.
 37. Park SY, Guo X. Adaptor protein complexes and intracellular transport. *Biosci Rep*. 2014;34(4):10.1042/BSR20140069. doi: 10.1042/BSR20140069 [doi].

38. Shu X, Lev-Ram V, Deerinck TJ, et al. A genetically encoded tag for correlated light and electron microscopy of intact cells, tissues, and organisms. *PLoS Biol.* 2011;9(4):e1001041. doi: 10.1371/journal.pbio.1001041 [doi].
39. Scheuring D, Viotti C, Kruger F, et al. Multivesicular bodies mature from the trans-Golgi network/early endosome in Arabidopsis. *Plant Cell.* 2011;23(9):3463-3481. doi: 10.1105/tpc.111.086918 [doi].
40. Ezougou CN, Ben-Rached F, Moss DK, et al. Plasmodium falciparum Rab5B is an N-terminally myristoylated Rab GTPase that is targeted to the parasite's plasma and food vacuole membranes. *PLoS One.* 2014;9(2):e87695. doi: 10.1371/journal.pone.0087695 [doi].
41. Ebine K, Miyakawa N, Fujimoto M, Uemura T, Nakano A, Ueda T. Endosomal trafficking pathway regulated by ARA6, a RAB5 GTPase unique to plants. *Small GTPases.* 2012;3(1):23-27.
42. Sakura T, Sindikubwabo F, Oesterlin LK, et al. A Critical Role for *Toxoplasma gondii* Vacuolar Protein Sorting VPS9 in Secretory Organelle Biogenesis and Host Infection. *Sci Rep.* 2016 Dec 14;6:38842-doi: 10.1038/srep38842.
43. Mizuno-Yamasaki E, Rivera-Molina F, Novick P. GTPase networks in membrane traffic. *Annu Rev Biochem.* 2012;81:637-659. doi: 10.1146/annurev-biochem-052810-093700 [doi].
44. Numrich J, Ungermann C. Endocytic Rabs in membrane trafficking and signaling. *Biol Chem.* 2014;395(3):327-333. doi: 10.1515/hsz-2013-0258 [doi].
45. Scott CC, Vacca F, Gruenberg J. Endosome maturation, transport and functions. *Semin Cell Dev Biol.* 2014;31:2-10. doi: 10.1016/j.semcdb.2014.03.034 [doi].
46. Viotti C, Bubeck J, Stierhof YD, et al. Endocytic and secretory traffic in Arabidopsis merge in the trans-Golgi network/early endosome, an independent and highly dynamic organelle. *Plant Cell.* 2010;22(4):1344-1357. doi: 10.1105/tpc.109.072637 [doi].
47. Kunzl F, Fruholz S, Fassler F, Li B, Pimpl P. Receptor-mediated sorting of soluble vacuolar proteins ends at the trans-Golgi network/early endosome. *Nat Plants.* 2016;2:16017. doi: 10.1038/nplants.2016.17 [doi].
48. V K, Qi H, Beckers CJ, et al. The protozoan parasite *Toxoplasma gondii* targets proteins to dense granules and the vacuolar space using both conserved and unusual mechanisms. *J Cell Biol.* 1998;141(6):1323-1333.
49. Striepen B, He CY, Matrajt M, Soldati D, Roos DS. Expression, selection, and organellar targeting of the green fluorescent protein in *Toxoplasma gondii*. *Mol Biochem Parasitol.* 1998;92(2):325-338.

50. Sloves PJ, Delhaye S, Mouveaux T, et al. Toxoplasma sortilin-like receptor regulates protein transport and is essential for apical secretory organelle biogenesis and host infection. *Cell Host Microbe*. 2012;11(5):515-527. doi: 10.1016/j.chom.2012.03.006; 10.1016/j.chom.2012.03.006.
51. Robinson DG, Neuhaus JM. Receptor-mediated sorting of soluble vacuolar proteins: myths, facts, and a new model. *J Exp Bot*. 2016;67(15):4435-4449. doi: 10.1093/jxb/erw222 [doi].
52. Kang H, Kim SY, Song K, et al. Trafficking of vacuolar proteins: the crucial role of Arabidopsis vacuolar protein sorting 29 in recycling vacuolar sorting receptor. *Plant Cell*. 2012;24(12):5058-5073. doi: 10.1105/tpc.112.103481 [doi].
53. Watanabe E, Shimada T, Kuroyanagi M, Nishimura M, Hara-Nishimura I. Calcium-mediated association of a putative vacuolar sorting receptor PV72 with a propeptide of 2S albumin. *J Biol Chem*. 2002;277(10):8708-8715. doi: 10.1074/jbc.M109346200 [doi].
54. Kirsch T, Paris N, Butler JM, Beevers L, Rogers JC. Purification and initial characterization of a potential plant vacuolar targeting receptor. *Proc Natl Acad Sci U S A*. 1994;91(8):3403-3407.
55. Saint-Jean B, Seveno-Carpentier E, Alcon C, Neuhaus JM, Paris N. The cytosolic tail dipeptide Ile-Met of the pea receptor BP80 is required for recycling from the prevacuole and for endocytosis. *Plant Cell*. 2010;22(8):2825-2837. doi: 10.1105/tpc.109.072215 [doi].
56. Braulke T, Bonifacino JS. Sorting of lysosomal proteins. *Biochim Biophys Acta*. 2009;1793(4):605-614. doi: 10.1016/j.bbamcr.2008.10.016 [doi].
57. Willnow TE, Petersen CM, Nykjaer A. VPS10P-domain receptors - regulators of neuronal viability and function. *Nat Rev Neurosci*. 2008;9(12):899-909. doi: 10.1038/nrn2516 [doi].
58. Tse YC, Mo B, Hillmer S, et al. Identification of multivesicular bodies as prevacuolar compartments in *Nicotiana tabacum* BY-2 cells. *Plant Cell*. 2004;16(3):672-693. doi: 10.1105/tpc.019703 [doi].
59. Lee GJ, Sohn EJ, Lee MH, Hwang I. The Arabidopsis rab5 homologs rha1 and ara7 localize to the prevacuolar compartment. *Plant Cell Physiol*. 2004;45(9):1211-1220. doi: 10.1007/s12275-004-0011-1 [pii].
60. Li P, Li J, Wang L, Di LJ. Proximity Labeling of Interacting Proteins: Application of BioID as a Discovery Tool. *Proteomics*. 2017;17(20):10.1002/pmic.201700002. Epub 2017 Apr 10. doi: 10.1002/pmic.201700002 [doi].

61. Bar DZ, Atkatsk K, Tavarez U, Erdos MR, Gruenbaum Y, Collins FS. Biotinylation by antibody recognition-a method for proximity labeling. *Nat Methods*. 2018;15(2):127-133. doi: 10.1038/nmeth.4533 [doi].
62. Herm-Gotz A, Agop-Nersesian C, Munter S, et al. Rapid control of protein level in the apicomplexan *Toxoplasma gondii*. *Nat Methods*. 2007;4(12):1003-1005. doi: nmeth11134 [pii].
63. Egeler EL, Urner LM, Rakhit R, Liu CW, Wandless TJ. Ligand-switchable substrates for a ubiquitin-proteasome system. *J Biol Chem*. 2011;286(36):31328-31336. doi: 10.1074/jbc.M111.264101 [doi].
64. Nishimura K, Fukagawa T, Takisawa H, Kakimoto T, Kanemaki M. An auxin-based degron system for the rapid depletion of proteins in nonplant cells. *Nat Methods*. 2009;6(12):917-922. doi: 10.1038/nmeth.1401 [doi].
65. Brown KM, Long S, Sibley LD. Plasma Membrane Association by N-Acylation Governs PKG Function in *Toxoplasma gondii*. *MBio*. 2017;8(3):10.1128/mBio.00375-17. doi: e00375-17 [pii].
66. Meshnick SR. Artemisinin: mechanisms of action, resistance and toxicity. *Int J Parasitol*. 2002;32(13):1655-1660. doi: S0020751902001947 [pii].
67. Slater AF. Chloroquine: mechanism of drug action and resistance in *Plasmodium falciparum*. *Pharmacol Ther*. 1993;57(2-3):203-235. doi: 0163-7258(93)90056-J [pii].
68. Pfefferkorn ER, Eckel M, Rebhun S. Interferon-gamma suppresses the growth of *Toxoplasma gondii* in human fibroblasts through starvation for tryptophan. *Mol Biochem Parasitol*. 1986;20(3):215-224.
69. Butcher BA, Fox BA, Rommereim LM, et al. *Toxoplasma gondii* rhoptry kinase ROP16 activates STAT3 and STAT6 resulting in cytokine inhibition and arginase-1-dependent growth control. *PLoS Pathog*. 2011;7(9):e1002236. doi: 10.1371/journal.ppat.1002236; 10.1371/journal.ppat.1002236.
70. McMahon HT, Boucrot E. Molecular mechanism and physiological function. *Nat Rev Mol Cell Biol*. 2011;12(8):517-533. doi: 10.1038/nrm3151 [doi].
71. Hermanns T, Muller UB, Konen-Waisman S, Howard JC, Steinfeldt T. The *Toxoplasma gondii* rhoptry protein ROP18 is an Irga6-specific kinase and regulated by the dense granule protein GRA7. *Cell Microbiol*. 2016;18(2):244-259. doi: 10.1111/cmi.12499 [doi].
72. Etheridge RD, Alaganan A, Tang K, Lou HJ, Turk BE, Sibley LD. The *Toxoplasma* pseudokinase ROP5 forms complexes with ROP18 and ROP17 kinases that synergize to control acute virulence in mice. *Cell Host Microbe*. 2014 May 14;15(5):537-550.

73. Ling YM, Shaw MH, Ayala C, et al. Vacuolar and plasma membrane stripping and autophagic elimination of *Toxoplasma gondii* in primed effector macrophages. *J Exp Med*. 2006;203(9):2063-2071. doi: jem.20061318 [pii].
74. Watts E, Zhao Y, Dhara A, Eller B, Patwardhan A, Sinai AP. Novel Approaches Reveal that *Toxoplasma gondii* Bradyzoites within Tissue Cysts Are Dynamic and Replicating Entities In Vivo. *MBio*. 2015;6(5):e01155-15. doi: 10.1128/mBio.01155-15 [doi].
75. Cui L, Mharakurwa S, Ndiaye D, Rathod PK, Rosenthal PJ. Antimalarial Drug Resistance: Literature Review and Activities and Findings of the ICEMR Network. *Am J Trop Med Hyg*. 2015;93(3 Suppl):57-68. doi: 10.4269/ajtmh.15-0007 [doi].
76. Chalmers RM, Davies AP. Minireview: clinical cryptosporidiosis. *Exp Parasitol*. 2010;124(1):138-146. doi: 10.1016/j.exppara.2009.02.003 [doi].